

**Synthesis, Characterization, and Reactivity Studies of Iridium Complexes
Bearing the Ligand Diphenylphosphidoboratabenzene**

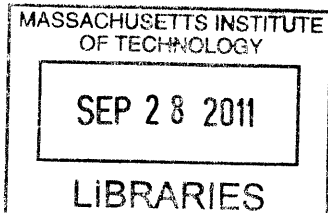
ARCHIVES

by

Luis Arizpe

B.A., Grinnell College

(2008)



**Submitted to the Department of Chemistry in Partial Fulfillment of the Requirements for
the Degree of**

MASTER OF SCIENCE

at the

Massachusetts Institute of Technology

September 2011

© Massachusetts Institute of Technology 2011

All rights reserved

A handwritten signature in black ink, appearing to read "Luis Arizpe".

Signature of Author

A handwritten signature in black ink, appearing to read "Luis Arizpe".

**Department of Chemistry
July 05, 2011**

Certified by _____

**Professor Gregory C. Fu
Department of Chemistry
Thesis Supervisor**

Accepted by _____

**Robert W. Field
Chairman, Departmental Committee on Graduate Studies**

**Synthesis, Characterization, and Reactivity Studies of Iridium Complexes Bearing the
Ligand Diphenylphosphidoboratabenzene**

by

Luis Arizpe

**Submitted to the Department of Chemistry
on July 05, 2011 in partial fulfillment of the
requirements for the Degree of Master of Science in
Chemistry**

Abstract

The synthesis, structure, and reactivity properties of three iridium square planar complexes bearing the anionic phosphine ligand diphenylphosphidoboratabenzene (DPB) are described. Reactivity studies show a rate enhancement for the oxidative addition of a substituted benzyl bromide and Me₃SnBr with DPB as a ligand in place of triphenylphosphine. Two products from the oxidative addition of *p*-chlorobenzyl bromide have been isolated and structurally characterized.

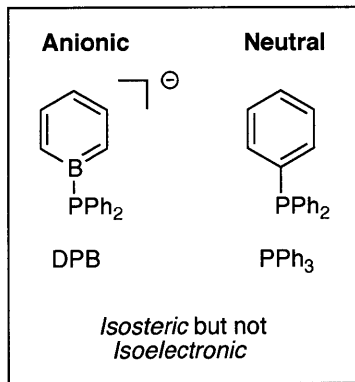
Thesis Supervisor: Gregory C. Fu
Title: Firmenich Professor of Chemistry

TABLE OF CONTENTS

1 Introduction	4
2 Discussion	
2.1 Synthesis and Structural Studies of $[K_2][IrCO(DPB)_3]$	6
2.2 Reactivity of $[K_2][IrCO(DPB)_3]$ Towards Electrophiles	9
2.3 Synthesis of and Addition Reactions to $[K_2][MeIrCO(DPB)_2]$	10
2.4 Synthesis of and Addition Reactions to $[K(18\text{-crown-}6)][MeIrCO(DPB)(PPh_3)]$	17
3 Synthetic Attempts Towards an Iron Cyclopentadienyl Azaborolyl Complex and Mechanistic Studies into Nickel- Catalyzed Carbon-Carbon Bond-Forming Reactions	
3.1 Iron Azaborolyl Chemistry	21
3.2 Isolation Attempts of a Nickel(I) Alkyl and Halo Species	22
4 Experimental	23
References	30
Appendix A: Crystal Structure Data	33

1 Introduction

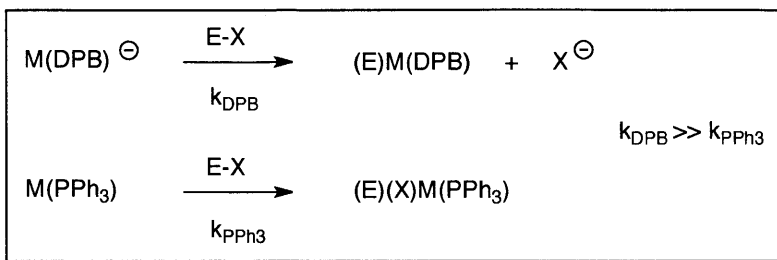
The reactivity of a metal center is in large part determined by the supporting ligands within its coordination sphere. This allows for the tuning of metal reactivity by altering the ligand structure in either a steric or electronic fashion. Typically, alterations of the electronic effects of ligands involve adding electron-withdrawing groups such as NO_2 , and CF_3 or electron-donating groups such as alkyl or methoxy groups to the backbone structure of the ligands. Changing the steric demand of a ligand may involve adding branched alkyl substituents near the reacting center. The particular interest of the work presented here lies in enhancing metal reactivity by altering the electronic properties of a ligand while keeping the steric parameters constant. It is not always a simple task to achieve a ligand structure, which is sterically identical to the base structure, but electronically distinct. Our lab has had success in developing an anionic variant of the ubiquitous triphenylphosphine (PPh_3) ligand by exchanging one of the phenyl rings for a borabenzene ring.¹² The resulting structure of diphenylphosphidoboratabenzene (DPB) is shown below.



It was further demonstrated that the electronic properties of a metal complex bearing this ligand are altered relative to PPh_3 by comparing the IR stretching frequencies of carbonyl ligands in two otherwise identical iron complexes ($(\eta^6\text{-C}_5\text{H}_5\text{Fe}(\text{CO})_2\text{DPB})$ versus $[\eta^6\text{-C}_5\text{H}_5\text{Fe}(\text{CO})_2\text{PPh}_3]\text{Cl}$).¹ These initial studies showed the metal binding ability of the ligand and its electron-donating properties.³ In continuation of these studies, insight on how metal reactivity can be affected was desired. With a more electron-rich ligand, reactions that involve electron transfer from a metal should be accelerated whereas decelerating effect is expected in reactions involving electron transfer to a metal. One particular class of reactions that follows this type of a

1 Introduction

behavior is the oxidative addition of an electrophile E-X to a metal center. Thus, an oxidative addition reaction with a metal DPB species M(DPB) should proceed faster relative to a metal PPh₃ species M(PPh₃) (Scheme 1). This hypothesis formed the basis our studies in beginning to understand the effect of DPB on metal reactivity.



Scheme 1.

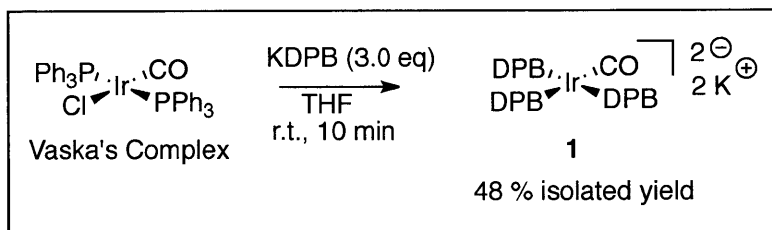
With the class of reaction in hand it still remained to choose a metal complex as a platform for our reactivity studies.⁴ Both the DPB and PPh₃ complexes had to be accessible. In light of the fact that much reactivity data had already been collected on square planar iridium(I) complexes, we decided to use these as our base structure for comparison. The most well-known example is *trans*-ClIrCO(PPh₃)₂, Vaska's Complex.⁵ This compound benefits from having a non-accessible reductive elimination pathway, which is useful for solely studying the oxidative addition reaction without facing the complications of an unstable product. However, a closer inspection at the reactivity of DPB shows that it undergoes substitutions of X type ligands and therefore exposure to *trans*-ClIrCO(PPh₃)₂ would likely not lead to the requisite complex [*trans*-ClIrCO(DPB)(PPh₃)]. As will be described in Section 2.1, the chloro and the two phosphine ligands are displaced to form [K₂][IrCO(DPB)₃] (**1**). Computational studies on the geometry of **1** and further reactivity studies are also described.

Our attention then turned to the methylated form of Vaska's complex (**MV**) *trans*-MeIrCO(PPh₃)₂.⁶ This was especially useful because Bergman and coworkers had already studied the rate of oxidative addition of methyl iodide (MeI).⁷ Section 2.2 describes the synthesis and the oxidative addition reactions to [MeIrCO(DPB)₂]²⁻, as this compound proved to be more straight forward to synthesize than the mono-substituted species. Section 2.3 shows our final success at obtaining [MeIrCO(DPB)(PPh₃)] along with its addition reactions described.

2 Discussion

2.1 Synthesis and Structural Studies of $[K_2][IrCO(DPB)_3]$

From the onset, MV was chosen instead of Vaska's complex for comparative reactivity studies due to the expected synthetic challenges brought on by the tendency of KDPB to displace both X- and L-type ligands in substitution reactions. Indeed, upon exposing *trans*-ClIrCO(PPh₃)₂ to one or two equivalents of KDPB a mixture of mono-, di-, and trisubstituted complexes was obtained. Exposure to three equivalents of KDPB, however, lead exclusively to the trisubstituted, dianionic complex $[K_2][IrCO(DPB)_3]$ (**1**) with concomitant precipitation of KCl from the reaction mixture (see Scheme 2). This complex was initially characterized by ³¹P NMR spectroscopy, which showed two distinct broad resonances in a ratio one to two (-6 and -17 ppm, respectively) as would be expected for a square-planar geometry. Structural analysis by X-ray crystallography confirmed this and showed that **1** adopts a distorted square planar geometry (Figure 1).⁸ The two *trans* DPB ligands (P1 and P3, Figure 1) are bent towards each other and are complimented by a similar bending of the carbonyl group and its *trans* DPB (see Table 1). The carbonyl ligand is coordinated in a linear fashion with a slight lengthening of the C-O bond (1.12 Å vs. 1.178(3) Å, Table 1) compared to its free form, as expected. The iridium-phosphine distances are in the range of square planar complexes of iridium, with a slight lengthening of the Ir-P bond to the DPB *trans* to the carbonyl (see Table 1), which is likely due to the steric encumbrance of the two *cis* DPB ligands.



Scheme 2.

2 Discussion

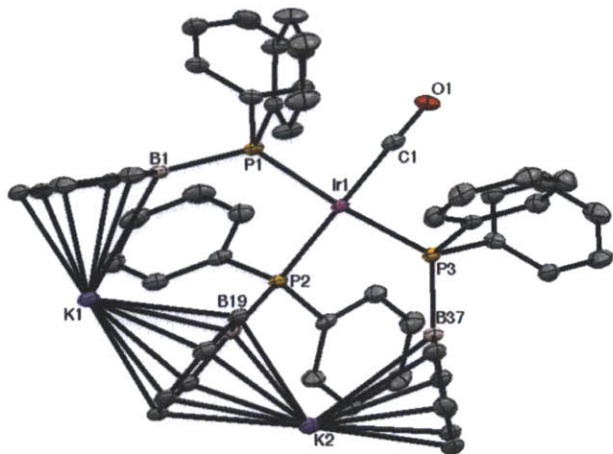


Table 1. Selected Bond Lengths and Angles for **1**.

Bond	Length (Å)	Angle	Angle Value (°)
Ir1-C1	1.928(2)	P1-Ir1-C1	94.8(3)
Ir1-P1	2.360(6)	P1-Ir1-P2	87.7(9)
Ir1-P2	2.490(1)	P1-Ir1-P3	163.9(0)
Ir1-P3	2.337(0)	P2-Ir1-C1	167.7(5)
C1-O1	1.178(3)	P2-Ir1-P3	104.1(3)
		P3-Ir1-C1	75.8(4)
		Ir1-C1-O1	173.1(2)

Figure 1. Molecular structure of **1**. Thermal ellipsoids drawn at 50% probability. Hydrogen atoms are omitted for clarity.

The geometry of **1** is striking in the context of its cationic PPh_3 analog $[\text{IrCO}(\text{PPh}_3)_3]^+$ (**2**), which adopts a tetrahedral geometry.⁸ It was reasoned that **2** adopts this arrangement in order to relieve steric congestion around the iridium center.⁵ However, the isosteric DPB ligands do not force on a tetrahedral geometry, and it is not immediately clear what brings about this structural difference. It was initially postulated that the potassium cations, which nicely arrange themselves with the borabenzene rings in a double-decker sandwich structure above the approximate plane of the molecule, are organizing the geometry. In order to get a clearer picture on whether the potassium cations were playing a role in determining the solid-state structure of **1**, a computational study was undertaken where geometry optimization calculations were carried out on the dianionic species of **1** without the potassium cations and on cationic **2** also without a counterion.

First, using electronic structure theory the ground-state geometry of **1** was explored. Geometry optimizations were carried out using the Q-chem 4 computational package⁹ at the DFT level with the B3LYP functional¹⁰ and the 6-31G* basis set¹¹ for all atoms except Ir where the LANL2DZ basis set¹² with an electron core potential was employed. Starting from either the crystallographically found geometry (**1a**, Figure 2) or an idealized tetrahedral geometry (**1b**, Figure 2), a structure similar to the first was obtained in both cases. With DPB as the phosphine

2 Discussion

there seems to be a preference in the solid state (with the potassium cations) and in the gas phase (computationally with no counter ions) for a more square-planar geometry.

A similar set of computational experiments was then carried with complex **2**. However, because a tetrahedral d⁸ complex would be expected to be paramagnetic both tetrahedral (**2a**) and square-planar (**2b**) geometries as starting points were optimized in the triplet (**2a-t**, **2b-t**) and singlet (**2a-s**, **2b-s**) spin states to give a total of four computations (Figure 3). The starting geometries **2a-t** and **2b-t** converged on a tetrahedral ground-state structure, while for **2a-s** and **2b-s** no ground-state structure was found either due to a large number of persistent imaginary stretching frequencies or since no SCF convergence was achieved after 500 cycles. The results are depicted in Figure 3.

These computational results taken together suggest that the structure-determining factors of the two molecules are not straightforward. Changing the neutral PPh₃ for the isosteric DPB has the effect of changing the preferred geometry and ultimately the spin state of the complex

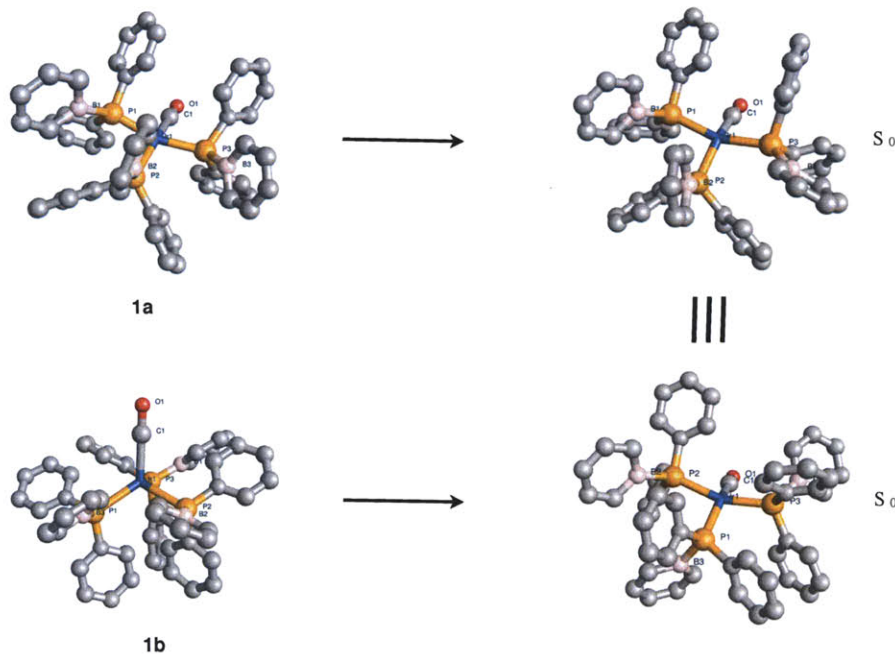


Figure 2. Theoretical geometry optimization studies of **1**.

2 Discussion

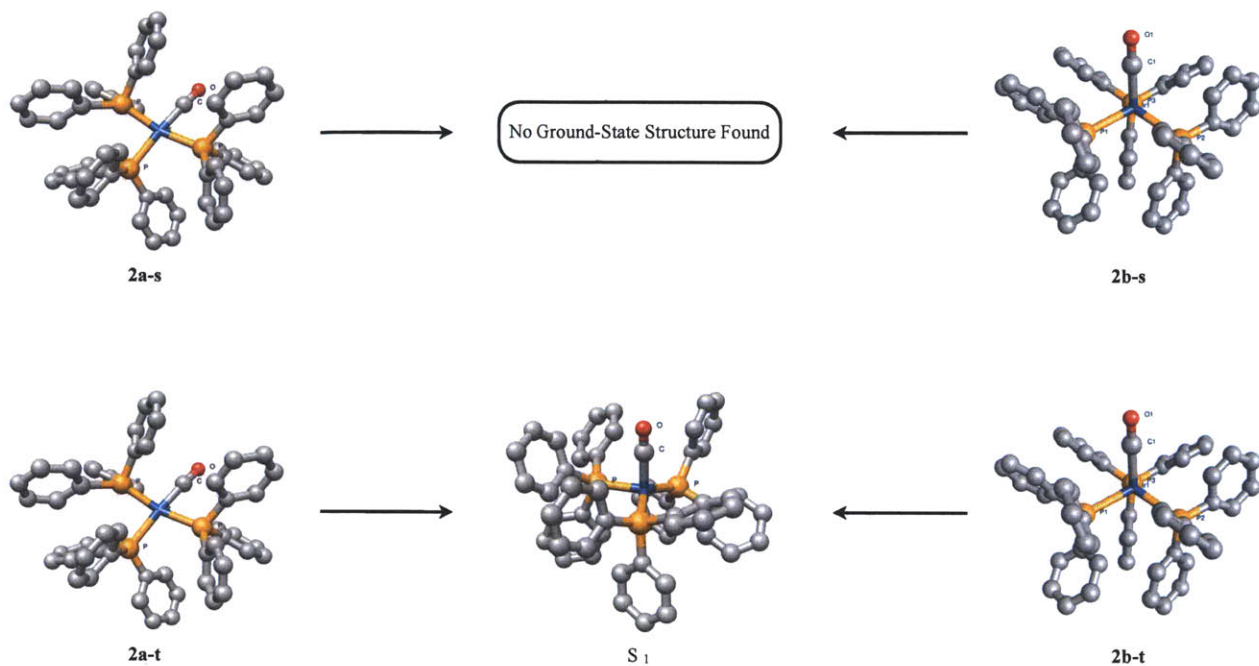


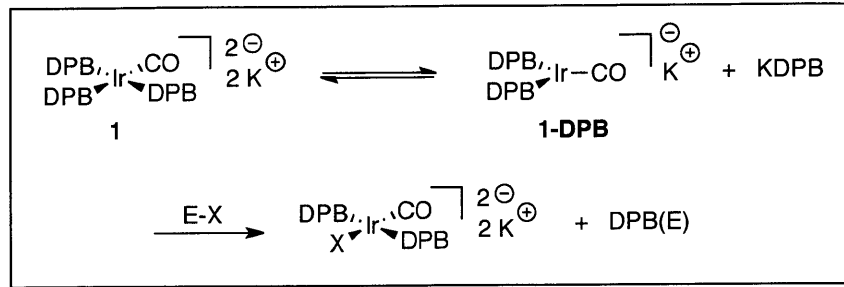
Figure 3. Theoretical geometry optimization studies of **2**.

2.2 Reactivity of 1 Towards Electrophiles

In light of the electron-richness of DPB, it was hypothesized that the carbonyl ligand would be poised for reaction at the oxygen with electrophiles due to significant back bonding from the iridium center (Scheme 3). As such, a variety of iodosilanes and anhydrides were exposed to **1**, but no product consistent with *O*-silylation or acylation was obtained. The major product observed in the most efficient reactions was from a direct reaction of DPB with the added electrophile, and was assigned based on a comparison of the ^{31}P NMR spectrum of the reaction mixture with a mixture containing only DPB and the electrophile. Two possible mechanistic pathways that could be operative in this reaction sequence are shown in Scheme 3. One DPB ligand dissociates from **1** to give **1-DPB**, a 14-electron tricoordinate species, and free KDPB, which then reacts with the electrophile E-X to form (DPB)E and KX. KX then adds to **1-DPB** to give the corresponding four-coordinate, 16 electron species. Another possibility is an iridium-mediated process. In this case **1** undergoes oxidative addition of E-X followed by a reductive elimination event that results in formation of a C-P bond. Due to the broad signals for DPB in its ^{31}P NMR spectrum¹³ suggesting some lability in these ligands, the noniridium-

2 Discussion

mediated pathway is favored (Scheme 3) although to date no mechanistic studies have been performed. Future addition reactions with **1** should focus on non-polar electrophiles such as H₂.¹⁴

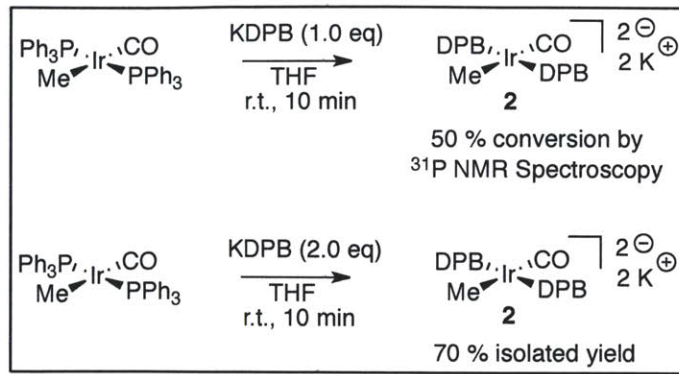


Scheme 3

2.3 Synthesis of and Addition Reactions to [K₂][MeIrCO(DPB)₂]

In order to probe the effects of substituting PPh₃ for DPB on the reactivity of **MV**, the monoDPB-monoPPh₃ derivative was a desired target. As in the synthesis of **1**, a simple ligand substitution reaction was expected to give the desired species. Exposure of one equivalent of KDPB to **MV** at room temperature however, gave the bisDPB species [MeIrCO(DPB)₂]²⁻, where both PPh₃ have been displaced, along with unreacted **MV** (Scheme 4). Presumably, the PPh₃ ligand in the initially formed mono-substituted complex is more labile towards substitution due to a stronger *trans* effect from DPB. Although an X-ray crystal structure of the dipotassium salt **3** was not obtained, a structure was obtained for the mixed cation species [K,Li][MeIrCO(DPB)₂] (**3'**)¹⁵ (Figure 4).

2 Discussion



Scheme 4

Compound **3'** adopts a slightly distorted from square-planar geometry with the potassium cation sandwiched between the two boratabenzene rings and a solvated lithium counterion (solvent not shown in Figure 4) removed from a DPB ligand showing a binding preference for a potassium cation over lithium.

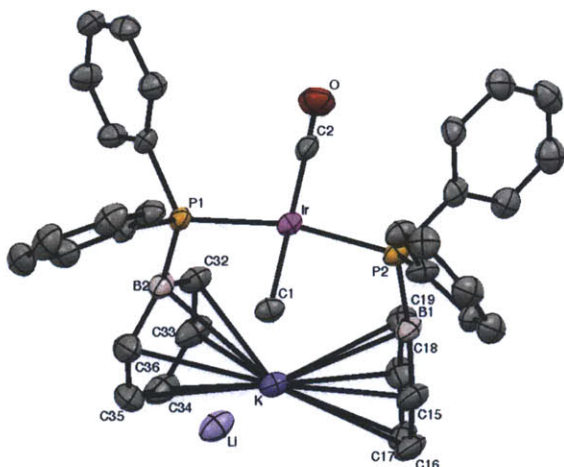


Table 2. Selected Bond Lengths and Angles for **3'**.

Bond	Length (Å)	Angle	Angle Value (°)
Ir-C1	2.156(3)	P1-Ir-C1	86.7(8)
Ir-C2	1.875(1)	P1-Ir-C2	93.4(2)
Ir-P1	2.295(2)	P2-Ir-C1	85.9(0)
Ir-P2	2.311(2)	P2-Ir-C2	94.2(2)
C2-O	1.137(0)	C1-Ir-C2	178.4(5)
		P1-Ir-P2	165.8(1)
		Ir-C1-O1	179.0(7)
		Ir-P1-B2	106.4(0)
		Ir-P2-B1	107.0(4)

Figure 4. Molecular structure of **3'**. Thermal ellipsoids drawn at 50% probability level. Hydrogen atoms are omitted for clarity.

The pertinent structural parameters are given in Table 2 and those of the most similar published structures in Table 3.¹⁶ A comparison shows that the bond lengths in **3'** are within the expected range and are ultimately not a particularly useful measure of the increased electron density transferred to the iridium center from DPB. The more common measure of the electron-richness of a metal is the vibrational stretching frequency of a bound carbonyl ligand and in this case a weaker stretching frequency is observed in **3'** (Table 3). In fact, with a value of 1893 cm^{-1} it is the weakest in the series.

2 Discussion

Table 3

PR_3	Ir-CO	Ir-P (avg)	Ir-CH_3	C-O	$\nu_{\text{CO}} (\text{cm}^{-1})$
PPh_3	1.835	2.300	2.17	1.14	1937
$\text{P}(p\text{-tol})_3$	1.87(2)	2.304	2.20(1)	1.12(2)	1935
$\text{P}(\text{Me}_2\text{C}_4\text{H}_6)\text{Ph}$	1.832(4)	2.282	2.134(5)	1.150(6)	1916
$\text{P}(p\text{-C}_6\text{H}_4\text{OMe})_3$	-	-	-	-	1926
PPh_2Me	-	-	-	-	1925
PPhMe_2	-	-	-	-	1938
PCy_3	-	-	-	-	1908
DPB ^a					1889

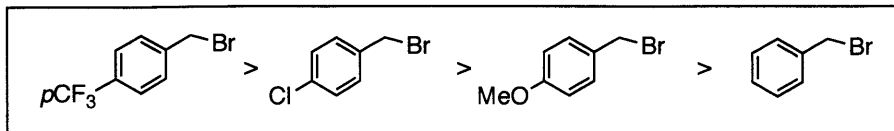
^aIn case of the DPB ligand the complex has an overall charge of 2-.

In addition to knowing the structural parameters of **3'**, we were also interested in the effects that DPB would have on the reactivity of the iridium center towards electrophiles in comparison to PPh_3 . Initial reactivity studies involved the exposure of **3** to methyl iodide in order to form a direct comparison with previously published work using MV, however, clean conversion to one product was not observed precluding mechanistic studies.⁷ Other electrophiles such as ethyl iodide, trimethylsilyl chloride and benzyl bromide were employed in search of a well-behaved reaction. Although all reacted with **3'**, the cleanest reaction was found with benzyl bromide, which gave peak-to-peak conversion according to its ^{31}P NMR spectrum.

Since no published structure of the oxidative addition product between benzyl bromide and **MV** was found, we first explored this reaction by Variable Temperature (VT) ^{31}P NMR Spectroscopy. Exposure of benzyl bromide to **MV** resulted in conversion of the starting material to predominantly one product (the ^{31}P NMR signal shifted from 32 ppm to -13 ppm). However, other products were also present that increased in concentration over time at expense of the presumed product. A variety of substituted benzyl bromides were then attempted using VT ^{31}P NMR spectroscopy to monitor the reaction in search for a structure and temperature that would give a clean reaction. The general qualitative trend in reactivity shown in Scheme 5 was observed in terms of the degree of consumption of **MV** at a certain temperature. Electron-withdrawing groups seemed to accelerate the reaction, while the benzyl chloride was the slowest reaction partner requiring heating at 50 °C, which resulted in many products. The best reactions were found for the *p*-trifluoromethyl- and the *p*-chlorobenzyl bromides¹⁷, and accordingly these were moved forward for test reactions with **3'**. While the reaction bewtween **3'** and *p*-

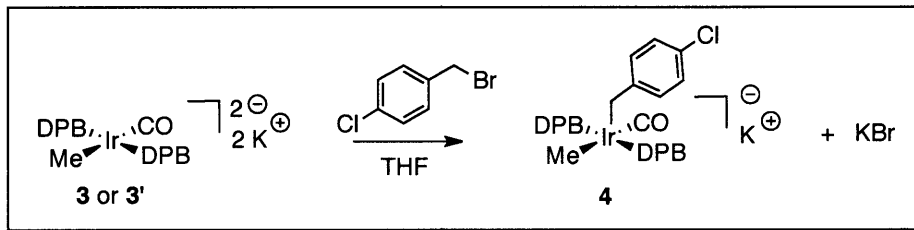
2 Discussion

trifluoromethylbenzyl bromide was too fast to monitor at -80 °C by ^{31}P NMR spectroscopy, the *p*-chlorobenzyl bromide gave a slower reaction that was complete upon warming to -10 °C over a one hour time period. The same reaction with MV was complete at 0 °C only after two days.



Scheme 5

The product observed and isolated from the reaction of **2** with *p*-chlorobenzyl bromide was the pentacoordinate iridium(III) complex K[MeIrCO(η^1 -CH₂-*p*-C₆H₄Cl)(DPB)₂] (**4**). This complex is the result of an initial iridium-carbon bond formation event followed by precipitation of KBr to give **4** (Scheme 6). The molecular structure is shown in Figure 5.



Scheme 6

The structure of **4** is best described as adopting a square-pyramidal geometry and possesses some features that are worthy of note. The first is the short Ir-B1 contact found that occupies the open coordination site *trans* to the benzylic carbon. Comparing this distance to the only published and structurally characterized iridium-borabenzene complex (η^6 -1-fluoro-3,5-dimethyl-1-borabenzene)Ir-(PEt₃)₃](BF₄)₂ with an iridium boron distance of 2.534(8) Å (0.115 Å shorter than **4**) shows a weaker but still significant interaction in **4**.¹⁸ The next closest contact in the boratabenzene ring and iridium is to C30 (Figure 2, Table 4), which is ~0.5 Å longer than in the iridium(II) borabenzene precedent mentioned above but still within the van der Waals radii of the two atoms. The best description of this interaction therefore seems to be a weak unsymmetrical η^2 interaction towards the boron between the B1-C30 π -bond and the vacant coordination spot on the iridium. This interaction results in an small Ir-P1-B1 angle which becomes apparent when compared to the corresponding angle on the other DPB ligand.

2 Discussion

Table 4. Selected Bond Lengths and Angles for **4**.

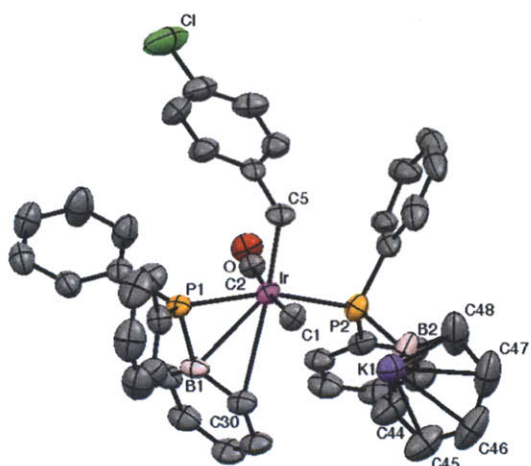
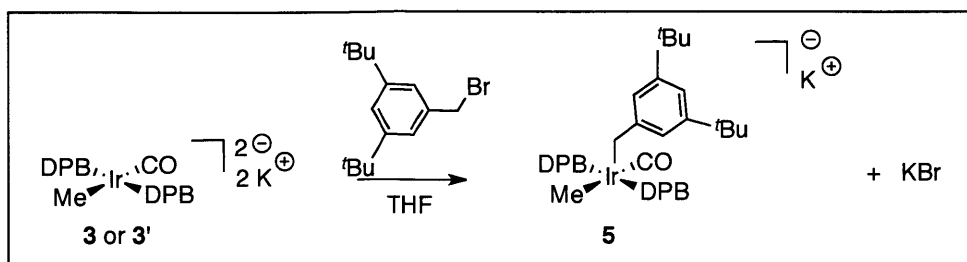


Figure 5. Molecular structure of **4**. Thermal ellipsoids drawn at 50 % probability. Hydrogen atoms have been omitted for clarity.

Although this interaction is termed as significant here, comment should be made on its strength. The static structure shown in Figure 5 is not the one observed in solution at room temperature where there is fast exchange of the potassium cations and coordination to the iridium between the borabenzene rings. This is easily observed in the ^{31}P NMR spectrum of the molecule, which features a singlet for the two phosphorus nuclei that upon cooling splits into two doublets as would be predicted by the structure in Figure 5. An illustrative variable temperature NMR experiment is presented in Figure 6 where 3,5-ditert-butylbenzyl bromide was used as the electrophilic partner in the reaction due to better resolution of the doublets in the product (**5**) (Scheme 7). It is currently unclear why the electron-density of the benzyl bromide has such a strong effect on the chemical shift of the phosphorus nuclei.

Bond	Length (Å)	Angle	Value (°)
Ir-C2	1.918(8)	P1-Ir-P2	162.7(9)
Ir-C1	2.139(5)	P1-Ir-C1	89.6(1)
Ir-P1	2.331(8)	P1-Ir-C2	95.6(8)
Ir-P2	2.379(8)	P2-Ir-C1	86.8(9)
Ir-C5	2.138(3)	P2-Ir-C2	89.0(6)
C2-O	1.115(5)	C1-Ir-C2	173.6(4)
Ir-B1	2.649(6)	C1-Ir-C5	81.8(9)
Ir-C30	2.822(2)	Ir-C2-O	173.8(1)
		Ir-P1-B1	76.5(3)

2 Discussion



Scheme 7

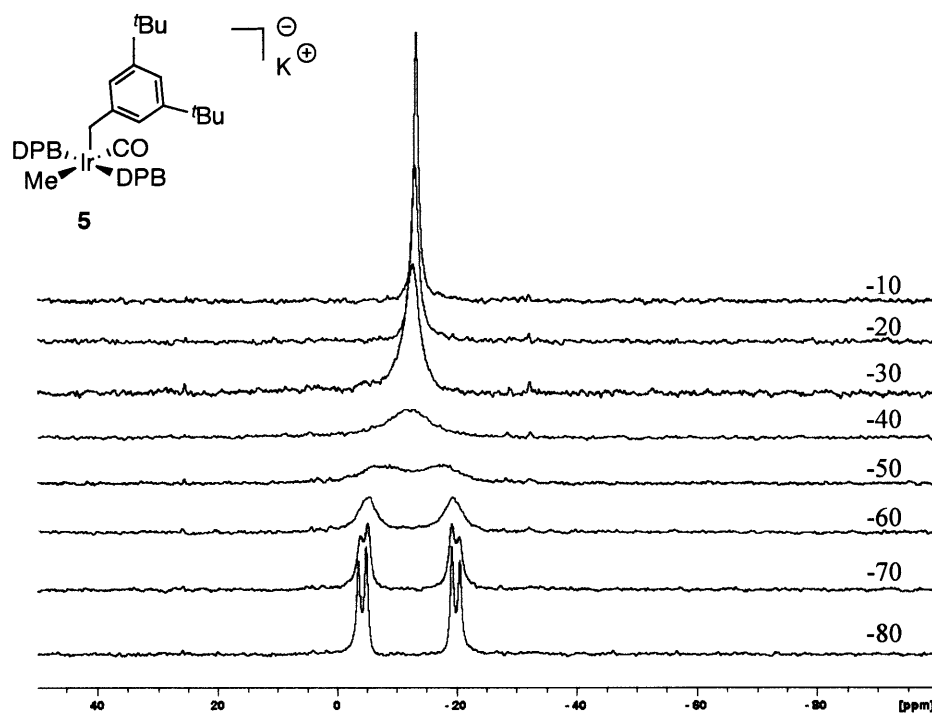


Figure 6. Variable Temperature ^{31}P NMR Spectrum of **5** in THF (temperatures in $^{\circ}\text{C}$).

The other structural parameters of **4** (Figure 5, Table 4) are as expected. The Ir-P bonds are almost unchanged relative to **2b** and lie in the range found for similar compounds. The C2-O bond of the carbonyl is slightly contracted and the Ir-C2 bond slightly lengthened relative to that in **2b** (Table 3 and 4) likely due to decreased back-bonding from the iridium (III) center.

Although the direct product from oxidative addition of the benzyl chloride to **MV** was not stable enough for crystal growth under the conditions attempted, the products from reductive elimination to Vaska's complex and its corresponding oxidative addition product **6** were crystallized at $-6\text{ }^{\circ}\text{C}$. The structure of **6** is displayed in Figure 7 and selected structural parameters in Table 5. Structural characterization of this compound is particularly interesting as to date there

2 Discussion

is no report on the structure of the product from oxidative addition of a benzyl halide to a *trans*- $\text{XIrCO}(\text{PR}_3)_2$ species, though spectroscopic data has been reported.^{19,20}

Table 5. Selected Bond Lengths and Angles for **6**.

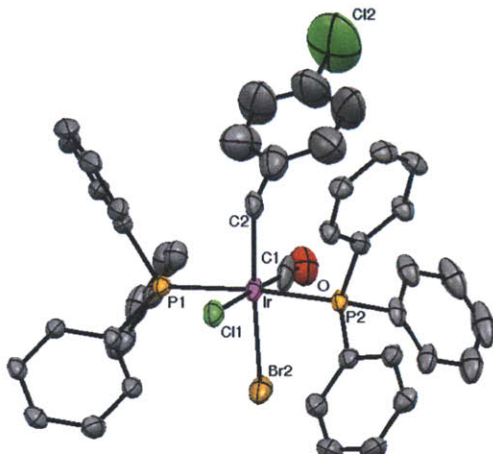


Figure 7. Molecular Structure of **6**. Thermal ellipsoids are drawn at 50 % probability. Hydrogen atoms have been omitted for clarity.

Bond	Length (Å)	Bond	Length (Å)
Ir-C1	1.97(1)	Ir-C11	2.632(2)
Ir-C2	2.110(8)	Ir-Br	2.6424(9)
Ir-P1	2.368(2)	C1-O	1.10(2)
Ir-P2	2.378(1)		

Angle	Value (°)	Angle	Value (°)
P1-Ir-P2	170.94(6)	P2-Ir-C1	94.7(3)
P1-Ir-C1	93.6(3)	P2-Ir-C2	91.1(2)
P1-Ir-C2	92.5(2)	P2-Ir-C11	83.82(6)
P1-Ir-C11	87.78(6)	P2-Ir-Br	90.15(4)
P1-Ir-Br	91.1(2)	C2-Ir-Br	170.2(2)
C1-Ir-C2	90.1(4)	C2-Ir-C11	91.2(2)
C1-Ir-C11	178.0(3)	Br-Ir-C11	98.63(5)
C1-Ir-Br	80.1(3)	Ir-C1-O	178.2(9)

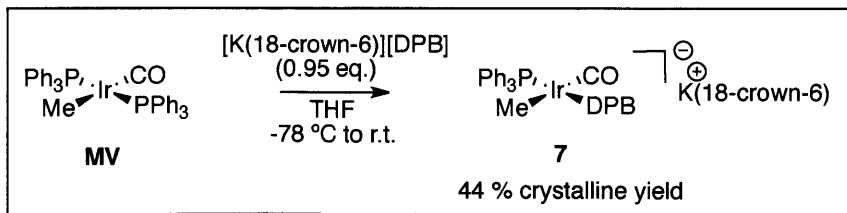
Complex **6** is best described as adopting an octahedral geometry with the benzylic carbon and the bromide *trans* to each other. The Ir-C1 and the Ir-C11 bond are elongated relative to Vaska's complex by 0.232 and 0.325 Å, respectively (Ir-Cl = 2.306(8) Å and Ir-C = 1.74(3) Å in *trans*-ClIrCO(PPh_3)₂).²¹ The elongation in the bond to the carbonyl carbon is as expected due to a reduction in the π -donating ability of the iridium (III) center versus iridium (I), however the reason for the severe elongation of the Ir-Cl bond is not entirely clear. All other structural parameters are within standard values. The large thermal motion of the benzyl bromide group is also of note as is displayed in the large size of the thermal ellipsoids (Figure 7). The unexpected presence of the chloro ligand is attributed to a halogen exchange reaction between an Ir-Br species and LiCl, which remained from the synthesis of **MV**. Since halide ligands are known to be labile in hexa-coordinated iridium species.

2 Discussion

From these experiments, we were thus able to qualitatively show an acceleration in the oxidative addition of *p*-chlorobenzyl bromide to **2** relative to **MV** giving us the first indication of the effects of DPB on metal reactivity.

2.4 Synthesis of and Addition Reactions to [K(18-crown-6)][MeIrCO(DPB)(PPh₃)]

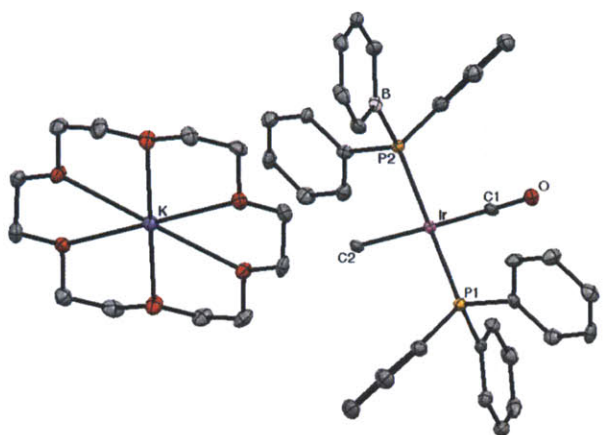
In our initial desire to quantify the effect that DPB would have on the reactivity of metal species, the mixed phosphine species [MeIrCO(DPB)(PPh₃)]⁻ was of high interest in order to allow for a comparison with **MV**. As described in Section 2.3, however, the rapid formation of **3** prevented the direct synthesis of the mono-DPB complex from simply mixing **MV** with one equivalent of KDPB at room temperature. Following the substitution reaction by variable temperature ³¹P NMR spectroscopy did give an indication (the presence of two corresponding doublets) that the desired product was indeed accessible, but only under conditions that would slow down the reactivity of the KDPB ligand. The first approach was simply to change the reaction solvent from THF to one in which KDPB expressed low solubility, which would limit the amount of reacting ligand. Attempts with solvents such as diethyl ether at toluene gave mostly **MV** after prolonged stirring. Low temperature reactions in THF gave a mixture of the mono- and disubstituted species, which proved difficult to separate. One technique that turned out successful, however, was to pre-complex the potassium cation in KDPB with a crown ether and then expose [K(18-crown-6)][DPB] to **MV** at low temperature (Scheme 8). In this reaction sequence the mono-substituted species precipitates from the THF upon warming to give [K(18-crown-6)][MeIrCO(DPB)(PPh₃)] **7** (Scheme 8).



Scheme 8

2 Discussion

Table 6. Selected Bond Lengths and Angles for **7**.



Bond	Length (Å)	Angle	Value (°)
Ir-C1	1.842(9)	P2-Ir-P1	178.2(7)
Ir-C2	2.151(4)	P2-Ir-C1	91.2(5)
Ir-P1	2.280(4)	P2-Ir-C2	88.5(9)
Ir-P2	2.341(4)	P1-Ir-C1	89.2(8)
C1-O	1.176(8)	P1-Ir-C2	90.8(2)
		C2-Ir-C1	177.9(6)
		Ir-C1-O	177.9(1)

Figure 8. Molecular Structure of **7**. Thermal ellipsoids are drawn at a 50% probability level. Hydrogen atoms have been omitted for clarity.

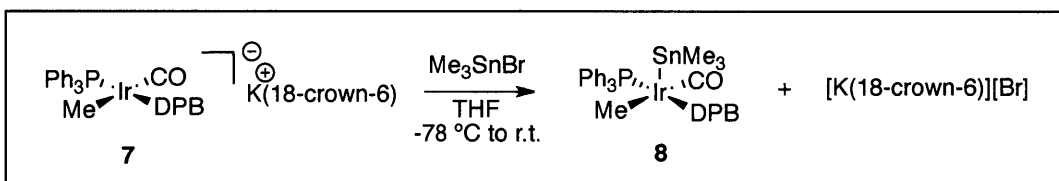
Compound **7** adopts a square-planar geometry (Figure 8) and is structurally very similar to **MV** (Table 6).⁶ The Ir-P distances in **MV** lie right in between the values for **7** (2.300 (1) Å), while the Ir-CO and Ir-Me bond distances are nearly identical (1.835 and 2.17 Å in **MV**). The C-O bond distances cannot be compared due to a disorder between the carbon of the methyl group and carbonyl carbon atom in **MV**, which allows for only an estimate of that value. In addition, the potassium cation has been completely removed from the borabenzene ring by the crown ether, which was desired in order to avoid removal of electron-density from the borabenzene ring through π-complexation to the potassium.

With **7** in hand we set out to perform reactivity studies. Exposure to Me-I in chlorobenzene did lead to formation of two new doublets in the ³¹P NMR spectrum at -30 °C, which suggests that some of the oxidative addition product does indeed form, however other unidentified products were also present. Attempts to lower the reaction temperature were unsuccessful due to the unfavorable solubility properties of **6** in solvents of lower melting points.²² The use of benzyl bromides, which were good reaction partners with **3**, did not result in a well-behaved reaction with **6**, that is formation of side-products before complete consumption of **6** was observed.

2 Discussion

Complex **7** was also found to react with a number of halo-silanes, but once again clean conversion to a single product was not possible through varying the solvent and the reaction temperature.

Moving further down in Group 14 of the periodic table, however, a well-behaved system was obtained. Exposure of **7** to Me₃SnBr in chlorobenzene resulted in complete conversion to essentially one product within 10 minutes at -30 °C (Scheme 9). A portion of the ³¹P NMR spectrum taken at -30 °C is shown in Figure 9, which displays two doublets of equal intensity assigned to the oxidative addition product **8**. It is predicted that the doublet at 4 ppm (Figure 9) is the DPB resonance leaving the other doublet as the PPh₃ resonance based on the assignments for **7**. Upon oxidation, the PPh₃ signal shifts upfield by 20 ppm, while the DPB signal shifts downfield by 7 ppm. This is a little surprising because with all other electrophiles both signals shift to more negative ppm values. If the structure of **8** is similar to that of **5**, as it is expected to be, then it could be that the interaction between the boratabenzene ring and the iridium center is affecting the electron density around the DPB phosphorus nuclei



Scheme 9

2 Discussion

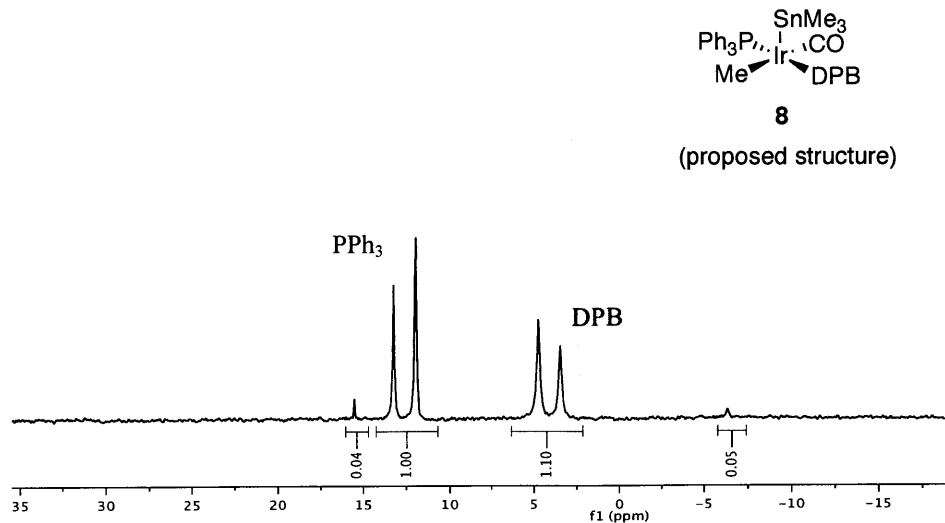


Figure 9. ³¹P NMR Spectrum of **8** at -30 °C in chlorobenzene.

The corresponding reaction with **MV** was also carried out. Addition of Me₃SnBr to **MV** in chlorobenzene did not result in any observable product by ³¹P NMR spectroscopy at room temperature. Upon heating to 90 °C, however, a new signal appeared at 24 ppm, which corresponds to *trans*-BrIrCO(PPh₃)₂ **9**. Complex **9** is formed from the initial oxidative addition of Me₃SnBr followed by reductive elimination of Me₄Sn. Further heating of the reaction mixture at 90 °C results in complete conversion after 25 hrs. Thus, the presence of DPB in place of PPh₃ in the coordination sphere of iridium greatly enhances the oxidative addition of Me₃SnBr.

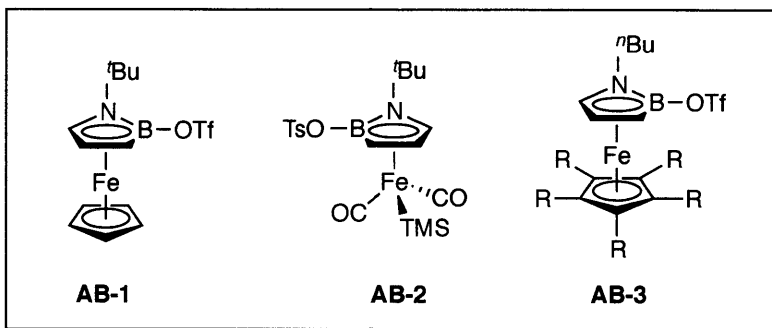
In hopes of finding a slower reaction that would allow for kinetic studies, the methyl groups were exchanged for more sterically demanding substituents. Employing Cy₃SnBr did result in a much slower reaction rate for the oxidative addition, however other products were also observed in the ³¹P NMR spectrum either from further reactivity of the oxidative addition product that was fast on the time-scale of the reaction of interest or from a background reaction. Tributyltin bromide was then used as an electrophile that fit sterically between trimethyl- and tricyclohexyltin bromide, but this reaction was also quite fast at -30 °C allowing only the observation of the oxidative addition product by ³¹P NMR spectroscopy.

Thus, DPB has been demonstrated to enhance the rate of oxidative addition of substituted benzyl bromides and trimethyltin bromide, and this effect is expected to be general. Furthermore, the reactivity of DPB is better understood now in terms of the types of ligands it can displace, how to tame its reactivity, and these studies have ultimately resulted in four new structurally characterized iridium-DPB complexes.

3 Synthetic Attempts Towards an Iron Cyclopentadienyl Azaborolyl Complex and Mechanistic Studies into Nickel-Catalyzed Carbon-Carbon Bond-Forming Reactions

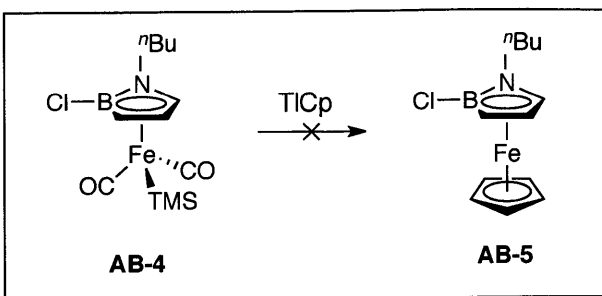
3.1 Iron Azaborolyl Chemistry

The iron azaborolyl (AB) complexes **AB-1** and **AB-2** depicted below in Scheme 10 have been reported by our group to be stoichiometric lewis acids in the stereoselective addition of Grignard reagents to imines and silyl enol ethers to aldehydes, respectively.²³



Scheme 10

These two reagents did not serve as catalyst due to the strong B-O and N-O bonds that result after addition of the nucleophile that are not cleaved by addition and substitution of a free aldehyde or imine. In the case of the aldol reaction, there was additional lack of transfer of the silyl moiety from the silyl enol ether to the oxygen of the aldehyde after nucleophilic attack as occurs in a standard Mukaiyama aldol reaction. In attempts to produce a catalytic Mukaiyama-type reaction, the goal of this project was to modify **AB-2** as displayed in Scheme 10 (complex **AB-3**). In **AB-3** the sterically encumbering 'Bu substituent on the nitrogen of the AB ring is replaced with an "Bu group in order to open up the nitrogen for service as a silicon shuttle from the enol ether to the aldehyde after addition. The carbonyl and silyl ligands are replaced with an electron-donating cyclopentadienyl ligand ($R = H$ or alkyl) that would result in a more electron-rich iron strengthening the Ir-B bond while weakening the B-O bond. Unfortunately, attempts to transmetallate a precursor to **AB-3** with TiCp (Cp^*) were unsuccessful (Scheme 11) and often lead to ferrocene as the predominant product instead of **AB-5**.



Scheme 11

3.2 Isolation Attempts of a Nickel(I) Alkyl or Halo Species

Both nickel(I) methyl and iodo species bearing the terpyridine ligand have been isolated and structurally characterized.²⁴ These two species are postulated intermediates in the nickel-catalyzed cross-coupling reaction and are, thus, of high interest, as work in our group has focused on this type of transformation. In order to understand the mechanism behind some of our nickel catalyzed cross-coupling reactions we set out to isolate and characterize nickel methyl and halo species with a pyridine bisoxolidinone (pybox) as the supporting ligand.²⁵

Unfortunately, even after trying similar techniques that were used for the terpyridine complex for synthesis and various substitution patterns on the pybox ligand in order to aid in crystallization no nickel(I) complex was crystallized.

4 Experimental

All experiments unless otherwise noted were carried out using standard dry box or Schlenk techniques under an inert atmosphere of argon or nitrogen. THF and toluene were passed through a column of packed alumina and degassed prior to use. Diethylether was passed through a column of packed alumina before use. All other solvents were purchased anhydrous in a sure-seal bottle from Aldrich and used as received. THF-*d*₈ and benzene-*d*₆ were distilled from Na/benzophenone, degassed, and stored over 4 Å molecular sieves in the glovebox. All other NMR solvents were degassed and stored over 4 Å molecular sieves for at least two days before use and kept in the glovebox. *p*-Chlorobenzyl bromide and 3,5-ditert-butylbenzyl bromide were purchased from Aldrich, recrystallized prior use, and stored in the glovebox. In addition, methyl iodide was passed through a short plug of neutral alumina after distillation and prior to use. Me₃SnBr and ⁿBu₃SnBr were purchased from Strem and Aldrich, respectively, and sublimed prior to use. *trans*-MeIrCO(PPh₃)₂ was synthesized according to a published procedure.⁵

The NMR spectra were recorded either on a Varian Mercury 300 MHz instrument, a Varian Unity 500 MHz instrument, or a Bruker DRX 400 MHz spectrometer. ¹H and ¹³C NMR spectra are referenced to the internal residual solvent peak, ³¹P NMR spectra are referenced externally to 85% H₃PO₄ at 0 ppm, and ¹¹B NMR spectra are referenced externally to BF₃·OEt₂ at 0 ppm. IR spectra were recorded on a Perkin-Elmer Series 1600 FT-IR spectrophotometer and obtained as indicated.

The following abbreviations are used throughout this section.

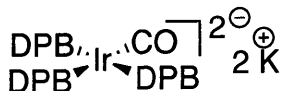
DPB = diphenylphosphidoboratabenzene

VT = Variable Temperature

MV = *trans*-MeIrCO(PPh₃)₂

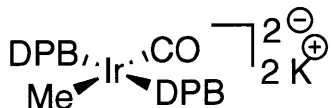
4 Experimental

Synthesis of $[K_2][IrCO(DPB)_3]$ (1)



In the glovebox, 100 mg (0.13 mmol, 1.0 eq.) of *trans*-ClIrCO(PPh₃)₂ along with 115 mg (0.39 mmol, 3.0 eq.) of KDPB are added to a 20 mL screw-cap vial with a 0.5-inch stir bar and diluted with 5.0 mL of THF. The intense red mixture was stirred for 15 min followed by removal of the THF *in vacuo*. The residue is triturated with toluene (2 x 3 mL) and then washed with benzene (100 mL) and Et₂O (100 mL) on a fritted glass filter. The orange-red solid collected resulted in 70 mg of **1**. X-ray quality crystals were grown by diffusion of Et₂O into a solution of **1** in THF. All bulk recrystallizations have been unsuccessful. ¹H NMR (THF-*d*₈, 298 K): δ 7.77 (m), 7.02 (m), 6.31 (m). ¹³C NMR (THF-*d*₈, 298 K): δ 186.5 (m, CO), 142.9 (broad, Ar), 137.6 (broad, Ar), 134.8 (broad, Ar), 133.5 (Ar), 128.7 (Ar), 128.5 (Ar), 117.1 (m, Ar), 115.42 (broad, Ar). ³¹P NMR (THF-*d*₈, 298 K): δ -6 (broad, 1P), -17 (broad, 2P). ¹¹B NMR (THF-*d*₈, 298 K): δ 31.5 (broad). IR (KBr): ν(C-O) 1937 cm⁻¹ (s).

Synthesis of $[K_2][MeIrCO(DPB)_2]$ (3)

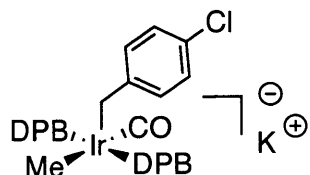


In the glovebox, to a 20 mL screw-cap vial were added 100.0 mg (0.13 mmol, 2 eq.) of **MV** and 78.0 mg (0.26, 2 eq.) of KPDB. A 0.5-inch stir bar was then introduced followed by 5.0 mL of THF. The red-orange reaction mixture was stirred for 10 min, after which complete consumption of **MV** was confirmed by ³¹P NMR spectroscopy. The THF was removed *in vacuo*, and the residue triturated with toluene (1 x 2 mL), then dried *in vacuo*. The residue was then thoroughly washed with benzene (100 mL) and diethyl ether (100 mL) on a fritted glass filter and the resultant yellow solid collected and dried *in vacuo* to give 88.2 mg of **3** (88% crude yield based on **MV**). X-ray quality crystals of $[KLi][MeIrCO(DPB)_2]$ (**3'**) were grown by layering a DME solution with hexanes at room temperature. ¹H NMR (500 MHz, THF-*d*₈): δ 7.98 (broad, 9H), 7.14 (t, 12H), 7.07 (broad t, 4H), 6.50 (broad d, 4H), 6.11 (broad t, 2H), -0.35 (t, ³J_{H-P} = 9 Hz, 3H). ¹³C{H} NMR (THF-*d*₈): δ 189.8 (t, ²J_{C-P} = 8 Hz), 142.3 (t, Ar), 136.8 (t, Ar), 132.9 (t,

4 Experimental

Ar), 131.3 (broad, Ar), 127.7 (broad s, Ar), 127.5 (broad t, Ar), 8.5 ($t, ^2J_{C-P} = 7$ Hz, CH₃). ³¹P{H} NMR (THF-*d*₈): δ 2 (s). ¹¹B NMR (THF-*d*₈): δ 31.5 (broad). IR (THF): ν (C-O) 1889 cm⁻¹ (m).

VT NMR Monitoring of the oxidative addition of *p*-chlorobenzyl bromide to **3**: Formation of [K][MeIrCO(η^1 -CH₂C₆H₄Cl)(DPB)₂] (**4**)



In the glovebox, 10.9 mg (0.013 mmol, 1.0 eq) of **3** and 2.8 mg *p*-chlorobenzyl bromide (0.014 mmol, 1.1 eq.) were massed into two separate 4 mL vials and dissolved in THF (0.4 mL for **2**, and 0.2 mL for *p*-chlorobenzyl bromide). The solution of **3** was transferred to a J. Young NMR tube and both solutions cooled to their freezing points in the cold well. The solution of *p*-chlorobenzyl was allowed to melt, quickly transferred to the J-Young tube, and the entire reaction mixture placed back in the cold well. Upon freezing of the reaction mixture, the J-Young tube was removed from the cold well, was quickly inverted three times, and allowed to freeze once again in the cold well. The J. Young Tube was then removed from the glovebox to a Dewar containing liquid nitrogen. The sample was introduced to the spectrometer with a probe pre-cooled to -90 °C. After 10 min, the probe was tuned to the sample and spectra (124 scans) were measured every 10 degrees after 10 min at each temperature from -90 °C to room temperature ³¹P{H} NMR (THF-*d*₈, 263 K): δ -22 (s).

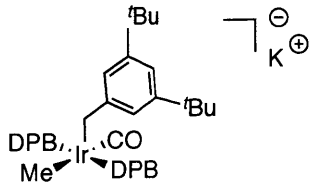
Synthesis of [K][MeIrCO(η^1 -CH₂-*p*-C₆H₄Cl)(DPB)₂] (on larger scale for characterization) (**4**)

In the glovebox, *p*-chlorobenzyl bromide (26 mg, 0.13 mmol) in 2.0 mL of THF was added dropwise to **3** (100 mg, 0.12 mmol) in 5.0 mL of THF at -78 °C in the cold well of the glovebox while stirring. After the addition was complete, the originally yellow solution turned red and was further allowed to stir at room temperature for 25 minutes, whereupon a precipitate formed.

4 Experimental

The endpoint of the reaction was determined by ^{31}P NMR Spectroscopy, and the reaction mixture filtered through an acrodisc with 5.0 mL of THF washings. X-ray quality crystals were grown by transferring 2.0 mL of this solution to a vapor diffusion setup with pentane and placing it in the glovebox freezer. Needle-like crystals grew after two weeks. ^1H NMR (400 MHz, THF- d_8): δ 7.38 (m, 4H), 7.16 (m, 13), 7.11 (t, 5H), 7.02 (m, 4H), 6.79 (m, 6H), 6.72 (m, 4H), 3.23 (t, $^3J_{\text{H-P}} = 4$ Hz, 2H, CH_2), 0.50 (t, $^3J_{\text{H-P}} = 8$ Hz). $^{13}\text{C}\{\text{H}\}$ NMR (THF- d_8 , 298 K): δ 178.8 (broad, CO), 154.2, 136.1 (d t, Ar), 135.2 (broad, Ar), 133.8 (broad, Ar), 131.4 (Ar), 130.2 (broad, Ar), 130.6 (Ar), 128.5 (Ar), 128.23 (Ar), 128.9 (Ar), 128.5 (Ar), 128.0 (Ar), 127.7 (t, Ar), 118.8, 11.2 (CH_2), 1.6 (t, $^2J_{\text{C-P}} = 7$ Hz). $^{31}\text{P}\{\text{H}\}$ NMR (THF- d_8 , 298 K): δ -22 (s). ^{11}B NMR (THF- d_8 , 298 K): δ 17.8 (broad s). IR (KBr): $\nu(\text{C-O})$ 2000 cm^{-1} (s).

Addition of 3,5-di-*tert*-butylbenzylbromide to 2: Formation of $[\text{K}][\text{MeIrCO}(\eta^1\text{-CH}_2\text{Ar})(\text{DPB})_2]$ (5)



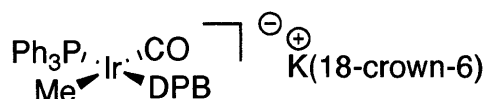
In the glovebox, **3** (10.0 mg, 0.012 mmol) and 3,5-di-*tert*-butylbenzylbromide (3.4 mg, 0.012 mmol) were added to two separate 4 mL vials and dissolved in THF (0.4 mL for **3** and 0.2 mL for 3,5-di-*tert*-butylbenzylbromide). The solution of **3** was then transferred to a J. Young NMR tube and both solutions cooled to their freezing points in the cold well. Upon freezing, the solution of 3,5-di-*tert*-butylbenzylbromide was allowed to melt and then quickly transferred to the NMR tube. Upon complete melting of the reaction mixture the tube was inverted three times and allowed to warm to room temperature, whereupon **3** was completely consumed. The reaction mixture was then analyzed by VT ^{31}P NMR spectroscopy every 10 degrees from -10 °C to -80 °C. $^{31}\text{P}\{\text{H}\}$ NMR (THF- d_8 , 298 K): δ -22 (s).

4 Experimental

Monitoring of the oxidative addition of *p*-chlorobenzyl bromide to MV: Formation of ClIrCOBr(η^1 -CH₂-*p*-C₆H₄Cl)(PPh₃)₂

In the glovebox, **MV** (10 mg, 0.013 mmol) and *p*-chlorobenzyl bromide (2.8 mg, 0.014 mmol) were massed out into two separate 4 mL vials and dissolved in THF (0.4 mL for **MV** and 0.2 mL for *p*-chlorobenzyl bromide). The solution of **MV** was transferred to a J. Young NMR Tube and cooled in the cold well of the glovebox at -78 °C for 10 min. The solution *p*-chlorobenzyl bromide was then transferred to the J. Young Tube and in the cold well. After a quick inversion the tube was removed from the glove box and kept in a bath at 0 °C. ³¹P NMR spectra were taken over the course of two days by removing from the cold bath to room temperature and returning as quickly as possible. ³¹P{H} NMR (THF, 298 K): δ -13 (s), -16 (s).

Synthesis of [K(18-crown-6)THF₂][MeIrCO(DPB)(PPh₃)] (7)

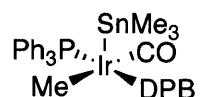


In the glovebox, a pre-stirred solution (10 minutes, r.t.) of KDB (36 mg, 0.12 mmol) and 18-crown-6 (63 mg, 0.24 mmol) in THF (3.0 mL) was added drop-wise via syringe to a solution of **MV** (100 mg, 0.13 mmol) in THF (5.0 mL) at -78 °C in the cold well. After stirring further for another 10 minutes at -78 °C, the homogenous yellow solution was allowed to warm to r.t. and stirred for 0.5 hrs., which resulted in the formation of a yellow precipitate. The THF was then removed *in vacuo* and the yellow residue triturated with toluene (1 x 2 mL). Washing the residue with Et₂O (100 mL) on a glass fritted funnel afforded a yellow solid that was recrystallized from THF/Et₂O to give 64 mg of yellow crystalline material after drying (44% yield based on KDPB). X-ray quality crystals were obtained by vapor diffusion of Et₂O into a saturated solution of **6** in THF. ¹H NMR (CD₃CN, 298 K): δ 7.83 (t, 4H), 7.65 (m, 6H), 7.38 (broad, 9H), 7.24 (m, 8H), 6.69 (d d, 2), 6.32 (t, 1H), 3.55 (s, 26H), -0.27 (t, *J*_{H-P} = 9 Hz). ¹³C{H} NMR (CD₃CN, 298 K): δ 189.2 (t, *J*_{C-P} = 8 Hz, CO), 142.1 (d, Ar), 136.9 (Ar), 136.3 (d, Ar), 135.3 (d, Ar), 132.5 (d, Ar), 130.4 (Ar), 128.7 (d, Ar) 128.2 (Ar), 127.8 (d, Ar), 118.34, 115.09, 70.9 (crown ether), 9.0 (dd, *J*_{C-P1} = 8, *J*_{C-P2} = 10, CH₃). ³¹P{H} NMR (CD₃CN, 298 K): δ 33 (d, *J*_{P-P} = 298 Hz, PPh₃), 1.8 (m, DPB). ³¹P{H} NMR (Cl-C₆H₅, 298 K): δ 32.6 (d, *J*_{P-P} = 300 Hz, PPh₃), -2.8 (d, *J*_{P-P} = 300

4 Experimental

Hz, DPB). ^{11}B NMR (CD_3CN , 298 K): δ 59.3 (d, $J_{\text{B-P}} = 86$ Hz). IR (KBr): $\nu(\text{C-O})$ 1917 cm^{-1} (s).

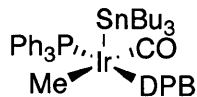
Addition of Me_3SnBr to 7 with VT ^{31}P NMR Spectroscopy Monitoring: Formation of $\text{MeIrCO}(\text{SnMe}_3)(\text{DPB})\text{PPh}_3$ (8)



(proposed structure)

In the glovebox, **7** (12 mg, 0.01 mmol) and Me_3SnBr (2.7 mg, 0.01 mmol) were added to two separate 4 mL vials and then both dissolved in chlorobenzene (0.4 mL for **7** and 0.2 mL for Me_3SnBr). The yellow solution of **7** was transferred to a J. Young Tube along with a sealed capillary tube containing a solution of $(o\text{-tol})_2\text{PH}$ (0.09 M, toluene), and the mixture cooled to its freezing point in the cold well. The solution of Me_3SnBr was then transferred to the J. Young NMR Tube where it also froze. Inverting the J. Young Tube in the cold well allowed the mixture to flow the opposite end of the NMR tube to wash down the sides. After inverting the NMR tube once again and allowing the mixture to flow to the bottom and freeze, the NMR tube was removed from the glovebox and placed in a dewar with liquid nitrogen. The sample was introduced to the spectrometer with a probe pre-cooled to -30 °C and the solvent as a partial solid-partial liquid mixture. After 10 minutes the probe was tuned and a ^{31}P NMR spectrum was measured. $^{31}\text{P}\{\text{H}\}$ NMR ($\text{Cl-C}_6\text{H}_5$, 258 K): 14.4 (d, $^2J_{\text{P-P}} = 259$ Hz, PPh_3), 4.1 (d, $^2J_{\text{P-P}} = 259$ Hz, DPB).

Addition of Bu_3SnBr to 7 with VT ^{31}P NMR Spectroscopy Monitoring: Formation of $\text{MeIrCO}(\text{SnBu}_3)(\text{DPB})(\text{PPh}_3)$ (9)



(proposed structure)

Same procedure as for **8**. $^{31}\text{P}\{\text{H}\}$ NMR ($\text{Cl-C}_6\text{H}_5$, 258 K): 13.2 (d, $^2J_{\text{P-P}} = 263$ Hz, PPh_3), 6.3 (d, $^2J_{\text{P-P}} = 263$ Hz, DPB).

4 Experimental

Computations

All computations were carried out using the Q-Chem 4 computational package.²⁷ The DFT calculations employed the B3LYP functional⁹ and 6-31G* basis set¹⁰ for all atoms except iridium for which the LANL2DZ basis set¹¹ with an electron core potential was used. All ground-state structures found had zero imaginary frequencies.

References

- ¹ Hoic, D. A.; Davis, W. M.; Fu, G. C. *J. Am. Chem. Soc.* **1996**, *118*, 8176-8177.
- ² For a recent review on anionic phosphines in catalysis see Snelders, D. J. M.; van Koten, G.; Klein Gebbink, R. J. M. *Chem. Eur. J.* **2011**, *17*, 42-57.
- ³ It is worth to note that DPB binds a metal through the phosphorus and not the boratabenzene ring in the complexes reported in 1 and 2. For a published example of a boratabenzene bound DPB complex see
- ⁴ For mechanistic details on the oxidative addition reaction to *trans*-ClIrCO(PPh₃)₂ see (a) Chock, P. B.; Halpern, J. *J. Am. Chem. Soc.* **1966**, *88*, 3511-3514. (b) Collman, J. P.; Sears, C. T. *Inorg. Chem.* **1967**, *7*, 27-32. (c) Ugo, R.; Pasini, A.; Cenini, S. *J. Am. Chem. Soc.* **1972**, *94*, 7364-7370. (d) Garrou, P. E.; Hartwell, G. E. *Inorg. Chem.* **1976**, *15*, 646-650. (e) van Doorn, J. A.; Masters, C.; van der Woude, C. *J.C.S. Dalton* **1978**, 1213-1220. (f) Mureinik, R. J.; Weitzberg, M.; Blum, J. *Inorg. Chem.* **1979**, *18*, 915-918. (g) Hall, T. L.; Lappert, M. F.; Lednor, P. W. *J.C.S. Dalton* **1980**, 1448-1456. (h) Labinger, J. A.; Osborn, J. A. *Inorg. Chem.* **1980**, *19*, 3230-3236. (h) Labinger, J. A.; Osborn, J. A.; Coville, N. J. *Inorg. Chem.* **1980**, *19*, 3236-3243.
- ⁵ Vaska, L.; DiLuzio, J. W. *J. Am. Chem. Soc.* **1961**, *83*, 2784-2785.
- ⁶ Rees, W. M.; Churchill, R.; Li, Y.-J.; Atwood, J. D. *Organometallics*, **1984**, *4*, 1162-1167.
- ⁷ (a) Hostetler, M. J.; Bergman, R. G. *J. Am. Chem. Soc.* **1992**, *114*, 787-788. (b) Hostetler, M. J.; Bergman, R. G. *J. Am. Chem. Soc.* **1992**, *114*, 7629-7636.
- ⁸ All data was collected at the M.I.T X-ray Diffraction Facility. All structures were solved by John Anderson from the Peters Group at the California Institute of Technology.
- ⁹ Xie, Z.; Jelínek, T.; Bau, R.; Reed, C. A. *J. Am. Chem. Soc.* **1994**, *116*, 1907-1913.
- ¹⁰ Shao, Y. *et. al. Phys. Chem. Chem. Phys.* **2006**, *8*, 3172
- ¹¹ (a) Becke, A. D. *J. Chem. Phys.* **1992**, *96*, 2155-2160. (b) Becke, A. D. *J. Chem. Phys.* **1993**, *98*, 5648-5652. (c) Becke, A. D. *J. Chem. Phys.* **1993**, *98*, 1372-1377. (d) Lee, C.; Yang, W.; Parr, R. G. *Phys. Rev. B; Condens. Matter* **1988**, *37*, 785-789. (e) Stephens, P. J.; Devlin, F. J.; Chabalowski, C. F.; Frisch, M. J. *J. Phys. Chem.* **1994**, *98*, 11623-11627.
- ¹² Krishnan, K.; Binkley, J. S.; Seeger, R.; Pople, J. A. *J. Chem. Phys.* **1980**, *72*, 650-654.

References

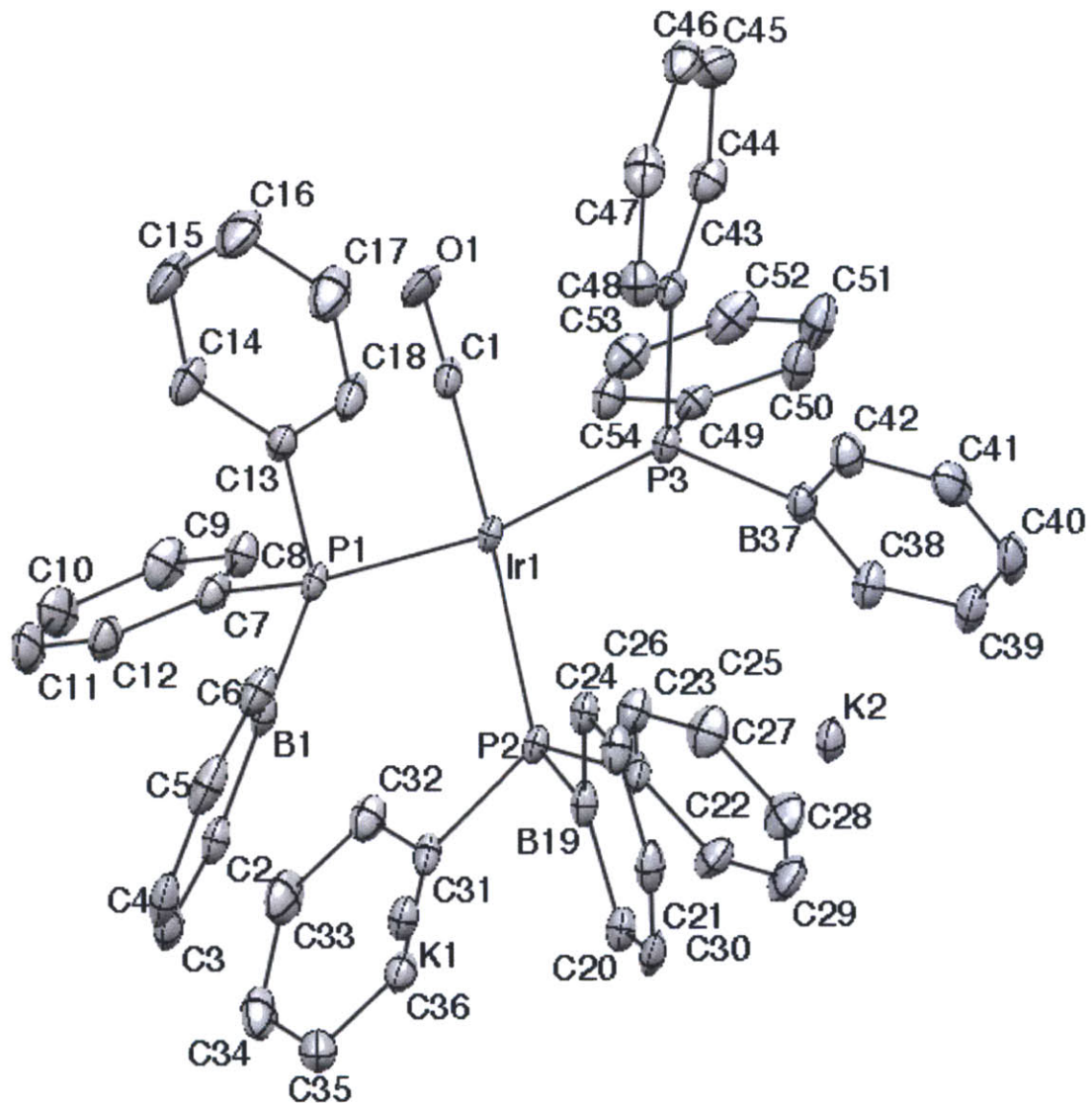
- ¹³ Cooling **1** in an NMR spectrometer to -80 °C did not reveal a doublet and triplet for the DPB resonances in the ³¹P NMR Spectrum, but rather a complex pattern that could not be deciphered.
- ¹⁴ In preliminary reactions, exposure of **1** to H₂ results in a bleaching of the red solution to give a colorless solution with four different phosphine signals in the ³¹P NMR spectrum.
- ¹⁵ It is believed that stray LiCl from the synthesis of **MV** is the source of the lithium cation in **3'**. The structure of **3** has not yet been obtained but will be used throughout this section.
- ¹⁶ (a) *trans*-MeIrCO(PPh₃)₂ see ref. 4. (b) *trans*-MeIrCO(P(*p*-tol)₃)₂ see Jankik, T. S.; Churchill, M. R.; See, R. F.; Randall, S. L.; McFarland, J. M.; Atwood, J. D. *Acta Cryst.* **1992**, C48, 1493-1495. (c) *trans*-MeIrCO(P(Me₂C₄H₆)Ph) see Shin, J. H.; Bridgewater, B. M.; Churchill, D. G.; Parkin, G. *Inorg. Chem.* **2001**, 40, 5626-5635. (d) all ν_{CO} from Lawson, H. J.; Atwood, J. D.; *J. Am. Chem. Soc.* **1989**, 111, 6223-6227.
- ¹⁷ Although these benzyl bromides gave the cleanest reaction a second shift at -16 ppm in the ³¹P NMR spectrum was always present in a ratio of 0.13 to 1.00 relative to the -13 ppm shift.
- ¹⁸ Bleake, J. R.; Behm, R.; Xie, Y.-F.; Chiang, M. Y.; Robinson, K. D.; Beatty, A. M. *Organometallics* **1997**, 16, 606-623.
- ¹⁹ Labinger, J. A.; Osborn, J. A.; Coville, N. J. *Inorg. Chem.* **1980**, 19, 3236-3243.
- ²⁰ The structurally similar complex IrCl₂(η¹-CH₂Ar)(CO)(PPh₃)₂ [Ar = Ph and *p*-tol] has been characterized but it was not the product of an oxidative addition reaction. Albertin, G.; Antoniutti, S.; Bacchi, A.; Pelizzi, G.; Piasente, F. *Dalton Trans.* **2003**, 32, 2881-2888.
- ²¹ Blake, A. J.; Ebsworth, E. A. V.; Murdoch, H. M.; Yellowless, L. J. *Acta Cryst.* **1991**, C47, 657-659.
- ²² **6** is soluble in methylene chloride, but also reacts with the solvent.
- ²³ (a) Liu, S.-Y.; Hills, I. D.; Fu, G. C. *J. Am. Chem. Soc.* **2005**, 127, 15352-15353. (b) Liu, S.-Y.; Lo, M. M.-C.; Fu, G. C. *Tetrahedron (Sympos.)* **2006**, 62, 11343-11349.
- ²⁴ (a) Anderson, T. J.; Jones, G. D.; Vicic D. A. *J. Am. Chem. Soc.* **2004**, 126, 8100-8101. (b) Jones, G. D.; Martin, J. L.; McFarland, C.; Allen, O. R. Hall; R. E.; Haley, A. D.; Brandon, R. J.; Konovalova, T.; Desrochers, P. E.; Pulay P.; Vici D. A. *J. Am. Chem. Soc.* **2006**, 128, 13175-13183.

References

- ²⁵ For examples of a cross-coupling reaction using pybox ligands see (a) Fischer, C.; Fu, G. C. *J. Am. Chem. Soc.* **2005**, *127*, 4594-4595. (b) Son, S.; Fu, G. C. *J. Am. Chem. Soc.* **2008**, *130*, 2756-2757.
- ²⁶ Shao, Y.; Fusti-Molnar, L.; Jung, Y.; Kussmann, J.; Ochsenfeld, C.; Brown, S. T.; Gilbert, A. T. B.; Slipchenko, L. V.; Levchenko, S. V.; O'Neill, D. P.; DiStasio Jr., R. A.; Lochan, R. C.; Wang, T.; Beran, G. J. O.; Besley, N. A.; Herbert, J. M.; Lin, C. Y.; Van Voorhis, T.; Chien, S. H.; Sodt, A.; Steele, R. P.; Rassolov, V. A.; Maslen, P. E.; Korambath, P. P.; Adamson, R. D.; Austin, B.; Baker, J.; Byrd, E. F. C.; Daschel, H.; Doerksen, R. J.; Dreuw, A.; Dunietz, B. D.; Dutoi, A. D.; Furlani, T. R.; Gwaltney, S. R.; Heyden, A.; Hirata, S.; Hsu, C.-P.; Kedziora, G.; Khaliullin, R. Z.; Klunzinger, P.; Lee, A. M.; Lee, M. S.; Liang, W.; Lotan, I.; Nair, N.; Peters, B.; Proynov, E. I.; Pieniazek, P. A.; Rhee, Y. M.; Ritchie, J.; Rosta, E.; Sherrill, C. D.; Simmonett, A. C.; Subotnik, J. E.; Woodcock III, H. L.; Zhang, W.; Bell, A. T.; Chakraborty, A. K.; Chipman, D. M.; Keil, F. J.; Warshel, A.; Hehre, W. J.; Schaefer III, H. F.; Kong, J.; Krylov, A. I.; Gill, P. M. W.; Head-Gordon M. *Phys. Chem. Chem. Phys.*, **2006**, *8*, 3172-3191.

Appendix A: Crystal Structure Data

Crystal data and structure refinement for 1



Appendix A

Table 1. Crystal data and structure refinement for **1**

Identification code	d8_10072_0m	
Empirical formula	C52 H45 B3 Ir K2 O P3	
Formula weight	1081.62	
Temperature	100(2) K	
Wavelength	1.54178 Å	
Crystal system		
Space group	P 2 _{1/n}	
Unit cell dimensions	a = 10.7052(6) Å b = 24.1467(11) Å c = 26.6144(13) Å	a= 90°. b= 90°. g = 90°.
Volume	6879.7(6) Å ³	
Z	6	
Density (calculated)	1.566 Mg/m ³	
Absorption coefficient	8.545 mm ⁻¹	
F(000)	3240	
Crystal size	0.20 x 0.10 x 0.05 mm ³	
Theta range for data collection	2.47 to 88.35°.	
Index ranges	-12<=h<=13, -31<=k<=31, -29<=l<=29	
Reflections collected	116833	
Independent reflections	12828 [R(int) = 0.0599]	
Completeness to theta = 88.35°	81.6 %	
Max. and min. transmission	0.6746 and 0.2798	
Refinement method	Full-matrix least-squares on F ²	
Data / restraints / parameters	12828 / 1735 / 850	
Goodness-of-fit on F ²	1.029	
Final R indices [I>2sigma(I)]	R1 = 0.0324, wR2 = 0.0767	
R indices (all data)	R1 = 0.0416, wR2 = 0.0823	
Largest diff. peak and hole	1.088 and -1.011 e.Å ⁻³	

Appendix A

Table 2. Bond lengths [\AA] and angles [$^\circ$] for D8_10072_0m.

Ir(1)-C(1)	1.929(3)	B(37)-C(42)	1.467(5)
Ir(1)-P(1)	2.3375(8)	B(37)-C(38)	1.470(5)
Ir(1)-P(3)	2.3605(8)	B(37)-K(2)	3.460(4)
Ir(1)-P(2)	2.4895(8)	C(38)-C(39)	1.271(4)
C(1)-O(1)	1.178(4)	C(38)-K(2)	3.444(4)
P(1)-C(7)	1.727(3)	C(39)-C(40)	1.376(5)
P(1)-C(13)	1.889(3)	C(39)-K(2)	3.337(4)
P(1)-B(1)	2.139(4)	C(40)-C(41)	1.365(6)
B(1)-C(6)	1.505(5)	C(40)-K(2)	3.249(4)
B(1)-C(2)	1.598(5)	C(41)-C(42)	1.276(5)
B(1)-K(1)	3.237(4)	C(41)-K(2)	3.320(4)
C(2)-C(3)	1.512(5)	C(42)-K(2)	3.412(4)
C(2)-K(1)	3.016(3)	C(43)-C(48)	1.409(5)
C(3)-C(4)	1.388(5)	C(43)-C(44)	1.520(5)
C(3)-K(1)	2.850(3)	C(44)-C(45)	1.461(5)
C(4)-C(5)	1.483(6)	C(45)-C(46)	1.387(6)
C(4)-K(1)	2.803(3)	C(46)-C(47)	1.526(6)
C(5)-C(6)	1.519(6)	C(47)-C(48)	1.453(5)
C(5)-K(1)	2.873(3)	C(49)-C(54)	1.294(4)
C(6)-K(1)	3.132(3)	C(49)-C(50)	1.386(5)
C(7)-C(12)	1.387(5)	C(50)-C(51)	1.433(5)
C(7)-C(8)	1.439(5)	C(51)-C(52)	1.282(5)
C(8)-C(9)	1.303(5)	C(52)-C(53)	1.379(6)
C(9)-C(10)	1.386(6)	C(53)-C(54)	1.420(5)
C(10)-C(11)	1.428(6)	K(1)-O(3)	2.708(3)
C(11)-C(12)	1.304(5)	K(1)-O(2)	2.879(3)
C(13)-C(14)	1.298(4)	O(2)-C(1E)	1.375(15)
C(13)-C(18)	1.347(5)	O(2)-C(4A)	1.422(13)
C(14)-C(15)	1.426(5)	O(2)-C(1A)	1.465(13)
C(15)-C(16)	1.330(6)	O(2)-C(4E)	1.594(15)
C(16)-C(17)	1.280(5)	C(1A)-C(2A)	1.567(12)
C(17)-C(18)	1.421(5)	C(2A)-C(3A)	1.511(12)
P(2)-C(25)	1.826(3)	C(3A)-C(4A)	1.574(12)
P(2)-C(31)	1.876(3)	C(1E)-C(2E)	1.564(11)
P(2)-B(19)	1.912(4)	C(2E)-C(3E)	1.527(12)
B(19)-C(24)	1.531(5)	C(3E)-C(4E)	1.578(11)
B(19)-C(20)	1.552(5)	O(3)-C(8A)	1.451(5)
B(19)-K(2)	2.978(3)	O(3)-C(5A)	1.485(5)
B(19)-K(1)	3.296(4)	C(5A)-C(6A)	1.530(5)
C(20)-C(21)	1.361(5)	C(6A)-C(7A)	1.636(6)
C(20)-K(1)	3.121(3)	C(7A)-C(8A)	1.494(5)
C(20)-K(2)	3.275(3)	K(2)-O(5)	2.608(3)
C(21)-C(22)	1.420(5)	K(2)-O(4C)	2.629(3)
C(21)-K(1)	2.981(3)	K(2)-C(12C)	3.326(4)
C(21)-K(2)	3.419(4)	K(2)-C(16A)	3.389(3)
C(22)-C(23)	1.442(5)	O(4C)-C(12C)	1.392(4)
C(22)-K(1)	2.976(3)	O(4C)-C(9C)	1.529(5)
C(22)-K(2)	3.321(4)	C(9C)-C(10C)	1.455(7)
C(23)-C(24)	1.375(5)	C(9C)-C(10D)	1.63(3)
C(23)-K(2)	3.101(3)	C(10C)-C(11C)	1.633(10)
C(23)-K(1)	3.183(3)	C(10D)-C(11C)	1.53(2)
C(24)-K(2)	2.926(3)	C(11C)-C(12C)	1.505(6)
C(24)-K(1)	3.355(3)	O(5)-C(16A)	1.344(4)
C(25)-C(30)	1.334(4)	O(5)-C(13A)	1.424(4)
C(25)-C(26)	1.427(5)	C(13A)-C(14A)	1.430(5)
C(26)-C(27)	1.377(5)	C(14A)-C(15A)	1.529(6)
C(27)-C(28)	1.322(5)	C(15A)-C(16A)	1.534(5)
C(28)-C(29)	1.422(6)	O(5X)-C(1X)	1.36(3)
C(29)-C(30)	1.377(5)	O(5X)-C(1Y)	1.456(10)
C(31)-C(32)	1.322(5)	O(5X)-C(4X)	1.514(8)
C(31)-C(36)	1.530(5)	C(1X)-C(2X)	1.38(4)
C(32)-C(33)	1.409(5)	C(2X)-C(3X)	1.41(3)
C(33)-C(34)	1.513(6)	C(1Y)-C(2Y)	1.382(12)
C(34)-C(35)	1.321(5)	C(2Y)-C(3X)	1.371(11)
C(35)-C(36)	1.404(5)	C(3X)-C(4X)	1.405(9)
P(3)-B(37)	1.808(3)		
P(3)-C(49)	1.881(3)	C(1)-Ir(1)-P(1)	94.81(10)
P(3)-C(43)	1.948(3)	C(1)-Ir(1)-P(3)	75.83(10)

Appendix A

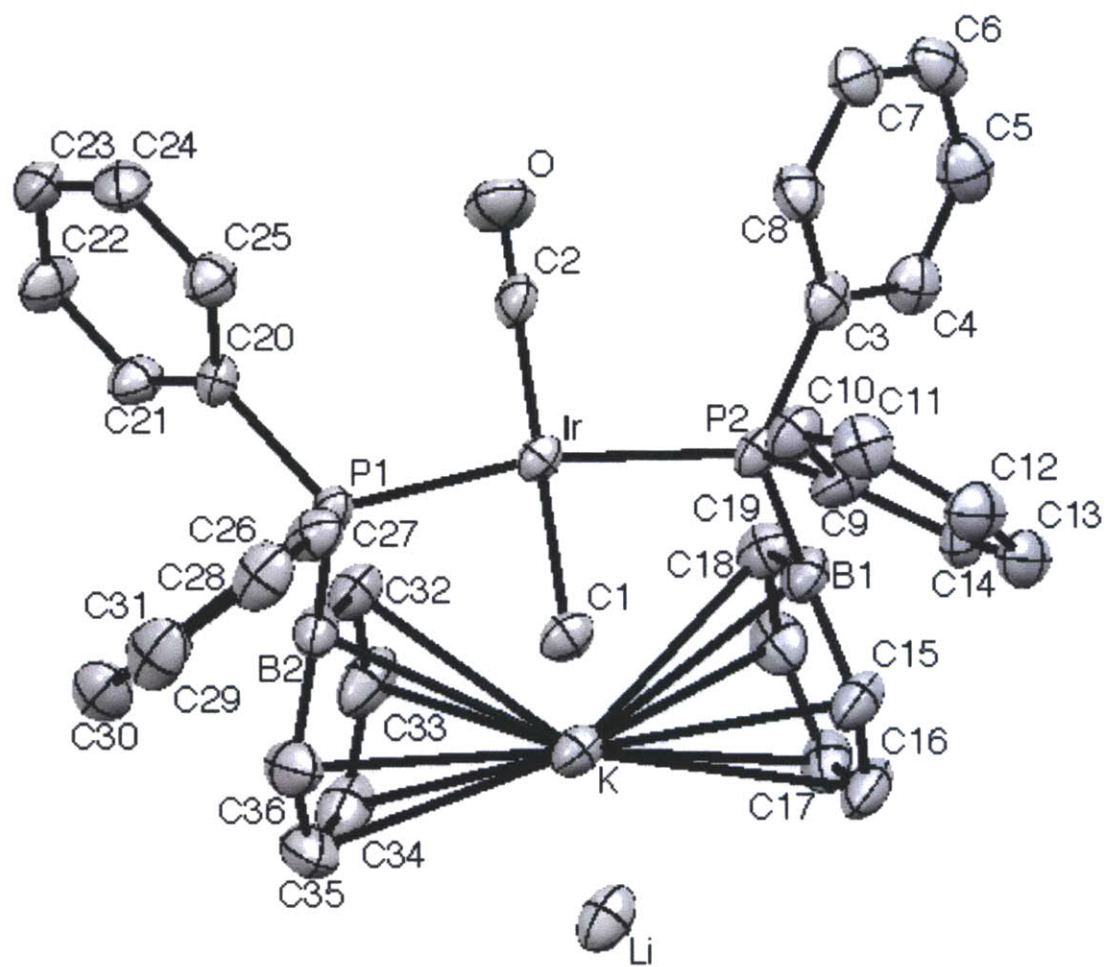
P(1)-Ir(1)-P(3)	163.91(3)	C(20)-C(21)-C(22)	120.3(3)
C(1)-Ir(1)-P(2)	167.75(10)	C(20)-C(21)-K(1)	82.93(18)
P(1)-Ir(1)-P(2)	87.79(3)	C(22)-C(21)-K(1)	76.01(18)
P(3)-Ir(1)-P(2)	104.14(3)	C(20)-C(21)-K(2)	72.4(2)
O(1)-C(1)-Ir(1)	173.1(3)	C(22)-C(21)-K(2)	74.0(2)
C(7)-P(1)-C(13)	106.14(15)	K(1)-C(21)-K(2)	122.97(11)
C(7)-P(1)-B(1)	103.20(16)	C(21)-C(22)-C(23)	124.0(3)
C(13)-P(1)-B(1)	105.20(15)	C(21)-C(22)-K(1)	76.41(18)
C(7)-P(1)-Ir(1)	107.70(12)	C(23)-C(22)-K(1)	84.63(18)
C(13)-P(1)-Ir(1)	99.72(10)	C(21)-C(22)-K(2)	81.7(2)
B(1)-P(1)-Ir(1)	132.57(9)	C(23)-C(22)-K(2)	68.60(19)
C(6)-B(1)-C(2)	113.2(3)	K(1)-C(22)-K(2)	126.58(11)
C(6)-B(1)-P(1)	120.2(3)	C(24)-C(23)-C(22)	121.3(3)
C(2)-B(1)-P(1)	126.4(2)	C(24)-C(23)-K(2)	69.80(18)
C(6)-B(1)-K(1)	72.50(18)	C(22)-C(23)-K(2)	85.74(19)
C(2)-B(1)-K(1)	67.65(16)	C(24)-C(23)-K(1)	85.0(2)
P(1)-B(1)-K(1)	132.93(14)	C(22)-C(23)-K(1)	68.55(18)
C(3)-C(2)-B(1)	124.1(3)	K(2)-C(23)-K(1)	127.14(11)
C(3)-C(2)-K(1)	69.06(16)	C(23)-C(24)-B(19)	116.8(3)
B(1)-C(2)-K(1)	83.01(17)	C(23)-C(24)-K(2)	84.03(19)
C(4)-C(3)-C(2)	120.5(3)	B(19)-C(24)-K(2)	76.87(17)
C(4)-C(3)-K(1)	73.91(18)	C(23)-C(24)-K(1)	70.9(2)
C(2)-C(3)-K(1)	81.25(17)	B(19)-C(24)-K(1)	74.55(19)
C(3)-C(4)-C(5)	117.6(3)	K(2)-C(24)-K(1)	127.11(11)
C(3)-C(4)-K(1)	77.68(19)	C(30)-C(25)-C(26)	118.9(3)
C(5)-C(4)-K(1)	77.49(18)	C(30)-C(25)-P(2)	118.2(3)
C(4)-C(5)-C(6)	127.0(3)	C(26)-C(25)-P(2)	122.9(2)
C(4)-C(5)-K(1)	72.25(18)	C(27)-C(26)-C(25)	124.4(3)
C(6)-C(5)-K(1)	85.08(18)	C(28)-C(27)-C(26)	116.2(4)
B(1)-C(6)-C(5)	117.6(3)	C(27)-C(28)-C(29)	119.9(3)
B(1)-C(6)-K(1)	80.22(19)	C(30)-C(29)-C(28)	124.0(3)
C(5)-C(6)-K(1)	66.04(17)	C(25)-C(30)-C(29)	116.5(3)
C(12)-C(7)-C(8)	124.1(3)	C(32)-C(31)-C(36)	120.0(3)
C(12)-C(7)-P(1)	115.6(3)	C(32)-C(31)-P(2)	110.4(3)
C(8)-C(7)-P(1)	120.3(2)	C(36)-C(31)-P(2)	129.6(2)
C(9)-C(8)-C(7)	119.9(3)	C(31)-C(32)-C(33)	113.1(4)
C(8)-C(9)-C(10)	115.4(4)	C(32)-C(33)-C(34)	126.4(3)
C(9)-C(10)-C(11)	125.1(3)	C(35)-C(34)-C(33)	121.3(3)
C(12)-C(11)-C(10)	119.5(3)	C(34)-C(35)-C(36)	112.3(4)
C(11)-C(12)-C(7)	116.0(4)	C(35)-C(36)-C(31)	127.0(3)
C(14)-C(13)-C(18)	111.9(3)	B(37)-P(3)-C(49)	105.91(16)
C(14)-C(13)-P(1)	124.7(3)	B(37)-P(3)-C(43)	101.35(15)
C(18)-C(13)-P(1)	123.4(2)	C(49)-P(3)-C(43)	96.15(15)
C(13)-C(14)-C(15)	121.6(3)	B(37)-P(3)-Ir(1)	120.42(13)
C(16)-C(15)-C(14)	126.0(3)	C(49)-P(3)-Ir(1)	118.44(10)
C(17)-C(16)-C(15)	112.7(4)	C(43)-P(3)-Ir(1)	110.61(10)
C(16)-C(17)-C(18)	122.1(4)	C(42)-B(37)-C(38)	122.1(3)
C(13)-C(18)-C(17)	125.7(3)	C(42)-B(37)-P(3)	116.8(3)
C(25)-P(2)-C(31)	96.65(14)	C(38)-B(37)-P(3)	120.7(3)
C(25)-P(2)-B(19)	114.30(15)	C(42)-B(37)-K(2)	75.9(2)
C(31)-P(2)-B(19)	100.84(16)	C(38)-B(37)-K(2)	77.1(2)
C(25)-P(2)-Ir(1)	108.54(11)	P(3)-B(37)-K(2)	125.64(17)
C(31)-P(2)-Ir(1)	121.22(10)	C(39)-C(38)-B(37)	116.3(3)
B(19)-P(2)-Ir(1)	114.22(12)	C(39)-C(38)-K(2)	74.5(2)
C(24)-B(19)-C(20)	119.3(3)	B(37)-C(38)-K(2)	78.3(2)
C(24)-B(19)-P(2)	113.1(3)	C(38)-C(39)-C(40)	119.7(4)
C(20)-B(19)-P(2)	127.5(3)	C(38)-C(39)-K(2)	84.0(2)
C(24)-B(19)-K(2)	73.10(17)	C(40)-C(39)-K(2)	74.4(2)
C(20)-B(19)-K(2)	86.59(17)	C(41)-C(40)-C(39)	125.8(3)
P(2)-B(19)-K(2)	109.36(16)	C(41)-C(40)-K(2)	81.0(2)
C(24)-B(19)-K(1)	78.85(19)	C(39)-C(40)-K(2)	81.6(2)
C(20)-B(19)-K(1)	69.79(18)	C(42)-C(41)-C(40)	120.3(3)
P(2)-B(19)-K(1)	122.45(14)	C(42)-C(41)-K(2)	83.2(2)
K(2)-B(19)-K(1)	127.43(12)	C(40)-C(41)-K(2)	75.1(2)
C(21)-C(20)-B(19)	118.3(3)	C(41)-C(42)-B(37)	115.7(3)
C(21)-C(20)-K(1)	71.43(18)	C(41)-C(42)-K(2)	75.0(2)
B(19)-C(20)-K(1)	82.39(18)	B(37)-C(42)-K(2)	79.5(2)
C(21)-C(20)-K(2)	84.3(2)	C(48)-C(43)-C(44)	118.5(3)
B(19)-C(20)-K(2)	65.19(17)	C(48)-C(43)-P(3)	113.8(3)
K(1)-C(20)-K(2)	123.22(11)	C(44)-C(43)-P(3)	127.7(2)

Appendix A

C(20)-K(2)-C(22)	42.88(8)	C(12C)-O(4C)-K(2)	107.6(2)
C(41)-K(2)-C(22)	139.92(10)	C(9C)-O(4C)-K(2)	134.0(2)
O(5)-K(2)-C(12C)	84.76(9)	C(10C)-C(9C)-O(4C)	106.0(4)
O(4C)-K(2)-C(12C)	23.52(9)	C(10C)-C(9C)-C(10D)	32.6(11)
C(24)-K(2)-C(12C)	149.82(10)	O(4C)-C(9C)-C(10D)	101.4(10)
B(19)-K(2)-C(12C)	128.52(11)	C(9C)-C(10C)-C(11C)	100.8(5)
C(23)-K(2)-C(12C)	131.49(10)	C(11C)-C(10D)-C(9C)	97.9(14)
C(40)-K(2)-C(12C)	79.95(10)	C(12C)-C(11C)-C(10D)	114.9(9)
C(20)-K(2)-C(12C)	102.18(9)	C(12C)-C(11C)-C(10C)	103.7(4)
C(41)-K(2)-C(12C)	99.41(10)	C(10D)-C(11C)-C(10C)	32.1(13)
C(22)-K(2)-C(12C)	106.90(10)	O(4C)-C(12C)-C(11C)	101.9(3)
O(5)-K(2)-C(39)	110.81(9)	O(4C)-C(12C)-K(2)	48.90(17)
O(4C)-K(2)-C(39)	99.40(9)	C(11C)-C(12C)-K(2)	128.6(3)
C(24)-K(2)-C(39)	125.59(9)	C(16A)-O(5)-C(13A)	108.4(3)
B(19)-K(2)-C(39)	117.03(9)	C(16A)-O(5)-K(2)	114.2(2)
C(23)-K(2)-C(39)	148.66(9)	C(13A)-O(5)-K(2)	135.1(2)
C(40)-K(2)-C(39)	24.07(9)	O(5)-C(13A)-C(14A)	109.5(3)
C(20)-K(2)-C(39)	128.99(9)	C(13A)-C(14A)-C(15A)	98.6(3)
C(41)-K(2)-C(39)	43.00(10)	C(14A)-C(15A)-C(16A)	100.3(3)
C(22)-K(2)-C(39)	169.77(8)	O(5)-C(16A)-C(15A)	106.0(3)
C(12C)-K(2)-C(39)	79.85(10)	O(5)-C(16A)-K(2)	44.56(16)
O(5)-K(2)-C(16A)	21.20(8)	C(15A)-C(16A)-K(2)	142.6(2)
O(4C)-K(2)-C(16A)	78.53(9)	C(1X)-O(5X)-C(1Y)	42.8(16)
C(24)-K(2)-C(16A)	119.44(9)	C(1X)-O(5X)-C(4X)	109.8(13)
B(19)-K(2)-C(16A)	145.28(10)	C(1Y)-O(5X)-C(4X)	102.9(5)
C(23)-K(2)-C(16A)	97.53(9)	O(5X)-C(1X)-C(2X)	106(2)
C(40)-K(2)-C(16A)	72.57(10)	C(1X)-C(2X)-C(3X)	114(3)
C(20)-K(2)-C(16A)	133.59(10)	C(2Y)-C(1Y)-O(5X)	100.0(6)
C(41)-K(2)-C(16A)	67.87(9)	C(3X)-C(2Y)-C(1Y)	118.9(7)
C(22)-K(2)-C(16A)	94.88(9)	C(2Y)-C(3X)-C(4X)	99.0(7)
C(12C)-K(2)-C(16A)	67.42(9)	C(2Y)-C(3X)-C(2X)	42.0(18)
C(39)-K(2)-C(16A)	94.84(9)	C(4X)-C(3X)-C(2X)	105.6(14)
C(12C)-O(4C)-C(9C)	112.6(3)	C(3X)-C(4X)-O(5X)	104.6(5)

Appendix A

Crystal data and structure refinement for 3'



Appendix A

Table 1. Crystal data and structure refinement for **3'**

Identification code	d8_10092_0m	
Empirical formula	C36 H33 B2 Ir K Li O P2	
Formula weight	803.42	
Temperature	100(2) K	
Wavelength	1.54178 Å	
Crystal system	Monoclinic	
Space group	P2(1)/n	
Unit cell dimensions	a = 14.8532(3) Å b = 20.8264(4) Å c = 18.8853(3) Å	$\alpha = 90^\circ$. $\beta = 90.0450(10)^\circ$. $\gamma = 90^\circ$.
Volume	5841.95(19) Å ³	
Z	8	
Density (calculated)	1.827 Mg/m ³	
Absorption coefficient	11.395 mm ⁻¹	
F(000)	3168	
Crystal size	0.25 x 0.20 x 0.10 mm ³	
Theta range for data collection	2.12 to 66.59°.	
Index ranges	-17 <= h <= 17, -24 <= k <= 21, -22 <= l <= 22	
Reflections collected	113420	
Independent reflections	10329 [R(int) = 0.0362]	
Completeness to theta = 66.59°	100.0 %	
Absorption correction	None	
Max. and min. transmission	0.3953 and 0.1629	
Refinement method	Full-matrix least-squares on F ²	
Data / restraints / parameters	10329 / 666 / 651	
Goodness-of-fit on F ²	1.118	
Final R indices [I>2sigma(I)]	R1 = 0.0483, wR2 = 0.1263	
R indices (all data)	R1 = 0.0489, wR2 = 0.1269	
Largest diff. peak and hole	3.580 and -1.692 e.Å ⁻³	

Appendix A

Table 2. Atomic coordinates ($\times 10^4$) and equivalent isotropic displacement parameters ($\text{\AA}^2 \times 10^3$) for D8_10092_0m. U(eq) is defined as one third of the trace of the orthogonalized U^{ij} tensor.

	x	y	z	U(eq)
Ir(1)	3436(1)	-1676(1)	-191(1)	24(1)
C(2)	2291(5)	-1297(3)	-190(4)	31(1)
O(1)	1597(4)	-1067(3)	-180(4)	51(1)
C(1)	4769(4)	-2086(3)	-193(5)	31(1)
K(1)	3817(1)	-3421(1)	-148(1)	32(1)
O(1D)	5337(4)	-4180(3)	-31(4)	56(2)
C(1D)	6163(7)	-3832(4)	6(8)	78(5)
C(2D)	5439(5)	-4839(4)	25(5)	46(2)
P(1)	3467(1)	-1787(1)	1018(1)	24(1)
C(3)	2578(6)	-1429(4)	-1915(4)	33(2)
C(4)	2007(6)	-1748(4)	-2401(5)	38(2)
C(5)	1370(6)	-1418(5)	-2784(5)	45(2)
C(6)	1291(6)	-765(5)	-2720(5)	43(2)
C(7)	1820(6)	-441(4)	-2261(5)	43(2)
C(8)	2470(6)	-762(4)	-1848(4)	36(2)
C(9)	4461(6)	-1519(4)	-1838(5)	34(2)
C(10)	4829(6)	-932(4)	-1623(5)	37(2)
C(11)	5541(6)	-657(4)	-1990(5)	41(2)
C(12)	5924(6)	-971(5)	-2559(5)	44(2)
C(13)	5551(7)	-1548(5)	-2785(5)	42(2)
C(14)	4813(6)	-1806(4)	-2461(4)	34(2)
B(1)	3359(7)	-2753(4)	-1560(4)	32(2)
C(15)	4108(7)	-3191(4)	-1739(5)	41(2)
C(16)	3978(8)	-3856(4)	-1718(5)	49(2)
C(17)	3166(7)	-4125(4)	-1517(4)	44(2)
C(18)	2423(6)	-3737(4)	-1351(5)	39(2)
C(19)	2482(6)	-3075(4)	-1359(5)	35(1)
P(2)	3456(2)	-1835(1)	-1402(1)	27(1)
C(20)	2623(5)	-1328(4)	1547(4)	26(1)
C(21)	2018(6)	-1610(4)	1994(5)	33(2)
C(22)	1423(6)	-1245(4)	2392(4)	38(2)
C(23)	1449(6)	-582(4)	2360(4)	36(2)
C(24)	2056(6)	-294(4)	1903(4)	38(2)
C(25)	2628(6)	-661(4)	1496(4)	35(2)
C(26)	4497(5)	-1502(4)	1465(4)	28(2)
C(27)	5004(5)	-1027(4)	1134(5)	36(2)
C(28)	5776(6)	-794(4)	1454(5)	42(2)
C(29)	6054(6)	-1034(5)	2099(5)	47(2)
C(30)	5573(6)	-1513(5)	2431(5)	45(2)
C(31)	4780(6)	-1752(4)	2086(5)	40(2)
B(2)	3276(6)	-2700(4)	1213(4)	31(2)
C(32)	2408(6)	-2991(4)	965(5)	36(2)
C(33)	2310(7)	-3657(4)	972(5)	46(2)
C(34)	2979(8)	-4065(4)	1202(5)	51(2)
C(35)	3814(8)	-3818(5)	1436(5)	55(2)
C(36)	3983(8)	-3157(5)	1456(5)	48(2)
C(1H)	6244(7)	443(5)	3598(6)	58(2)
O(2H)	6037(6)	542(3)	4329(4)	68(2)
C(3H)	6363(9)	104(6)	4806(7)	79(3)
C(4H)	6100(8)	280(6)	5552(6)	68(3)
O(5H)	6692(5)	681(4)	5855(3)	59(2)
C(6H)	6404(9)	845(7)	6552(6)	78(4)
Li(1)	8531(10)	-1740(6)	-179(10)	43(2)
C(1S)	10262(7)	-2517(5)	-488(7)	67(3)
O(1S)	9512(4)	-2459(3)	-57(3)	52(2)
C(2S)	9163(10)	-2993(6)	206(9)	95(4)
C(3S)	8473(10)	-2834(6)	760(6)	75(3)
O(2S)	7837(5)	-2364(4)	474(4)	67(2)
C(4S)	7171(9)	-2221(6)	954(5)	68(3)
C(5S)	9815(7)	-798(5)	-1079(5)	55(2)
O(3S)	7897(5)	-2162(4)	-1106(4)	67(2)
C(6S)	8961(8)	-1500(6)	-1748(6)	59(3)
C(7S)	8052(7)	-1820(6)	-1784(5)	55(2)
O(4S)	9049(5)	-1203(4)	-1078(4)	60(2)

Appendix A

C(8S)	7131(11)	-2553(8)	-1142(8)	96(5)
C(9S)	6830(8)	-944(7)	-545(6)	76(3)
O(5S)	7527(5)	-1009(3)	-36(4)	71(2)
C(10S)	7884(7)	-426(4)	171(6)	56(2)
C(11S)	8545(9)	-620(6)	801(6)	72(3)
O(6S)	9164(5)	-1144(4)	584(4)	66(2)
C(12S)	9782(10)	-1276(8)	1042(6)	81(4)

Table 3. Bond lengths [\AA] and angles [$^\circ$] for 3'.

Ir(1)-C(2)	1.875(7)	C(32)-C(33)	1.394(13)
Ir(1)-C(1)	2.156(6)	C(33)-C(34)	1.379(15)
Ir(1)-P(1)	2.2954(17)	C(34)-C(35)	1.413(16)
Ir(1)-P(2)	2.3114(18)	C(35)-C(36)	1.400(14)
Ir(1)-K(1)	3.6789(14)	C(1H)-O(2H)	1.430(13)
C(2)-O(1)	1.137(8)	O(2H)-C(3H)	1.369(14)
K(1)-O(1D)	2.765(6)	C(3H)-C(4H)	1.508(15)
K(1)-C(15)	3.073(9)	C(4H)-O(5H)	1.342(13)
K(1)-B(1)	3.083(9)	O(5H)-C(6H)	1.426(12)
K(1)-B(2)	3.083(8)	Li(1)-O(2S)	2.068(16)
K(1)-C(36)	3.089(9)	Li(1)-O(1S)	2.103(16)
K(1)-C(32)	3.099(8)	Li(1)-O(6S)	2.121(18)
K(1)-C(35)	3.104(10)	Li(1)-O(5S)	2.148(15)
K(1)-C(16)	3.109(9)	Li(1)-O(4S)	2.174(18)
K(1)-C(19)	3.110(9)	Li(1)-O(3S)	2.174(19)
K(1)-C(33)	3.119(9)	C(1S)-O(1S)	1.385(12)
K(1)-C(17)	3.124(8)	O(1S)-C(2S)	1.323(13)
K(1)-C(34)	3.139(9)	C(2S)-C(3S)	1.502(16)
O(1D)-C(2D)	1.386(9)	C(3S)-O(2S)	1.464(14)
O(1D)-C(1D)	1.426(11)	O(2S)-C(4S)	1.375(12)
C(2D)-C(2D) ^{#1}	1.469(16)	C(5S)-O(4S)	1.416(12)
P(1)-C(26)	1.843(8)	O(3S)-C(8S)	1.400(14)
P(1)-C(20)	1.867(7)	O(3S)-C(7S)	1.483(13)
P(1)-B(2)	1.957(9)	C(6S)-O(4S)	1.415(13)
C(3)-C(8)	1.405(12)	C(6S)-C(7S)	1.508(15)
C(3)-C(4)	1.415(13)	C(9S)-O(5S)	1.418(13)
C(3)-P(2)	1.831(9)	O(5S)-C(10S)	1.383(11)
C(4)-C(5)	1.375(13)	C(10S)-C(11S)	1.594(17)
C(5)-C(6)	1.370(14)	C(11S)-O(6S)	1.483(14)
C(6)-C(7)	1.350(13)	O(6S)-C(12S)	1.291(15)
C(7)-C(8)	1.409(12)		
C(9)-C(10)	1.397(12)	C(2)-Ir(1)-C(1)	178.4(3)
C(9)-C(14)	1.420(12)	C(2)-Ir(1)-P(1)	93.4(3)
C(9)-P(2)	1.829(9)	C(1)-Ir(1)-P(1)	86.8(2)
C(10)-C(11)	1.388(12)	C(2)-Ir(1)-P(2)	94.2(3)
C(11)-C(12)	1.382(13)	C(1)-Ir(1)-P(2)	85.9(2)
C(12)-C(13)	1.389(14)	P(1)-Ir(1)-P(2)	165.83(5)
C(13)-C(14)	1.366(13)	C(2)-Ir(1)-K(1)	123.7(2)
B(1)-C(15)	1.478(13)	C(1)-Ir(1)-K(1)	57.84(18)
B(1)-C(19)	1.513(13)	P(1)-Ir(1)-K(1)	82.86(5)
B(1)-P(2)	1.941(8)	P(2)-Ir(1)-K(1)	82.97(6)
C(15)-C(16)	1.398(12)	O(1)-C(2)-Ir(1)	179.0(8)
C(16)-C(17)	1.383(14)	O(1D)-K(1)-C(15)	92.9(2)
C(17)-C(18)	1.404(13)	O(1D)-K(1)-B(1)	120.4(2)
C(18)-C(19)	1.382(12)	C(15)-K(1)-B(1)	27.8(2)
C(20)-C(21)	1.365(11)	O(1D)-K(1)-B(2)	115.2(2)
C(20)-C(25)	1.392(11)	C(15)-K(1)-B(2)	140.9(2)
C(21)-C(22)	1.388(11)	B(1)-K(1)-B(2)	116.4(2)
C(22)-C(23)	1.382(12)	O(1D)-K(1)-C(36)	87.6(2)
C(23)-C(24)	1.386(12)	C(15)-K(1)-C(36)	156.9(2)
C(24)-C(25)	1.379(12)	B(1)-K(1)-C(36)	141.8(2)
C(26)-C(31)	1.351(13)	B(2)-K(1)-C(36)	28.0(2)
C(26)-C(27)	1.391(12)	O(1D)-K(1)-C(32)	131.5(2)
C(27)-C(28)	1.384(11)	C(15)-K(1)-C(32)	135.6(3)
C(28)-C(29)	1.379(14)	B(1)-K(1)-C(32)	107.9(3)
C(29)-C(30)	1.379(15)	B(2)-K(1)-C(32)	28.0(2)
C(30)-C(31)	1.434(13)	C(36)-K(1)-C(32)	48.5(3)
B(2)-C(36)	1.491(13)	O(1D)-K(1)-C(35)	76.8(3)
B(2)-C(32)	1.498(13)	C(15)-K(1)-C(35)	169.7(3)

Appendix A

B(1)-K(1)-C(35)	162.5(3)	C(11)-C(10)-C(9)	120.9(8)
B(2)-K(1)-C(35)	47.6(2)	C(12)-C(11)-C(10)	120.4(8)
C(36)-K(1)-C(35)	26.1(3)	C(11)-C(12)-C(13)	119.0(8)
C(32)-K(1)-C(35)	54.7(3)	C(14)-C(13)-C(12)	121.4(9)
O(1D)-K(1)-C(16)	81.1(3)	C(13)-C(14)-C(9)	120.1(9)
C(15)-K(1)-C(16)	26.1(2)	C(15)-B(1)-C(19)	115.7(7)
B(1)-K(1)-C(16)	47.5(2)	C(15)-B(1)-P(2)	125.9(7)
B(2)-K(1)-C(16)	163.1(3)	C(19)-B(1)-P(2)	117.5(6)
C(36)-K(1)-C(16)	168.7(3)	C(15)-B(1)-K(1)	75.7(5)
C(32)-K(1)-C(16)	141.6(3)	C(19)-B(1)-K(1)	76.8(5)
C(35)-K(1)-C(16)	147.3(2)	P(2)-B(1)-K(1)	107.1(3)
O(1D)-K(1)-C(19)	135.4(2)	C(16)-C(15)-B(1)	120.0(9)
C(15)-K(1)-C(19)	48.4(2)	C(16)-C(15)-K(1)	78.4(5)
B(1)-K(1)-C(19)	28.3(2)	B(1)-C(15)-K(1)	76.5(5)
B(2)-K(1)-C(19)	109.5(2)	C(17)-C(16)-C(15)	122.0(9)
C(36)-K(1)-C(19)	136.9(3)	C(17)-C(16)-K(1)	77.8(5)
C(32)-K(1)-C(19)	90.1(2)	C(15)-C(16)-K(1)	75.5(5)
C(35)-K(1)-C(19)	140.3(3)	C(16)-C(17)-C(18)	120.9(8)
C(16)-K(1)-C(19)	54.3(3)	C(16)-C(17)-K(1)	76.5(5)
O(1D)-K(1)-C(33)	116.3(2)	C(18)-C(17)-K(1)	77.8(5)
C(15)-K(1)-C(33)	142.1(3)	C(19)-C(18)-C(17)	121.5(8)
B(1)-K(1)-C(33)	120.0(3)	C(19)-C(18)-K(1)	75.9(5)
B(2)-K(1)-C(33)	47.5(2)	C(17)-C(18)-K(1)	76.3(5)
C(36)-K(1)-C(33)	54.5(3)	C(18)-C(19)-B(1)	119.9(8)
C(32)-K(1)-C(33)	25.9(2)	C(18)-C(19)-K(1)	78.6(5)
C(35)-K(1)-C(33)	45.8(3)	B(1)-C(19)-K(1)	74.9(5)
C(16)-K(1)-C(33)	131.0(3)	C(9)-P(2)-C(3)	100.2(4)
C(19)-K(1)-C(33)	94.4(3)	C(9)-P(2)-B(1)	110.3(4)
O(1D)-K(1)-C(17)	92.9(2)	C(3)-P(2)-B(1)	108.7(4)
C(15)-K(1)-C(17)	46.2(2)	C(9)-P(2)-Ir(1)	113.9(3)
B(1)-K(1)-C(17)	55.1(2)	C(3)-P(2)-Ir(1)	116.6(3)
B(2)-K(1)-C(17)	146.9(3)	B(1)-P(2)-Ir(1)	107.0(3)
C(36)-K(1)-C(17)	156.8(3)	C(21)-C(20)-C(25)	118.4(7)
C(32)-K(1)-C(17)	119.2(2)	C(21)-C(20)-P(1)	123.6(6)
C(35)-K(1)-C(17)	132.2(3)	C(25)-C(20)-P(1)	118.0(6)
C(16)-K(1)-C(17)	25.6(3)	C(20)-C(21)-C(22)	121.3(7)
C(19)-K(1)-C(17)	45.9(2)	C(23)-C(22)-C(21)	120.3(8)
C(33)-K(1)-C(17)	105.4(3)	C(22)-C(23)-C(24)	118.6(7)
O(1D)-K(1)-C(34)	90.9(2)	C(25)-C(24)-C(23)	120.5(7)
C(15)-K(1)-C(34)	156.5(3)	C(24)-C(25)-C(20)	120.8(7)
B(1)-K(1)-C(34)	143.9(3)	C(31)-C(26)-C(27)	119.6(8)
B(2)-K(1)-C(34)	55.1(2)	C(31)-C(26)-P(1)	122.1(7)
C(36)-K(1)-C(34)	46.4(3)	C(27)-C(26)-P(1)	118.3(6)
C(32)-K(1)-C(34)	45.9(2)	C(28)-C(27)-C(26)	120.2(8)
C(35)-K(1)-C(34)	26.2(3)	C(29)-C(28)-C(27)	120.4(9)
C(16)-K(1)-C(34)	132.9(3)	C(30)-C(29)-C(28)	120.6(8)
C(19)-K(1)-C(34)	116.3(3)	C(29)-C(30)-C(31)	118.1(9)
C(33)-K(1)-C(34)	25.5(3)	C(26)-C(31)-C(30)	121.1(9)
C(17)-K(1)-C(34)	110.4(2)	C(36)-B(2)-C(32)	116.4(8)
C(2D)-O(1D)-C(1D)	113.9(6)	C(36)-B(2)-P(1)	125.2(7)
C(2D)-O(1D)-K(1)	131.4(5)	C(32)-B(2)-P(1)	117.3(6)
C(1D)-O(1D)-K(1)	114.6(5)	C(36)-B(2)-K(1)	76.2(5)
O(1D)-C(2D)-C(2D) ^{#1}	110.5(8)	C(32)-B(2)-K(1)	76.6(4)
C(26)-P(1)-C(20)	98.5(3)	P(1)-B(2)-K(1)	106.2(3)
C(26)-P(1)-B(2)	110.4(4)	C(33)-C(32)-B(2)	119.3(8)
C(20)-P(1)-B(2)	107.4(4)	C(33)-C(32)-K(1)	77.8(5)
C(26)-P(1)-Ir(1)	116.0(3)	B(2)-C(32)-K(1)	75.4(4)
C(20)-P(1)-Ir(1)	117.9(2)	C(34)-C(33)-C(32)	122.7(9)
B(2)-P(1)-Ir(1)	106.4(3)	C(34)-C(33)-K(1)	78.1(5)
C(8)-C(3)-C(4)	117.0(8)	C(32)-C(33)-K(1)	76.2(5)
C(8)-C(3)-P(2)	119.5(7)	C(33)-C(34)-C(35)	120.4(8)
C(4)-C(3)-P(2)	123.6(7)	C(33)-C(34)-K(1)	76.5(5)
C(5)-C(4)-C(3)	121.2(9)	C(35)-C(34)-K(1)	75.6(5)
C(6)-C(5)-C(4)	120.6(9)	C(36)-C(35)-C(34)	121.6(9)
C(7)-C(6)-C(5)	120.2(9)	C(36)-C(35)-K(1)	76.3(6)
C(6)-C(7)-C(8)	121.1(9)	C(34)-C(35)-K(1)	78.3(5)
C(3)-C(8)-C(7)	119.9(8)	C(35)-C(36)-B(2)	119.6(9)
C(10)-C(9)-C(14)	117.7(8)	C(35)-C(36)-K(1)	77.6(5)
C(10)-C(9)-P(2)	120.2(6)	B(2)-C(36)-K(1)	75.8(5)
C(14)-C(9)-P(2)	121.5(7)	C(3H)-O(2H)-C(1H)	117.5(8)

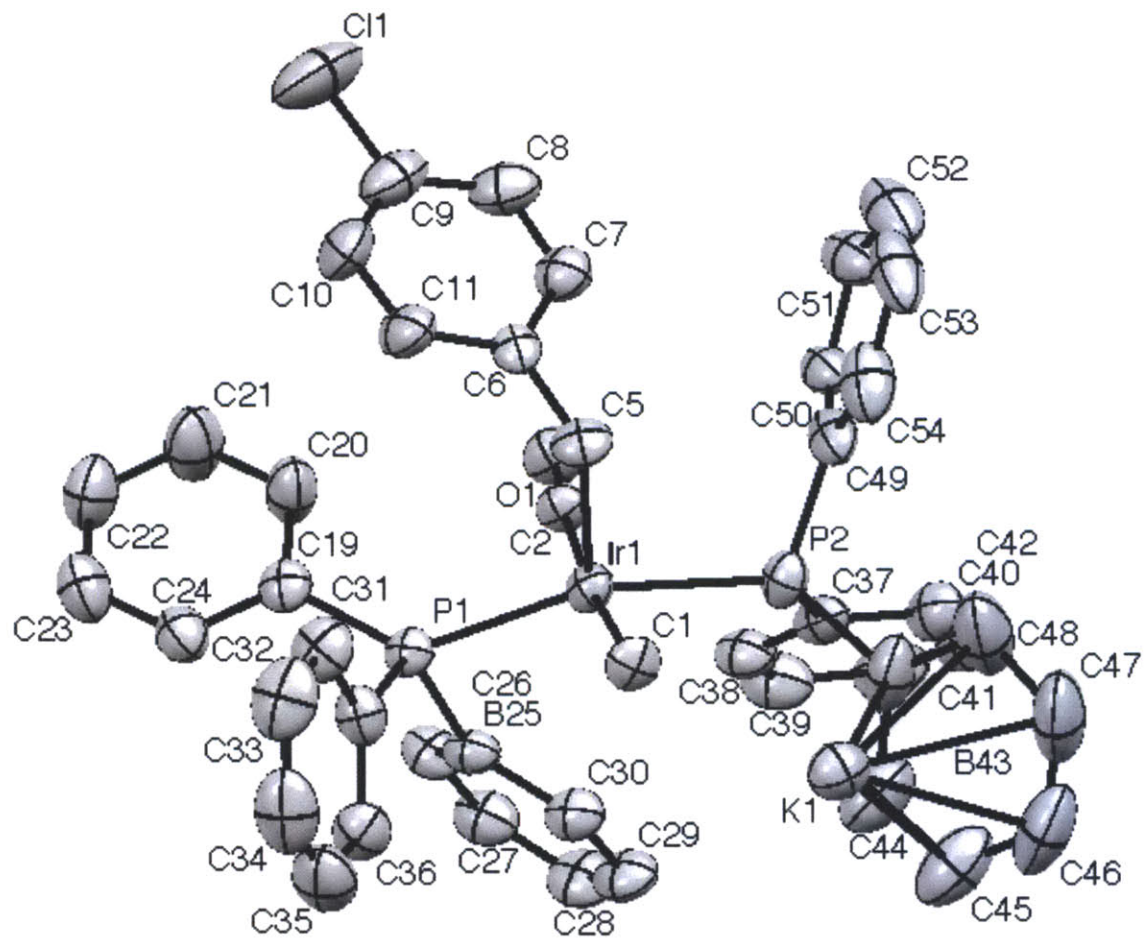
Appendix A

O(2H)-C(3H)-C(4H)	111.1(9)	O(1S)-C(2S)-C(3S)	110.1(10)
O(5H)-C(4H)-C(3H)	112.3(11)	O(2S)-C(3S)-C(2S)	109.3(10)
C(4H)-O(5H)-C(6H)	110.2(9)	C(4S)-O(2S)-C(3S)	111.5(8)
O(2S)-Li(1)-O(1S)	80.3(6)	C(4S)-O(2S)-Li(1)	128.1(8)
O(2S)-Li(1)-O(6S)	100.5(9)	C(3S)-O(2S)-Li(1)	108.6(8)
O(1S)-Li(1)-O(6S)	92.1(8)	C(8S)-O(3S)-C(7S)	111.3(9)
O(2S)-Li(1)-O(5S)	91.3(7)	C(8S)-O(3S)-Li(1)	128.7(9)
O(1S)-Li(1)-O(5S)	166.5(10)	C(7S)-O(3S)-Li(1)	115.7(7)
O(6S)-Li(1)-O(5S)	78.9(5)	O(4S)-C(6S)-C(7S)	108.4(9)
O(2S)-Li(1)-O(4S)	165.0(10)	O(3S)-C(7S)-C(6S)	108.2(9)
O(1S)-Li(1)-O(4S)	101.9(7)	C(6S)-O(4S)-C(5S)	109.4(8)
O(6S)-Li(1)-O(4S)	94.2(6)	C(6S)-O(4S)-Li(1)	116.2(8)
O(5S)-Li(1)-O(4S)	88.9(6)	C(5S)-O(4S)-Li(1)	126.3(8)
O(2S)-Li(1)-O(3S)	90.6(6)	C(10S)-O(5S)-C(9S)	112.8(9)
O(1S)-Li(1)-O(3S)	95.7(6)	C(10S)-O(5S)-Li(1)	113.0(7)
O(6S)-Li(1)-O(3S)	167.4(9)	C(9S)-O(5S)-Li(1)	119.3(9)
O(5S)-Li(1)-O(3S)	95.0(8)	O(5S)-C(10S)-C(11S)	103.0(8)
O(4S)-Li(1)-O(3S)	74.5(7)	O(6S)-C(11S)-C(10S)	111.2(8)
C(2S)-O(1S)-C(1S)	117.5(8)	C(12S)-O(6S)-C(11S)	114.4(9)
C(2S)-O(1S)-Li(1)	111.6(8)	C(12S)-O(6S)-Li(1)	130.1(10)
C(1S)-O(1S)-Li(1)	123.7(8)	C(11S)-O(6S)-Li(1)	110.1(8)

Symmetry transformations used to generate equivalent atoms:
#1 -x+1,-y-1,-z

Appendix A

Crystal data and structure refinement for 4



Appendix A

Table 1. Crystal data and structure refinement for **4**

Identification code	d8_10118_0m	
Empirical formula	C9.83 H11.83 B0.33 Br0 Cl0.17 Ir0.17 K0.17 O0.83 P0.33	
Formula weight	201.74	
Temperature	173(2) K	
Wavelength	1.54178 Å	
Crystal system	Monoclinic	
Space group	P2(1)/c	
Unit cell dimensions	a = 20.8109(3) Å b = 19.0414(3) Å c = 29.6086(4) Å	a = 90°. b = 104.1270(10)°. g = 90°.
Volume	11378.1(3) Å ³	
Z	12	
Density (calculated)	0.353 Mg/m ³	
Absorption coefficient	1.630 mm ⁻¹	
F(000)	1236	
Crystal size	0.25 x 0.20 x 0.15 mm ³	
Theta range for data collection	2.19 to 66.59°.	
Index ranges	-24<=h<=24, -22<=k<=22, -35<=l<=35	
Reflections collected	242454	
Independent reflections	20092 [R(int) = 0.0633]	
Completeness to theta = 66.59°	100.0 %	
Absorption correction	None	
Max. and min. transmission	0.7920 and 0.6860	
Refinement method	Full-matrix least-squares on F ²	
Data / restraints / parameters	20092 / 3825 / 1521	
Goodness-of-fit on F ²	1.141	
Final R indices [I>2sigma(I)]	R1 = 0.0639, wR2 = 0.1683	
R indices (all data)	R1 = 0.0902, wR2 = 0.1897	
Largest diff. peak and hole	2.021 and -1.940 e.Å ⁻³	

Appendix A

Table 2. Atomic coordinates ($\times 10^4$) and equivalent isotropic displacement parameters ($\text{\AA}^2 \times 10^3$) for D8_10118_0m. U(eq) is defined as one third of the trace of the orthogonalized U^{ij} tensor.

	x	y	z	U(eq)
Ir(1)	4462(1)	7396(1)	632(1)	34(1)
P(1)	4283(1)	6282(1)	298(1)	34(1)
O(1)	4675(3)	8171(3)	-214(2)	51(2)
C(1)	4247(4)	6993(4)	1253(3)	38(2)
Cl(1)	2243(2)	8429(3)	-1505(1)	101(1)
K(1)	4488(1)	7195(1)	2399(1)	54(1)
O(1L)	-274(4)	7667(5)	-1714(3)	81(2)
O(1O)	173(5)	9005(4)	-2539(3)	81(2)
O(1T)	4501(5)	7233(5)	3339(3)	82(2)
Ir(2)	-477(1)	7591(1)	-4412(1)	35(1)
C(2)	4610(4)	7853(4)	88(3)	35(2)
P(2)	4951(1)	8376(1)	1086(1)	40(1)
O(2)	-263(3)	6887(4)	-5283(2)	60(2)
Cl(2)	-3080(20)	7030(40)	-6485(11)	109(9)
Cl(2A)	-2960(30)	6850(30)	-6475(7)	128(8)
K(2)	-337(1)	7695(1)	-2643(1)	50(1)
C(2T)	5071(7)	7405(8)	3703(5)	86(3)
C(2L)	-17(7)	7051(8)	-1465(5)	87(3)
C(2O)	19(9)	9508(8)	-2885(5)	103(5)
P(3)	110(1)	6652(1)	-3958(1)	37(1)
C(3)	-680(4)	7970(5)	-3785(3)	43(2)
C(3T)	5330(7)	6708(8)	3919(5)	88(3)
C(3L)	624(8)	7245(9)	-1130(5)	101(4)
C(3O)	633(10)	9860(12)	-2888(6)	145(7)
C(4)	-333(4)	7166(5)	-4966(3)	38(2)
P(4)	-744(1)	8688(1)	-4753(1)	37(1)
C(4T)	4749(7)	6211(7)	3778(4)	81(3)
C(4L)	603(7)	8024(8)	-1103(5)	94(4)
C(4O)	1063(9)	9734(13)	-2416(7)	147(7)
C(5)	3460(4)	7753(5)	510(3)	43(2)
C(5O)	689(8)	9271(8)	-2188(5)	100(5)
C(5T)	4172(7)	6690(8)	3517(5)	88(4)
C(5L)	-90(8)	8231(9)	-1391(5)	97(4)
C(6)	3130(4)	7922(4)	17(3)	37(2)
C(7)	3198(4)	8576(5)	-169(3)	49(2)
C(8)	2922(5)	8741(6)	-628(4)	60(2)
C(9)	2553(5)	8227(7)	-913(4)	62(2)
C(10)	2454(5)	7586(6)	-735(4)	68(3)
C(11)	2731(5)	7446(5)	-277(4)	55(2)
C(12)	-1432(4)	7125(6)	-4495(3)	48(2)
C(13)	-1847(4)	7038(5)	-4981(3)	39(2)
C(14)	-2369(4)	7490(5)	-5158(3)	49(2)
C(15)	-2736(5)	7456(6)	-5609(4)	61(2)
C(16)	-2587(5)	6951(7)	-5892(4)	68(3)
C(17)	-2105(6)	6466(7)	-5723(4)	75(3)
C(18)	-1748(5)	6501(5)	-5269(4)	59(2)
C(19)	3990(4)	6092(5)	-324(3)	39(2)
C(20)	3850(6)	6623(5)	-650(3)	59(3)
C(21)	3650(7)	6466(6)	-1122(4)	74(3)
C(22)	3586(6)	5780(6)	-1267(4)	64(3)
C(23)	3730(5)	5257(5)	-949(4)	56(2)
C(24)	3934(5)	5417(5)	-477(3)	48(2)
B(25)	5228(4)	6368(5)	461(4)	38(2)
C(26)	5622(4)	6411(5)	88(4)	45(2)
C(27)	6284(4)	6540(5)	225(4)	52(2)
C(28)	6610(5)	6678(6)	696(4)	58(2)
C(29)	6276(4)	6686(5)	1040(4)	53(2)
C(30)	5585(4)	6536(5)	951(3)	44(2)
C(31)	3940(4)	5565(4)	575(3)	40(2)
C(32)	3267(5)	5490(6)	506(4)	56(2)
C(33)	3011(6)	4941(7)	717(4)	69(3)
C(34)	3416(7)	4472(6)	997(4)	69(3)
C(35)	4096(7)	4539(6)	1064(4)	68(3)
C(36)	4364(5)	5082(5)	856(3)	52(2)

Appendix A

C(37)	5756(4)	8654(5)	966(3)	42(2)
C(38)	6038(4)	8319(5)	660(3)	48(2)
C(39)	6627(5)	8556(6)	577(4)	59(2)
C(40)	6918(5)	9158(6)	812(4)	62(3)
C(41)	6640(5)	9482(6)	1126(4)	63(3)
C(42)	6051(5)	9249(5)	1208(4)	53(2)
B(43)	5201(8)	8307(7)	1774(4)	67(2)
C(44)	5720(6)	7785(8)	1972(4)	75(2)
C(45)	5973(6)	7756(9)	2448(4)	85(3)
C(46)	5785(8)	8202(8)	2744(4)	91(3)
C(47)	5261(9)	8671(7)	2589(4)	94(3)
C(48)	4945(8)	8749(6)	2103(4)	88(3)
C(49)	4463(4)	9165(5)	907(3)	45(2)
C(50)	4552(4)	9587(5)	540(4)	48(2)
C(51)	4137(5)	10157(6)	381(5)	67(3)
C(52)	3635(5)	10322(7)	599(6)	82(3)
C(53)	3545(6)	9930(7)	937(5)	81(3)
C(54)	3931(5)	9350(6)	1101(4)	67(3)
C(55)	-399(4)	5853(5)	-4067(3)	39(2)
C(56)	-387(4)	5415(5)	-4440(3)	48(2)
C(57)	-835(5)	4856(5)	-4552(4)	60(2)
C(58)	-1276(5)	4727(6)	-4282(4)	65(3)
C(59)	-1279(5)	5141(6)	-3919(4)	62(2)
C(60)	-839(5)	5709(5)	-3794(4)	53(2)
C(61)	859(4)	6381(5)	-4154(3)	40(2)
C(62)	1165(4)	5757(5)	-3992(4)	59(3)
C(63)	1729(5)	5546(6)	-4135(5)	68(3)
C(64)	1976(5)	5946(6)	-4438(4)	62(3)
C(65)	1666(4)	6576(6)	-4591(4)	55(2)
C(66)	1106(4)	6790(5)	-4454(3)	47(2)
B(67)	476(5)	6769(6)	-3281(4)	47(2)
C(68)	432(5)	6228(6)	-2934(4)	57(2)
C(69)	760(6)	6336(7)	-2467(4)	65(2)
C(70)	1125(5)	6938(7)	-2317(4)	63(2)
C(71)	1194(5)	7439(7)	-2633(4)	63(2)
C(72)	884(5)	7380(6)	-3104(3)	55(2)
C(73)	-1085(4)	8846(5)	-5376(3)	39(2)
C(74)	-1086(4)	9509(5)	-5550(3)	46(2)
C(75)	-1341(5)	9652(5)	-6020(3)	53(2)
C(76)	-1595(5)	9102(5)	-6318(3)	53(2)
C(77)	-1590(5)	8437(5)	-6152(3)	54(2)
C(78)	-1335(5)	8300(5)	-5676(3)	48(2)
C(79)	-1134(4)	9363(5)	-4472(3)	40(2)
C(80)	-1818(5)	9420(6)	-4570(4)	60(3)
C(81)	-2103(6)	9918(7)	-4348(4)	72(3)
C(82)	-1729(6)	10365(6)	-4030(4)	70(3)
C(83)	-1051(6)	10322(6)	-3932(4)	67(3)
C(84)	-748(5)	9827(5)	-4152(3)	52(2)
B(85)	205(5)	8686(5)	-4614(4)	42(2)
C(86)	574(4)	8678(5)	-4999(4)	48(2)
C(87)	1248(5)	8590(5)	-4884(4)	53(2)
C(88)	1603(5)	8472(5)	-4417(4)	56(2)
C(89)	1288(4)	8443(5)	-4061(4)	51(2)
C(90)	596(4)	8551(5)	-4132(3)	47(2)
O(1F)	3430(40)	8050(40)	2060(20)	88(5)
C(2F)	3460(50)	8410(50)	2490(20)	101(5)
C(3F)	3030(50)	9010(40)	2360(30)	99(10)
C(4F)	2480(40)	8720(70)	1990(40)	92(9)
C(5F)	2790(50)	8190(70)	1770(30)	88(9)
O(1FA)	3254(6)	7798(9)	2166(5)	97(3)
C(2FA)	3093(10)	8042(11)	2573(5)	108(6)
C(3FA)	2751(8)	8693(9)	2480(6)	90(4)
C(4FA)	2501(12)	8695(13)	1969(7)	101(5)
C(5FA)	2727(10)	8063(13)	1789(6)	91(5)
O(1S)	-1420(15)	6860(30)	-2872(15)	70(4)
C(2S)	-1990(20)	7010(20)	-3230(11)	76(6)
C(3S)	-2562(16)	6980(40)	-3039(11)	83(7)
C(4S)	-2307(12)	6960(20)	-2529(10)	84(6)
C(5S)	-1619(12)	6790(20)	-2449(12)	81(5)
O(1SA)	-1407(13)	6780(30)	-2889(13)	70(4)

Appendix A

C(2SA)	-1966(19)	6800(20)	-3277(10)	84(6)
C(3SA)	-2532(15)	6930(30)	-3089(11)	83(6)
C(4SA)	-2357(11)	6510(20)	-2653(11)	92(7)
C(5SA)	-1654(11)	6600(20)	-2497(11)	80(6)
O(1E)	3547(12)	6140(13)	2399(11)	111(6)
C(2E)	2891(15)	6235(16)	2130(14)	134(9)
C(3E)	2553(15)	5590(20)	2100(16)	155(11)
C(4E)	2969(17)	5128(17)	2456(15)	149(10)
C(5E)	3572(14)	5486(16)	2625(12)	124(8)
O(1EA)	3667(12)	6055(12)	2271(11)	107(5)
C(2EA)	3079(16)	6059(16)	1905(13)	134(9)
C(3EA)	2753(13)	5409(18)	1925(14)	136(10)
C(4EA)	3264(14)	4934(13)	2195(14)	120(8)
C(5EA)	3853(12)	5338(14)	2324(14)	126(8)
O(1V)	-1401(14)	8642(14)	-2728(9)	92(4)
C(2V)	-1820(20)	9053(17)	-3076(8)	103(7)
C(3V)	-1962(17)	9696(14)	-2867(10)	104(7)
C(4V)	-1761(17)	9585(14)	-2356(10)	111(7)
C(5V)	-1373(19)	8966(17)	-2293(8)	109(7)
O(1VA)	-1450(20)	8510(20)	-2675(13)	89(5)
C(2VA)	-1800(30)	8870(30)	-3078(12)	98(8)
C(3VA)	-2240(20)	9370(30)	-2943(14)	114(9)
C(4VA)	-2000(30)	9410(20)	-2427(14)	115(9)
C(5VA)	-1730(20)	8720(20)	-2304(12)	98(7)
O(1H)	5465(18)	6134(17)	2574(13)	88(5)
C(2H)	5770(30)	5640(30)	2921(14)	91(7)
C(3H)	6360(20)	5410(30)	2807(14)	100(8)
C(4H)	6300(20)	5620(30)	2314(15)	109(9)
C(5H)	5640(20)	5900(30)	2164(11)	105(7)
O(1HA)	5146(7)	5991(7)	2472(5)	76(3)
C(2HA)	5688(10)	5786(14)	2835(6)	84(5)
C(3HA)	6184(10)	5541(18)	2607(8)	123(6)
C(4HA)	5809(12)	5358(15)	2128(7)	122(7)
C(5HA)	5129(11)	5509(11)	2110(6)	102(6)

Appendix A

Table 3. Bond lengths [\AA] and angles [$^\circ$] for 4.

Ir(1)-C(2)	1.919(7)	C(4O)-C(5O)	1.45(2)
Ir(1)-C(5)	2.138(8)	C(5)-C(6)	1.490(12)
Ir(1)-C(1)	2.140(7)	C(6)-C(7)	1.383(13)
Ir(1)-P(1)	2.332(2)	C(6)-C(11)	1.385(12)
Ir(1)-P(2)	2.380(2)	C(7)-C(8)	1.376(14)
Ir(1)-B(25)	2.650(10)	C(8)-C(9)	1.393(16)
P(1)-C(31)	1.827(8)	C(9)-C(10)	1.367(16)
P(1)-C(19)	1.829(9)	C(10)-C(11)	1.364(15)
P(1)-B(25)	1.914(9)	C(12)-C(13)	1.495(12)
O(1)-C(2)	1.115(9)	C(13)-C(18)	1.379(14)
Cl(1)-C(9)	1.754(11)	C(13)-C(14)	1.384(12)
K(1)-O(1HA)	2.652(12)	C(14)-C(15)	1.370(14)
K(1)-O(1F)	2.73(6)	C(15)-C(16)	1.359(16)
K(1)-O(1EA)	2.731(19)	C(16)-C(17)	1.364(17)
K(1)-O(1FA)	2.742(11)	C(17)-C(18)	1.370(16)
K(1)-O(1T)	2.776(8)	C(19)-C(24)	1.359(12)
K(1)-O(1E)	2.80(2)	C(19)-C(20)	1.379(13)
K(1)-O(1H)	2.82(2)	C(20)-C(21)	1.389(14)
K(1)-C(2F)	3.20(6)	C(21)-C(22)	1.371(16)
K(1)-C(47)	3.218(13)	C(22)-C(23)	1.354(15)
K(1)-C(45)	3.240(12)	C(23)-C(24)	1.391(14)
K(1)-C(46)	3.265(13)	B(25)-C(30)	1.495(14)
K(1)-C(48)	3.293(13)	B(25)-C(26)	1.528(13)
O(1L)-C(2L)	1.419(16)	C(26)-C(27)	1.360(12)
O(1L)-C(5L)	1.426(16)	C(27)-C(28)	1.420(15)
O(1L)-K(2)	2.720(8)	C(28)-C(29)	1.366(14)
O(1O)-C(2O)	1.382(15)	C(29)-C(30)	1.425(11)
O(1O)-C(5O)	1.395(15)	C(31)-C(32)	1.373(13)
O(1O)-K(2)	2.698(8)	C(31)-C(36)	1.400(13)
O(1T)-C(5T)	1.412(15)	C(32)-C(33)	1.389(14)
O(1T)-C(2T)	1.432(16)	C(33)-C(34)	1.362(17)
Ir(2)-C(4)	1.918(8)	C(34)-C(35)	1.386(17)
Ir(2)-C(3)	2.127(8)	C(35)-C(36)	1.388(14)
Ir(2)-C(12)	2.137(8)	C(37)-C(38)	1.354(13)
Ir(2)-P(4)	2.327(2)	C(37)-C(42)	1.400(13)
Ir(2)-P(3)	2.387(2)	C(38)-C(39)	1.384(13)
Ir(2)-B(85)	2.670(10)	C(39)-C(40)	1.400(16)
P(2)-C(49)	1.817(10)	C(40)-C(41)	1.356(16)
P(2)-C(37)	1.870(9)	C(41)-C(42)	1.379(14)
P(2)-B(43)	1.982(12)	B(43)-C(44)	1.48(2)
O(2)-C(4)	1.118(10)	B(43)-C(48)	1.481(19)
Cl(2)-C(16)	1.81(4)	C(44)-C(45)	1.379(16)
Cl(2A)-C(16)	1.72(2)	C(45)-C(46)	1.34(2)
K(2)-O(1S)	2.71(4)	C(46)-C(47)	1.40(2)
K(2)-O(1VA)	2.77(3)	C(47)-C(48)	1.436(18)
K(2)-O(1SA)	2.78(4)	C(49)-C(50)	1.399(14)
K(2)-O(1V)	2.818(18)	C(49)-C(54)	1.412(13)
K(2)-C(71)	3.217(10)	C(50)-C(51)	1.397(13)
K(2)-C(72)	3.222(10)	C(51)-C(52)	1.391(17)
K(2)-C(70)	3.291(11)	C(52)-C(53)	1.30(2)
K(2)-B(67)	3.333(11)	C(53)-C(54)	1.382(18)
K(2)-C(5S)	3.34(3)	C(55)-C(60)	1.388(12)
K(2)-C(69)	3.405(11)	C(55)-C(56)	1.390(13)
C(2T)-C(3T)	1.514(19)	C(56)-C(57)	1.400(13)
C(2L)-C(3L)	1.503(18)	C(57)-C(58)	1.378(16)
C(2O)-C(3O)	1.45(2)	C(58)-C(59)	1.337(16)
P(3)-C(55)	1.837(9)	C(59)-C(60)	1.406(15)
P(3)-C(61)	1.866(8)	C(61)-C(66)	1.371(13)
P(3)-B(67)	1.974(11)	C(61)-C(62)	1.380(13)
C(3T)-C(4T)	1.511(19)	C(62)-C(63)	1.400(14)
C(3L)-C(4L)	1.49(2)	C(63)-C(64)	1.370(16)
C(3O)-C(4O)	1.48(2)	C(64)-C(65)	1.383(15)
P(4)-C(79)	1.825(8)	C(65)-C(66)	1.386(12)
P(4)-C(73)	1.833(9)	B(67)-C(72)	1.459(15)
P(4)-B(85)	1.916(10)	B(67)-C(68)	1.475(15)
C(4T)-C(5T)	1.555(18)	C(68)-C(69)	1.398(14)
C(4L)-C(5L)	1.54(2)	C(69)-C(70)	1.386(16)

Appendix A

C(70)-C(71)	1.369(16)		
C(71)-C(72)	1.391(14)	C(2)-Ir(1)-C(5)	93.7(3)
C(73)-C(74)	1.362(12)	C(2)-Ir(1)-C(1)	173.6(3)
C(73)-C(78)	1.386(13)	C(5)-Ir(1)-C(1)	81.8(3)
C(74)-C(75)	1.391(13)	C(2)-Ir(1)-P(1)	95.7(3)
C(75)-C(76)	1.389(15)	C(5)-Ir(1)-P(1)	99.8(3)
C(76)-C(77)	1.356(14)	C(1)-Ir(1)-P(1)	89.6(2)
C(77)-C(78)	1.402(13)	C(2)-Ir(1)-P(2)	89.1(3)
C(79)-C(80)	1.388(13)	C(5)-Ir(1)-P(2)	96.3(3)
C(79)-C(84)	1.398(13)	C(1)-Ir(1)-P(2)	86.9(2)
C(80)-C(81)	1.370(15)	P(1)-Ir(1)-P(2)	162.83(8)
C(81)-C(82)	1.364(17)	C(2)-Ir(1)-B(25)	87.0(3)
C(82)-C(83)	1.371(17)	C(5)-Ir(1)-B(25)	144.1(3)
C(83)-C(84)	1.382(14)	C(1)-Ir(1)-B(25)	99.3(3)
B(85)-C(90)	1.484(14)	P(1)-Ir(1)-B(25)	44.6(2)
B(85)-C(86)	1.522(13)	P(2)-Ir(1)-B(25)	119.5(2)
C(86)-C(87)	1.371(13)	C(31)-P(1)-C(19)	103.6(4)
C(87)-C(88)	1.417(15)	C(31)-P(1)-B(25)	116.2(4)
C(88)-C(89)	1.373(14)	C(19)-P(1)-B(25)	109.9(4)
C(89)-C(90)	1.418(12)	C(31)-P(1)-Ir(1)	121.9(3)
O(1F)-C(2F)	1.422(15)	C(19)-P(1)-Ir(1)	125.9(3)
O(1F)-C(5F)	1.424(15)	B(25)-P(1)-Ir(1)	76.5(3)
C(2F)-C(3F)	1.433(16)	O(1HA)-K(1)-O(1F)	154.4(16)
C(3F)-C(4F)	1.48(2)	O(1HA)-K(1)-O(1EA)	67.5(7)
C(4F)-C(5F)	1.432(15)	O(1F)-K(1)-O(1EA)	90(2)
O(1FA)-C(2FA)	1.406(11)	O(1HA)-K(1)-O(1FA)	144.7(5)
O(1FA)-C(5FA)	1.453(12)	O(1F)-K(1)-O(1FA)	15.3(17)
C(2FA)-C(3FA)	1.420(13)	O(1EA)-K(1)-O(1FA)	77.5(7)
C(3FA)-C(4FA)	1.475(17)	O(1HA)-K(1)-O(1T)	93.6(4)
C(4FA)-C(5FA)	1.440(13)	O(1F)-K(1)-O(1T)	99.4(12)
O(1S)-C(5S)	1.417(13)	O(1EA)-K(1)-O(1T)	90.7(7)
O(1S)-C(2S)	1.417(13)	O(1FA)-K(1)-O(1T)	91.2(3)
C(2S)-C(3S)	1.431(14)	O(1HA)-K(1)-O(1E)	74.2(7)
C(3S)-C(4S)	1.473(18)	O(1F)-K(1)-O(1E)	86(2)
C(4S)-C(5S)	1.429(14)	O(1EA)-K(1)-O(1E)	10.8(10)
O(1SA)-C(2SA)	1.422(13)	O(1FA)-K(1)-O(1E)	71.9(7)
O(1SA)-C(5SA)	1.422(13)	O(1T)-K(1)-O(1E)	81.7(7)
C(2SA)-C(3SA)	1.440(14)	O(1HA)-K(1)-O(1H)	14.5(8)
C(3SA)-C(4SA)	1.483(18)	O(1F)-K(1)-O(1H)	167.5(15)
C(4SA)-C(5SA)	1.433(14)	O(1EA)-K(1)-O(1H)	81.6(10)
O(1E)-C(5E)	1.407(14)	O(1FA)-K(1)-O(1H)	159.0(10)
O(1E)-C(2E)	1.415(14)	O(1T)-K(1)-O(1H)	90.3(7)
C(2E)-C(3E)	1.412(14)	O(1E)-K(1)-O(1H)	87.6(10)
C(3E)-C(4E)	1.474(18)	O(1HA)-K(1)-C(2F)	164(2)
C(4E)-C(5E)	1.408(14)	O(1F)-K(1)-C(2F)	26.2(7)
O(1EA)-C(5EA)	1.417(14)	O(1EA)-K(1)-C(2F)	100(2)
O(1EA)-C(2EA)	1.424(14)	O(1FA)-K(1)-C(2F)	27.9(16)
C(2EA)-C(3EA)	1.418(14)	O(1T)-K(1)-C(2F)	75.2(12)
C(3EA)-C(4EA)	1.475(18)	O(1E)-K(1)-C(2F)	92(2)
C(4EA)-C(5EA)	1.418(14)	O(1H)-K(1)-C(2F)	165.3(13)
O(1V)-C(2V)	1.411(13)	O(1HA)-K(1)-C(47)	120.9(5)
O(1V)-C(5V)	1.419(13)	O(1F)-K(1)-C(47)	82.2(18)
C(2V)-C(3V)	1.435(14)	O(1EA)-K(1)-C(47)	170.9(7)
C(3V)-C(4V)	1.484(17)	O(1FA)-K(1)-C(47)	94.3(5)
C(4V)-C(5V)	1.415(14)	O(1T)-K(1)-C(47)	85.4(3)
O(1VA)-C(2VA)	1.415(14)	O(1E)-K(1)-C(47)	160.8(7)
O(1VA)-C(5VA)	1.424(14)	O(1H)-K(1)-C(47)	106.6(9)
C(2VA)-C(3VA)	1.439(15)	C(2F)-K(1)-C(47)	71(2)
C(3VA)-C(4VA)	1.489(18)	O(1HA)-K(1)-C(45)	79.2(5)
C(4VA)-C(5VA)	1.432(15)	O(1F)-K(1)-C(45)	119.6(19)
O(1H)-C(2H)	1.420(14)	O(1EA)-K(1)-C(45)	145.7(7)
O(1H)-C(5H)	1.425(14)	O(1FA)-K(1)-C(45)	134.2(5)
C(2H)-C(3H)	1.431(15)	O(1T)-K(1)-C(45)	99.8(3)
C(3H)-C(4H)	1.486(18)	O(1E)-K(1)-C(45)	153.4(7)
C(4H)-C(5H)	1.425(15)	O(1H)-K(1)-C(45)	65.9(9)
O(1HA)-C(5HA)	1.405(12)	C(2F)-K(1)-C(45)	114(2)
O(1HA)-C(2HA)	1.410(12)	C(47)-K(1)-C(45)	43.4(4)
C(2HA)-C(3HA)	1.442(13)	O(1HA)-K(1)-C(46)	96.3(5)
C(3HA)-C(4HA)	1.483(17)	O(1F)-K(1)-C(46)	107.1(19)
C(4HA)-C(5HA)	1.434(14)	O(1EA)-K(1)-C(46)	162.1(7)

Appendix A

O(1FA)-K(1)-C(46)	119.0(5)	O(1O)-K(2)-C(72)	83.8(3)
O(1T)-K(1)-C(46)	82.3(3)	O(1S)-K(2)-C(72)	118.6(9)
O(1E)-K(1)-C(46)	160.8(7)	O(1L)-K(2)-C(72)	125.2(3)
O(1H)-K(1)-C(46)	81.9(9)	O(1VA)-K(2)-C(72)	146.0(9)
C(2F)-K(1)-C(46)	94(2)	O(1SA)-K(2)-C(72)	116.0(8)
C(47)-K(1)-C(46)	24.9(4)	O(1V)-K(2)-C(72)	139.8(6)
C(45)-K(1)-C(46)	23.8(4)	C(71)-K(2)-C(72)	25.0(2)
O(1HA)-K(1)-C(48)	128.4(5)	O(1O)-K(2)-C(70)	93.5(3)
O(1F)-K(1)-C(48)	67.8(19)	O(1S)-K(2)-C(70)	118.0(11)
O(1EA)-K(1)-C(48)	152.8(7)	O(1L)-K(2)-C(70)	83.2(3)
O(1FA)-K(1)-C(48)	82.6(5)	O(1VA)-K(2)-C(70)	163.9(8)
O(1T)-K(1)-C(48)	108.1(3)	O(1SA)-K(2)-C(70)	115.4(10)
O(1E)-K(1)-C(48)	153.0(7)	O(1V)-K(2)-C(70)	163.0(6)
O(1H)-K(1)-C(48)	116.7(9)	C(71)-K(2)-C(70)	24.3(3)
C(2F)-K(1)-C(48)	67(2)	C(72)-K(2)-C(70)	43.5(3)
C(47)-K(1)-C(48)	25.4(3)	O(1O)-K(2)-B(67)	108.3(3)
C(45)-K(1)-C(48)	51.7(4)	O(1S)-K(2)-B(67)	93.1(9)
C(46)-K(1)-C(48)	44.3(4)	O(1L)-K(2)-B(67)	131.1(3)
C(2L)-O(1L)-C(5L)	105.6(10)	O(1VA)-K(2)-B(67)	144.4(8)
C(2L)-O(1L)-K(2)	117.4(8)	O(1SA)-K(2)-B(67)	90.4(8)
C(5L)-O(1L)-K(2)	127.0(8)	O(1V)-K(2)-B(67)	141.6(5)
C(2O)-O(1O)-C(5O)	107.2(10)	C(71)-K(2)-B(67)	44.4(3)
C(2O)-O(1O)-K(2)	122.9(8)	C(72)-K(2)-B(67)	25.7(3)
C(5O)-O(1O)-K(2)	129.1(8)	C(70)-K(2)-B(67)	51.2(3)
C(5T)-O(1T)-C(2T)	105.8(10)	O(1O)-K(2)-C(5S)	140.0(8)
C(5T)-O(1T)-K(1)	118.0(8)	O(1S)-K(2)-C(5S)	24.3(5)
C(2T)-O(1T)-K(1)	124.3(7)	O(1L)-K(2)-C(5S)	70.2(7)
C(4)-Ir(2)-C(3)	174.4(4)	O(1VA)-K(2)-C(5S)	66.3(13)
C(4)-Ir(2)-C(12)	93.5(4)	O(1SA)-K(2)-C(5S)	25.8(12)
C(3)-Ir(2)-C(12)	82.2(4)	O(1V)-K(2)-C(5S)	72.7(9)
C(4)-Ir(2)-P(4)	94.5(3)	C(71)-K(2)-C(5S)	138.7(7)
C(3)-Ir(2)-P(4)	89.8(3)	C(72)-K(2)-C(5S)	136.2(8)
C(12)-Ir(2)-P(4)	101.9(3)	C(70)-K(2)-C(5S)	116.3(7)
C(4)-Ir(2)-P(3)	90.0(3)	B(67)-K(2)-C(5S)	111.2(8)
C(3)-Ir(2)-P(3)	86.9(2)	O(1O)-K(2)-C(69)	117.0(3)
C(12)-Ir(2)-P(3)	95.0(3)	O(1S)-K(2)-C(69)	94.5(11)
P(4)-Ir(2)-P(3)	162.19(8)	O(1L)-K(2)-C(69)	88.1(3)
C(4)-Ir(2)-B(85)	86.3(3)	O(1VA)-K(2)-C(69)	162.6(10)
C(3)-Ir(2)-B(85)	99.3(3)	O(1SA)-K(2)-C(69)	91.8(10)
C(12)-Ir(2)-B(85)	146.0(3)	O(1V)-K(2)-C(69)	169.3(7)
P(4)-Ir(2)-B(85)	44.4(2)	C(71)-K(2)-C(69)	42.1(3)
P(3)-Ir(2)-B(85)	119.0(2)	C(72)-K(2)-C(69)	49.8(3)
O(1)-C(2)-Ir(1)	173.8(8)	C(70)-K(2)-C(69)	23.8(3)
C(49)-P(2)-C(37)	100.1(4)	B(67)-K(2)-C(69)	43.2(3)
C(49)-P(2)-B(43)	110.0(6)	C(5S)-K(2)-C(69)	96.6(7)
C(37)-P(2)-B(43)	101.0(5)	O(1T)-C(2T)-C(3T)	105.2(12)
C(49)-P(2)-Ir(1)	110.6(3)	O(1L)-C(2L)-C(3L)	107.5(12)
C(37)-P(2)-Ir(1)	113.2(3)	O(1O)-C(2O)-C(3O)	106.3(14)
B(43)-P(2)-Ir(1)	119.8(4)	C(55)-P(3)-C(61)	101.9(4)
O(1O)-K(2)-O(1S)	148.4(11)	C(55)-P(3)-B(67)	109.6(5)
O(1O)-K(2)-O(1L)	89.0(3)	C(61)-P(3)-B(67)	101.7(4)
O(1S)-K(2)-O(1L)	94.2(9)	C(55)-P(3)-Ir(2)	109.2(3)
O(1O)-K(2)-O(1VA)	77.8(10)	C(61)-P(3)-Ir(2)	112.5(3)
O(1S)-K(2)-O(1VA)	71.5(17)	B(67)-P(3)-Ir(2)	120.3(4)
O(1L)-K(2)-O(1VA)	83.0(8)	C(4T)-C(3T)-C(2T)	104.8(11)
O(1O)-K(2)-O(1SA)	151.0(10)	C(4L)-C(3L)-C(2L)	104.4(13)
O(1S)-K(2)-O(1SA)	2.9(19)	C(2O)-C(3O)-C(4O)	104.5(14)
O(1L)-K(2)-O(1SA)	95.2(8)	O(2)-C(4)-Ir(2)	176.5(9)
O(1VA)-K(2)-O(1SA)	74.3(11)	C(79)-P(4)-C(73)	103.7(4)
O(1O)-K(2)-O(1V)	72.4(7)	C(79)-P(4)-B(85)	117.0(4)
O(1S)-K(2)-O(1V)	76.5(11)	C(73)-P(4)-B(85)	110.0(4)
O(1L)-K(2)-O(1V)	86.9(5)	C(79)-P(4)-Ir(2)	121.4(3)
O(1VA)-K(2)-O(1V)	6.7(14)	C(73)-P(4)-Ir(2)	125.2(3)
O(1SA)-K(2)-O(1V)	79.2(13)	B(85)-P(4)-Ir(2)	77.3(3)
O(1O)-K(2)-C(71)	77.2(3)	C(3T)-C(4T)-C(5T)	103.7(11)
O(1S)-K(2)-C(71)	132.5(11)	C(3L)-C(4L)-C(5L)	105.1(13)
O(1L)-K(2)-C(71)	100.7(3)	C(5O)-C(4O)-C(3O)	105.5(15)
O(1VA)-K(2)-C(71)	154.6(10)	C(6)-C(5)-Ir(1)	115.5(5)
O(1SA)-K(2)-C(71)	129.6(9)	O(1O)-C(5O)-C(4O)	106.2(13)
O(1V)-K(2)-C(71)	148.5(7)	O(1T)-C(5T)-C(4T)	103.3(11)

Appendix A

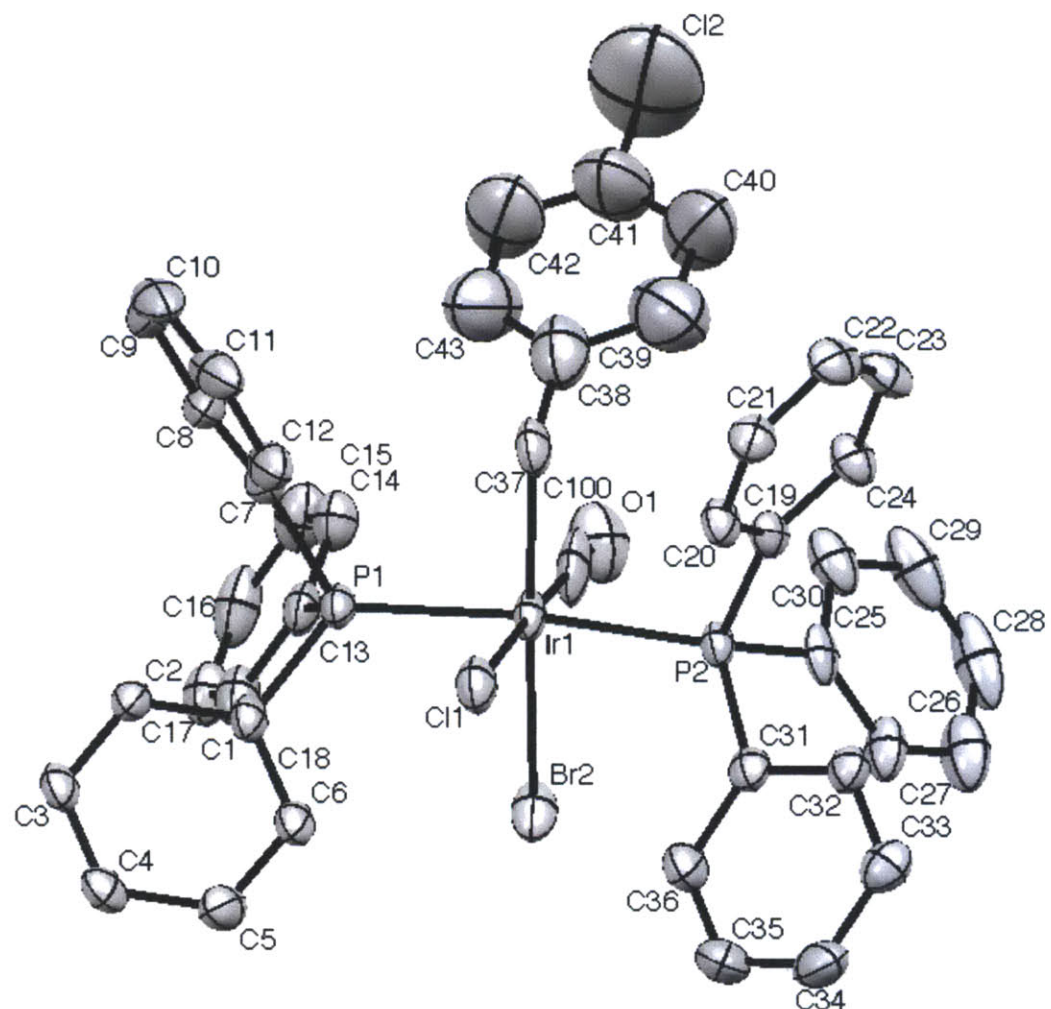
O(1L)-C(5L)-C(4L)	104.0(12)	C(46)-C(45)-K(1)	79.1(8)
C(7)-C(6)-C(11)	116.3(9)	C(44)-C(45)-K(1)	81.1(7)
C(7)-C(6)-C(5)	121.2(8)	C(45)-C(46)-C(47)	121.1(13)
C(11)-C(6)-C(5)	122.5(8)	C(45)-C(46)-K(1)	77.0(7)
C(8)-C(7)-C(6)	122.7(9)	C(47)-C(46)-K(1)	75.7(8)
C(7)-C(8)-C(9)	118.3(10)	C(46)-C(47)-C(48)	121.7(14)
C(10)-C(9)-C(8)	120.4(10)	C(46)-C(47)-K(1)	79.5(8)
C(10)-C(9)-Cl(1)	121.9(9)	C(48)-C(47)-K(1)	80.2(7)
C(8)-C(9)-Cl(1)	117.7(9)	C(47)-C(48)-B(43)	116.7(14)
C(11)-C(10)-C(9)	119.4(10)	C(47)-C(48)-K(1)	74.4(7)
C(10)-C(11)-C(6)	122.7(10)	B(43)-C(48)-K(1)	80.6(7)
C(13)-C(12)-Ir(2)	117.3(6)	C(50)-C(49)-C(54)	115.9(10)
C(18)-C(13)-C(14)	116.8(9)	C(50)-C(49)-P(2)	122.0(7)
C(18)-C(13)-C(12)	122.5(8)	C(54)-C(49)-P(2)	121.8(9)
C(14)-C(13)-C(12)	120.7(9)	C(51)-C(50)-C(49)	121.5(10)
C(15)-C(14)-C(13)	122.6(10)	C(52)-C(51)-C(50)	119.4(12)
C(16)-C(15)-C(14)	118.5(10)	C(53)-C(52)-C(51)	119.7(12)
C(15)-C(16)-C(17)	120.8(11)	C(52)-C(53)-C(54)	123.3(12)
C(15)-C(16)-Cl(2A)	125(3)	C(53)-C(54)-C(49)	120.3(12)
C(17)-C(16)-Cl(2A)	114(3)	C(60)-C(55)-C(56)	119.1(9)
C(15)-C(16)-Cl(2)	112(2)	C(60)-C(55)-P(3)	119.7(7)
C(17)-C(16)-Cl(2)	127(2)	C(56)-C(55)-P(3)	121.0(7)
Cl(2A)-C(16)-Cl(2)	13(3)	C(55)-C(56)-C(57)	120.2(9)
C(16)-C(17)-C(18)	120.1(11)	C(58)-C(57)-C(56)	119.9(11)
C(17)-C(18)-C(13)	120.9(10)	C(59)-C(58)-C(57)	119.7(10)
C(24)-C(19)-C(20)	118.3(9)	C(58)-C(59)-C(60)	122.3(10)
C(24)-C(19)-P(1)	120.2(7)	C(55)-C(60)-C(59)	118.7(10)
C(20)-C(19)-P(1)	121.5(7)	C(66)-C(61)-C(62)	120.1(8)
C(19)-C(20)-C(21)	120.5(10)	C(66)-C(61)-P(3)	121.3(7)
C(22)-C(21)-C(20)	120.1(11)	C(62)-C(61)-P(3)	118.6(7)
C(23)-C(22)-C(21)	119.7(10)	C(61)-C(62)-C(63)	119.4(10)
C(22)-C(23)-C(24)	120.0(10)	C(64)-C(63)-C(62)	121.0(10)
C(19)-C(24)-C(23)	121.4(10)	C(63)-C(64)-C(65)	118.6(9)
C(30)-B(25)-C(26)	117.5(8)	C(64)-C(65)-C(66)	121.1(10)
C(30)-B(25)-P(1)	120.0(7)	C(61)-C(66)-C(65)	119.9(9)
C(26)-B(25)-P(1)	121.4(7)	C(72)-B(67)-C(68)	115.8(9)
C(30)-B(25)-Ir(1)	80.6(5)	C(72)-B(67)-P(3)	120.1(8)
C(26)-B(25)-Ir(1)	123.5(6)	C(68)-B(67)-P(3)	123.7(8)
P(1)-B(25)-Ir(1)	58.8(3)	C(72)-B(67)-K(2)	72.9(6)
C(27)-C(26)-B(25)	118.5(9)	C(68)-B(67)-K(2)	81.2(6)
C(26)-C(27)-C(28)	122.3(9)	P(3)-B(67)-K(2)	120.8(4)
C(29)-C(28)-C(27)	121.7(9)	C(69)-C(68)-B(67)	119.2(10)
C(28)-C(29)-C(30)	122.3(10)	C(69)-C(68)-K(2)	77.1(7)
C(29)-C(30)-B(25)	117.5(9)	B(67)-C(68)-K(2)	73.7(6)
C(32)-C(31)-C(36)	119.6(8)	C(70)-C(69)-C(68)	122.4(11)
C(32)-C(31)-P(1)	120.5(8)	C(70)-C(69)-K(2)	73.5(6)
C(36)-C(31)-P(1)	119.9(7)	C(68)-C(69)-K(2)	79.3(6)
C(31)-C(32)-C(33)	119.9(11)	C(71)-C(70)-C(69)	119.8(10)
C(34)-C(33)-C(32)	121.3(10)	C(71)-C(70)-K(2)	74.8(6)
C(33)-C(34)-C(35)	119.1(10)	C(69)-C(70)-K(2)	82.7(6)
C(34)-C(35)-C(36)	120.7(11)	C(70)-C(71)-C(72)	122.0(11)
C(35)-C(36)-C(31)	119.3(10)	C(70)-C(71)-K(2)	80.9(6)
C(38)-C(37)-C(42)	121.0(9)	C(72)-C(71)-K(2)	77.7(6)
C(38)-C(37)-P(2)	123.3(7)	C(71)-C(72)-B(67)	120.7(10)
C(42)-C(37)-P(2)	115.7(7)	C(71)-C(72)-K(2)	77.3(6)
C(37)-C(38)-C(39)	120.9(10)	B(67)-C(72)-K(2)	81.4(6)
C(38)-C(39)-C(40)	118.2(11)	C(74)-C(73)-C(78)	119.2(9)
C(41)-C(40)-C(39)	120.6(9)	C(74)-C(73)-P(4)	119.8(7)
C(40)-C(41)-C(42)	121.4(10)	C(78)-C(73)-P(4)	121.0(7)
C(41)-C(42)-C(37)	117.9(10)	C(73)-C(74)-C(75)	121.7(9)
C(44)-B(43)-C(48)	117.8(11)	C(76)-C(75)-C(74)	118.7(9)
C(44)-B(43)-P(2)	115.8(10)	C(77)-C(76)-C(75)	120.4(9)
C(48)-B(43)-P(2)	126.3(11)	C(76)-C(77)-C(78)	120.3(10)
C(44)-B(43)-K(1)	74.9(7)	C(73)-C(78)-C(77)	119.7(9)
C(48)-B(43)-K(1)	73.8(7)	C(80)-C(79)-C(84)	118.8(9)
P(2)-B(43)-K(1)	124.4(5)	C(80)-C(79)-P(4)	120.5(8)
C(45)-C(44)-B(43)	119.4(13)	C(84)-C(79)-P(4)	120.6(7)
C(45)-C(44)-K(1)	74.6(7)	C(81)-C(80)-C(79)	119.8(11)
B(43)-C(44)-K(1)	79.6(7)	C(82)-C(81)-C(80)	121.5(11)
C(46)-C(45)-C(44)	122.8(15)	C(81)-C(82)-C(83)	119.6(10)

Appendix A

C(82)-C(83)-C(84)	120.3(11)	C(5SA)-C(4SA)-C(3SA)	103.4(13)
C(83)-C(84)-C(79)	120.0(10)	O(1SA)-C(5SA)-C(4SA)	108.1(12)
C(90)-B(85)-C(86)	117.4(8)	C(5E)-O(1E)-C(2E)	107.3(13)
C(90)-B(85)-P(4)	120.1(7)	C(5E)-O(1E)-K(1)	133.6(16)
C(86)-B(85)-P(4)	121.4(7)	C(2E)-O(1E)-K(1)	119.1(16)
C(90)-B(85)-Ir(2)	81.1(6)	C(3E)-C(2E)-O(1E)	108.7(14)
C(86)-B(85)-Ir(2)	123.5(7)	C(2E)-C(3E)-C(4E)	106.0(13)
P(4)-B(85)-Ir(2)	58.2(3)	C(5E)-C(4E)-C(3E)	106.5(12)
C(87)-C(86)-B(85)	119.2(9)	O(1E)-C(5E)-C(4E)	109.5(13)
C(86)-C(87)-C(88)	121.3(9)	C(5EA)-O(1EA)-C(2EA)	104.4(15)
C(89)-C(88)-C(87)	121.6(9)	C(5EA)-O(1EA)-K(1)	127.3(15)
C(88)-C(89)-C(90)	122.5(9)	C(2EA)-O(1EA)-K(1)	119.6(17)
C(89)-C(90)-B(85)	117.9(9)	C(3EA)-C(2EA)-O(1EA)	107.1(14)
C(2F)-O(1F)-C(5F)	106.0(18)	C(2EA)-C(3EA)-C(4EA)	105.6(13)
C(2F)-O(1F)-K(1)	96(3)	C(5EA)-C(4EA)-C(3EA)	105.9(13)
C(5F)-O(1F)-K(1)	152(5)	O(1EA)-C(5EA)-C(4EA)	107.4(14)
O(1F)-C(2F)-C(3F)	105(2)	C(2V)-O(1V)-C(5V)	107.6(12)
O(1F)-C(2F)-K(1)	58(3)	C(2V)-O(1V)-K(2)	138.8(17)
C(3F)-C(2F)-K(1)	160(4)	C(5V)-O(1V)-K(2)	109.9(15)
C(2F)-C(3F)-C(4F)	102.5(19)	O(1V)-C(2V)-C(3V)	108.4(13)
C(5F)-C(4F)-C(3F)	104.5(19)	C(2V)-C(3V)-C(4V)	106.3(12)
O(1F)-C(5F)-C(4F)	108.1(14)	C(5V)-C(4V)-C(3V)	105.3(12)
C(2FA)-O(1FA)-C(5FA)	104.5(10)	C(4V)-C(5V)-O(1V)	110.3(12)
C(2FA)-O(1FA)-K(1)	109.2(9)	C(2VA)-O(1VA)-C(5VA)	106.7(15)
C(5FA)-O(1FA)-K(1)	145.5(11)	C(2VA)-O(1VA)-K(2)	124(2)
O(1FA)-C(2FA)-C(3FA)	109.6(11)	C(5VA)-O(1VA)-K(2)	129(2)
O(1FA)-C(2FA)-K(1)	48.3(7)	O(1VA)-C(2VA)-C(3VA)	108.4(13)
C(3FA)-C(2FA)-K(1)	140.7(13)	C(2VA)-C(3VA)-C(4VA)	104.2(15)
C(2FA)-C(3FA)-C(4FA)	103.6(10)	C(5VA)-C(4VA)-C(3VA)	103.0(15)
C(5FA)-C(4FA)-C(3FA)	108.3(11)	O(1VA)-C(5VA)-C(4VA)	105.8(15)
C(4FA)-C(5FA)-O(1FA)	105.0(10)	C(2H)-O(1H)-C(5H)	104.3(17)
C(5S)-O(1S)-C(2S)	107.7(12)	C(2H)-O(1H)-K(1)	141.2(19)
C(5S)-O(1S)-K(2)	104(2)	C(5H)-O(1H)-K(1)	113.2(19)
C(2S)-O(1S)-K(2)	125(3)	O(1H)-C(2H)-C(3H)	107.1(17)
O(1S)-C(2S)-C(3S)	109.0(12)	C(2H)-C(3H)-C(4H)	105.4(13)
C(2S)-C(3S)-C(4S)	106.2(13)	C(5H)-C(4H)-C(3H)	105.3(14)
C(5S)-C(4S)-C(3S)	105.9(13)	C(4H)-C(5H)-O(1H)	106.1(17)
O(1S)-C(5S)-C(4S)	109.2(13)	C(5HA)-O(1HA)-C(2HA)	105.4(11)
O(1S)-C(5S)-K(2)	52(2)	C(5HA)-O(1HA)-K(1)	125.9(10)
C(4S)-C(5S)-K(2)	132(2)	C(2HA)-O(1HA)-K(1)	127.1(12)
C(2SA)-O(1SA)-C(5SA)	106.1(13)	O(1HA)-C(2HA)-C(3HA)	105.3(12)
C(2SA)-O(1SA)-K(2)	130(3)	C(2HA)-C(3HA)-C(4HA)	104.7(11)
C(5SA)-O(1SA)-K(2)	111(2)	C(5HA)-C(4HA)-C(3HA)	105.8(11)
O(1SA)-C(2SA)-C(3SA)	106.0(14)	O(1HA)-C(5HA)-C(4HA)	105.2(12)
C(2SA)-C(3SA)-C(4SA)	101.4(16)		

Appendix A

Crystal data and structure refinement for 6



Appendix A

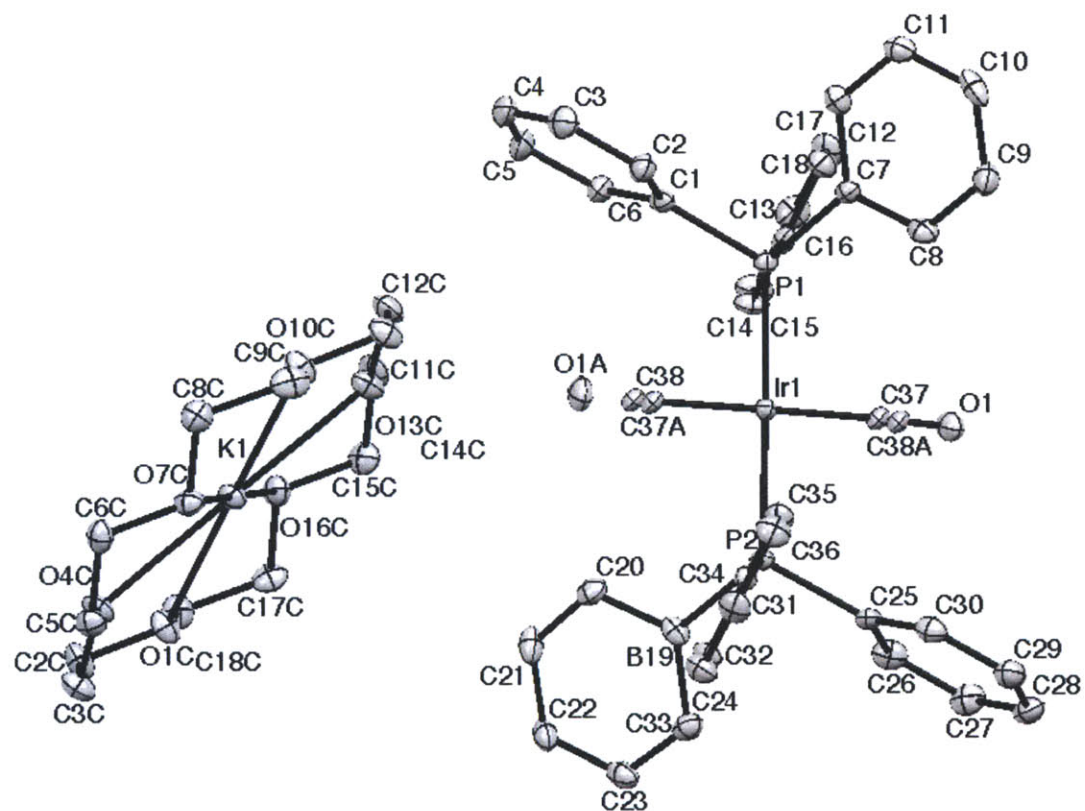
Table 3. Bond lengths [Å] and angles [°] for 6.

Number	Atom1	Atom2	Length					
1	Ir1	Br2	2.6424(9)	48	C8	C9	1.40(1)	
2	Ir1	P2	2.378(1)	49	C9	H9	0.950(8)	
3	Ir1	P1	2.368(2)	50	C9	C10	1.43(2)	
4	Ir1	C100	1.97(1)	51	C11	H11	0.95(1)	
5	Ir1	C37	2.110(8)	52	C11	C10	1.35(1)	
6	Ir1	C11	2.632(2)	53	C10	H10	0.948(9)	
7	P2	C19	1.838(7)	54	C30	H30	0.951(8)	
8	P2	C25	1.82(1)	55	C24	H24	0.949(9)	
9	P2	C31	1.825(5)	56	C32	H32	0.951(6)	
10	P1	C1	1.835(6)	57	C32	C31	1.403(9)	
11	P1	C7	1.827(8)	58	C32	C33	1.393(8)	
12	P1	C13	1.808(8)	59	C31	C36	1.394(8)	
13	C19	C20	1.36(1)	60	C13	C18	1.400(9)	
14	C19	C24	1.382(8)	61	C13	C14	1.412(9)	
15	C20	H20	0.949(6)	62	C33	H33	0.950(7)	
16	C20	C21	1.38(1)	63	C33	C34	1.41(1)	
17	C3	H3	0.949(7)	64	O1	C100	1.10(2)	
18	C3	C2	1.391(8)	65	C37	H37A	0.989(9)	
19	C3	C4	1.373(8)	66	C37	H37B	0.991(7)	
20	C2	H2	0.950(5)	67	C37	C38	1.55(1)	
21	C2	C1	1.395(9)	68	C34	H34	0.950(6)	
22	C21	H21	0.951(9)	69	C34	C35	1.35(1)	
23	C21	C22	1.396(9)	70	C36	H36	0.951(7)	
24	C25	C26	1.37(1)	71	C36	C35	1.383(9)	
25	C25	C30	1.414(9)	72	C18	H18	0.950(7)	
26	C1	C6	1.403(8)	73	C18	C17	1.41(1)	
27	C22	H22	0.950(8)	74	C17	H17	0.951(8)	
28	C22	C23	1.37(1)	75	C17	C16	1.33(1)	
29	C4	H4	0.951(6)	76	C14	H14	0.951(7)	
30	C4	C5	1.40(1)	77	C14	C15	1.40(1)	
31	C26	H26	0.949(6)	78	C35	H35	0.949(7)	
32	C26	C27	1.38(2)	79	C15	H15	0.950(7)	
33	C12	H12	0.951(6)	80	C15	C16	1.39(1)	
34	C12	C7	1.41(1)	81	C16	H16	0.95(1)	
35	C12	C11	1.38(1)	82	C28	H28	0.95(1)	
36	C6	H6	0.950(7)	83	C12	C41	1.76(1)	
37	C6	C5	1.391(9)	84	C38	C43	1.35(2)	
38	C7	C8	1.399(8)	85	C38	C39	1.38(2)	
39	C23	H23	0.949(6)	86	C43	H43	0.95(1)	
40	C23	C24	1.39(1)	87	C43	C42	1.46(2)	
41	C5	H5	0.950(6)	88	C39	H39	0.95(1)	
42	C27	H27	0.95(1)	89	C39	C40	1.45(2)	
43	C27	C28	1.40(1)	90	C40	H40	0.95(2)	
44	C29	H29	0.949(7)	91	C40	C41	1.35(2)	
45	C29	C30	1.41(2)	92	C41	C42	1.35(2)	
46	C29	C28	1.34(2)	93	C42	H42	0.95(1)	
47	C8	H8	0.951(9)					
Number	Atom1	Atom2	Atom3	Angle				
1	Br2	Ir1	P2	90.15(4)	20	C19	P2	C31 100.4(3)
2	Br2	Ir1	P1	87.77(5)	21	C25	P2	C31 101.9(3)
3	Br2	Ir1	C100	80.1(3)	22	Ir1	P1	C1 116.8(2)
4	Br2	Ir1	C37	170.2(2)	23	Ir1	P1	C7 115.3(2)
5	Br2	Ir1	C11	98.63(5)	24	Ir1	P1	C13 115.6(2)
6	P2	Ir1	P1	170.94(6)	25	C1	P1	C7 100.1(3)
7	P2	Ir1	C100	94.7(3)	26	C1	P1	C13 102.3(3)
8	P2	Ir1	C37	91.1(2)	27	C7	P1	C13 104.6(3)
9	P2	Ir1	C11	83.82(6)	28	P2	C19	C20 119.1(5)
10	P1	Ir1	C100	93.6(3)	29	P2	C19	C24 123.1(5)
11	P1	Ir1	C37	92.5(2)	30	C20	C19	C24 117.8(6)
12	P1	Ir1	C11	87.78(6)	31	C19	C20	H20 118.8(7)
13	C100	Ir1	C37	90.1(4)	32	C19	C20	C21 122.4(6)
14	C100	Ir1	C11	178.0(3)	33	H20	C20	C21 118.8(7)
15	C37	Ir1	C11	91.2(2)	34	H3	C3	C2 119.8(7)
16	Ir1	P2	C19	113.9(2)	35	H3	C3	C4 119.8(7)
17	Ir1	P2	C25	114.0(2)	36	C2	C3	C4 120.4(6)
18	Ir1	P2	C31	119.1(2)	37	C3	C2	H2 120.0(7)
19	C19	P2	C25	105.6(3)	38	C3	C2	C1 119.9(6)

Appendix A

39	H2	C2	C1 120.1(6)	101	P2	C31 C36 123.8(5)
40	C20	C21	H21 120.4(7)	102	C32	C31 C36 118.0(6)
41	C20	C21	C22 119.1(7)	103	P1	C13 C18 122.2(6)
42	H21	C21	C22 120.5(7)	104	P1	C13 C14 120.7(6)
43	P2	C25	C26 121.7(6)	105	C18	C13 C14 117.1(7)
44	P2	C25	C30 118.0(5)	106	C32	C33 H33 120.5(7)
45	C26	C25	C30 120.3(7)	107	C32	C33 C34 119.2(7)
46	P1	C1	C2 118.4(5)	108	H33	C33 C34 120.3(8)
47	P1	C1	C6 121.5(5)	109	Ir1	C100 O1 178.2(9)
48	C2	C1	C6 119.9(6)	110	Ir1	C37 H37A 107.3(5)
49	C21	C22	H22 120.3(7)	111	Ir1	C37 H37B 107.4(5)
50	C21	C22	C23 119.4(7)	112	Ir1	C37 C38 120.0(6)
51	H22	C22	C23 120.3(7)	113	H37A	C37 H37B 106.8(7)
52	C3	C4	H4 119.9(7)	114	H37A	C37 C38 107.3(7)
53	C3	C4	C5 120.4(7)	115	H37B	C37 C38 107.3(7)
54	H4	C4	C5 119.8(7)	116	C33	C34 H34 120.7(8)
55	C25	C26	H26 119.9(7)	117	C33	C34 C35 118.8(8)
56	C25	C26	C27 120.3(8)	118	H34	C34 C35 120.5(8)
57	H26	C26	C27 119.9(8)	119	C31	C36 H36 120.1(8)
58	H12	C12	C7 120.3(7)	120	C31	C36 C35 119.7(7)
59	H12	C12	C11 119.9(8)	121	H36	C36 C35 120.0(8)
60	C7	C12	C11 119.7(7)	122	C13	C18 C18 119.5(7)
61	C1	C6	H6 120.1(7)	123	C13	C18 C17 121.1(7)
62	C1	C6	C5 119.5(6)	124	H18	C18 C17 119.4(8)
63	H6	C6	C5 120.3(7)	125	C18	C17 H17 120.4(8)
64	P1	C7	C12 117.0(5)	126	C18	C17 C16 119.3(8)
65	P1	C7	C8 123.7(5)			
66	C12	C7	C8 119.3(7)	127	H17	C17 C16 120.3(9)
67	C22	C23	H23 119.9(7)	128	C13	C14 H14 119.2(8)
68	C22	C23	C24 120.1(7)	129	C13	C14 C15 121.5(7)
69	H23	C23	C24 120.0(7)	130	H14	C14 C15 119.3(8)
70	C4	C5	C6 119.9(7)	131	C34	C35 C36 122.7(8)
71	C4	C5	H5 120.2(7)	132	C34	C35 H35 118.6(8)
72	C6	C5	H5 119.9(7)	133	C36	C35 H35 118.7(8)
73	C26	C27	H27 120(1)	134	C14	C15 H15 121.0(8)
74	C26	C27	C28 120(1)	135	C14	C15 C16 117.8(8)
75	H27	C27	C28 120(1)	136	H15	C15 C16 121.2(9)
76	H29	C29	C30 119.6(9)	137	C17	C16 C15 123(1)
77	H29	C29	C28 120(1)	138	C17	C16 H16 119(1)
78	C30	C29	C28 120.8(9)	139	C15	C16 H16 118(1)
79	C7	C8	H8 119.9(7)	140	C27	C28 C29 121(1)
80	C7	C8	C9 120.4(7)	141	C27	C28 H28 120(1)
81	H8	C8	C9 119.8(8)	142	C29	C28 H28 119(1)
82	C8	C9	H9 120.8(9)	143	C37	C38 C43 123(1)
83	C8	C9	C10 118.7(8)	144	C37	C38 C39 122(1)
84	H9	C9	C10 120.6(9)	145	C43	C38 C39 115(1)
85	C12	C11	H11 1119.3(8)	146	C38	C43 H43 118(1)
86	C12	C11	C10 121.8(8)	147	C38	C43 C42 125(1)
87	H11	C11	C10 118.9(8)	148	H43	C43 C42 118(1)
88	C9	C10	C11 120.1(8)	149	C38	C39 H39 118(2)
89	C9	C10	H10 119.9(8)	150	C38	C39 C40 124(1)
90	C11	C10	H10 120.0(8)	151	H39	C39 C40 118(2)
91	C25	C30	C29 117.9(8)	152	C39	C40 H40 122(2)
92	C25	C30	H30 120.8(8)	153	C39	C40 C41 116(2)
93	C29	C30	H30 121.3(8)	154	H40	C40 C41 122(2)
94	C19	C24	C23 121.2(7)	155	C12	C41 C40 118(1)
95	C19	C24	H24 119.4(7)	156	C12	C41 C42 118(1)
96	C23	C24	H24 119.4(7)	157	C40	C41 C42 125(2)
97	H32	C32	C31 119.5(7)	158	C43	C42 C41 116(1)
98	H32	C32	C33 119.3(7)	159	C43	C42 H42 122(1)
99	C31	C32	C33 121.2(7)	160	C41	C42 H42 122(2)
100	P2	C31	C32 118.1(5)			

Crystal data and structure refinement for 7



Appendix A

Table 3. Bond lengths [\AA] and angles [$^\circ$] for 7.

Ir(1)-C(37)	1.843(9)	C(17)-C(18)	1.389(5)
Ir(1)-C(37A)	1.867(8)	C(17C)-C(18C)	1.486(5)
Ir(1)-C(38A)	2.148(8)	B(19)-C(20)	1.475(5)
Ir(1)-C(38)	2.152(9)	B(19)-C(24)	1.487(5)
Ir(1)-P(1)	2.2800(9)	C(20)-C(21)	1.393(4)
Ir(1)-P(2)	2.3415(9)	C(21)-C(22)	1.387(5)
O(1)-C(37)	1.175(10)	C(22)-C(23)	1.397(5)
O(1A)-C(37A)	1.167(9)	C(23)-C(24)	1.381(4)
P(1)-C(7)	1.842(3)	C(25)-C(30)	1.398(5)
P(1)-C(1)	1.843(3)	C(25)-C(26)	1.415(5)
P(1)-C(13)	1.843(3)	C(26)-C(27)	1.371(5)
O(1C)-C(2C)	1.420(4)	C(27)-C(28)	1.391(5)
O(1C)-C(18C)	1.433(4)	C(28)-C(29)	1.401(5)
O(1C)-K(1)	2.777(2)	C(29)-C(30)	1.384(5)
C(1)-C(2)	1.391(5)	C(31)-C(36)	1.396(4)
C(1)-C(6)	1.397(5)	C(31)-C(32)	1.401(4)
K(1)-O(1H)	2.752(3)	C(32)-C(33)	1.389(5)
K(1)-O(10C)	2.764(3)	C(33)-C(34)	1.385(5)
K(1)-O(1T)	2.767(3)	C(34)-C(35)	1.379(5)
K(1)-O(4C)	2.774(3)	C(35)-C(36)	1.402(5)
K(1)-O(13C)	2.789(3)		
K(1)-O(7C)	2.827(3)	C(37)-Ir(1)-C(37A)	179.0(5)
K(1)-O(16C)	2.845(3)	C(37)-Ir(1)-C(38A)	1.9(7)
K(1)-C(5T)	3.415(4)	C(37A)-Ir(1)-C(38A)	177.6(6)
K(1)-C(2H)	3.416(4)	C(37)-Ir(1)-C(38)	177.9(7)
O(1H)-C(5H)	1.434(4)	C(37A)-Ir(1)-C(38)	2.0(7)
O(1H)-C(2H)	1.446(4)	C(38A)-Ir(1)-C(38)	178.8(4)
O(1T)-C(5T)	1.413(4)	C(37)-Ir(1)-P(1)	89.3(4)
O(1T)-C(2T)	1.431(4)	C(37A)-Ir(1)-P(1)	91.7(4)
P(2)-C(31)	1.832(4)	C(38A)-Ir(1)-P(1)	90.3(3)
P(2)-C(25)	1.849(4)	C(38)-Ir(1)-P(1)	90.8(3)
P(2)-B(19)	1.931(4)	C(37)-Ir(1)-P(2)	91.2(4)
C(2C)-C(3C)	1.497(5)	C(37A)-Ir(1)-P(2)	87.8(4)
C(2)-C(3)	1.404(5)	C(38A)-Ir(1)-P(2)	90.3(3)
C(2H)-C(3H)	1.511(5)	C(38)-Ir(1)-P(2)	88.6(3)
C(2T)-C(3T)	1.520(6)	P(1)-Ir(1)-P(2)	178.26(4)
C(3)-C(4)	1.384(5)	O(1)-C(37)-Ir(1)	177.9(11)
C(3C)-O(4C)	1.419(4)	O(1A)-C(37A)-Ir(1)	176.6(10)
C(3H)-C(4H)	1.507(5)	C(7)-P(1)-C(1)	101.74(14)
C(3T)-C(4T)	1.543(5)	C(7)-P(1)-C(13)	104.56(14)
O(4C)-C(5C)	1.428(4)	C(1)-P(1)-C(13)	100.99(15)
C(4)-C(5)	1.368(5)	C(7)-P(1)-Ir(1)	117.70(10)
C(4T)-C(5T)	1.513(5)	C(1)-P(1)-Ir(1)	117.12(11)
C(4H)-C(5H)	1.531(6)	C(13)-P(1)-Ir(1)	112.61(11)
C(5)-C(6)	1.396(4)	C(2C)-O(1C)-C(18C)	113.5(3)
C(5C)-C(6C)	1.491(5)	C(2C)-O(1C)-K(1)	116.5(2)
C(6C)-O(7C)	1.434(4)	C(18C)-O(1C)-K(1)	115.09(19)
O(7C)-C(8C)	1.423(4)	C(2)-C(1)-C(6)	118.9(3)
C(7)-C(8)	1.405(4)	C(2)-C(1)-P(1)	120.2(3)
C(7)-C(12)	1.406(4)	C(6)-C(1)-P(1)	120.8(3)
C(8)-C(9)	1.378(4)	O(1H)-K(1)-O(10C)	102.54(9)
C(8C)-C(9C)	1.499(5)	O(1H)-K(1)-O(1T)	178.17(12)
C(9)-C(10)	1.392(5)	O(10C)-K(1)-O(1T)	76.93(8)
C(9C)-O(10C)	1.423(4)	O(1H)-K(1)-O(4C)	98.51(8)
O(10C)-C(11C)	1.422(4)	O(10C)-K(1)-O(4C)	121.45(8)
C(10)-C(11)	1.371(5)	O(1T)-K(1)-O(4C)	83.24(8)
C(11)-C(12)	1.382(4)	O(1H)-K(1)-O(1C)	76.79(8)
C(11C)-C(12C)	1.503(5)	O(10C)-K(1)-O(1C)	179.33(12)
C(12C)-O(13C)	1.417(4)	O(1T)-K(1)-O(1C)	103.74(9)
O(13C)-C(14C)	1.431(4)	O(4C)-K(1)-O(1C)	58.80(7)
C(13)-C(18)	1.393(4)	O(1H)-K(1)-O(13C)	80.63(8)
C(13)-C(14)	1.394(4)	O(10C)-K(1)-O(13C)	58.80(7)
C(14C)-C(15C)	1.495(5)	O(1T)-K(1)-O(13C)	97.63(8)
C(14)-C(15)	1.381(5)	O(4C)-K(1)-O(13C)	179.14(11)
C(15C)-O(16C)	1.419(4)	O(1C)-K(1)-O(13C)	120.94(8)
C(15)-C(16)	1.388(5)	O(1H)-K(1)-O(7C)	101.18(9)
O(16C)-C(17C)	1.433(4)	O(10C)-K(1)-O(7C)	61.83(7)
C(16)-C(17)	1.381(5)	O(1T)-K(1)-O(7C)	80.15(8)

Appendix A

O(4C)-K(1)-O(7C)	60.74(7)	O(7C)-C(8C)-C(9C)	109.5(3)
O(1C)-K(1)-O(7C)	118.28(8)	C(8)-C(9)-C(10)	120.2(3)
O(13C)-K(1)-O(7C)	119.32(8)	O(10C)-C(9C)-C(8C)	108.6(3)
O(1H)-K(1)-O(16C)	78.49(8)	C(11C)-O(10C)-C(9C)	111.5(3)
O(10C)-K(1)-O(16C)	118.21(8)	C(11C)-O(10C)-K(1)	118.0(2)
O(1T)-K(1)-O(16C)	100.18(9)	C(9C)-O(10C)-K(1)	115.1(2)
O(4C)-K(1)-O(16C)	119.29(8)	C(11)-C(10)-C(9)	120.0(3)
O(1C)-K(1)-O(16C)	61.67(7)	C(10)-C(11)-C(12)	120.4(3)
O(13C)-K(1)-O(16C)	60.65(7)	O(10C)-C(11C)-C(12C)	108.4(3)
O(7C)-K(1)-O(16C)	179.67(11)	O(13C)-C(12C)-C(11C)	108.5(3)
O(1H)-K(1)-C(5T)	154.58(10)	C(11)-C(12)-C(7)	120.8(3)
O(10C)-K(1)-C(5T)	72.43(9)	C(12C)-O(13C)-C(14C)	113.4(3)
O(1T)-K(1)-C(5T)	23.59(8)	C(12C)-O(13C)-K(1)	119.4(2)
O(4C)-K(1)-C(5T)	105.32(9)	C(14C)-O(13C)-K(1)	116.12(19)
O(1C)-K(1)-C(5T)	108.15(9)	C(18)-C(13)-C(14)	118.6(3)
O(13C)-K(1)-C(5T)	75.54(9)	C(18)-C(13)-P(1)	124.7(3)
O(7C)-K(1)-C(5T)	98.12(9)	C(14)-C(13)-P(1)	116.6(2)
O(16C)-K(1)-C(5T)	82.20(9)	O(13C)-C(14C)-C(15C)	108.5(3)
O(1H)-K(1)-C(2H)	24.18(8)	C(15)-C(14)-C(13)	120.8(3)
O(10C)-K(1)-C(2H)	107.53(9)	O(16C)-C(15C)-C(14C)	109.8(3)
O(1T)-K(1)-C(2H)	157.66(10)	C(14)-C(15)-C(16)	120.1(3)
O(4C)-K(1)-C(2H)	75.79(8)	C(15C)-O(16C)-C(17C)	110.2(3)
O(1C)-K(1)-C(2H)	71.88(8)	C(15C)-O(16C)-K(1)	111.21(19)
O(13C)-K(1)-C(2H)	103.35(9)	C(17C)-O(16C)-K(1)	107.90(19)
O(7C)-K(1)-C(2H)	82.91(9)	C(17)-C(16)-C(15)	119.8(3)
O(16C)-K(1)-C(2H)	96.78(9)	C(16)-C(17)-C(18)	120.2(3)
C(5T)-K(1)-C(2H)	178.75(13)	O(16C)-C(17C)-C(18C)	109.7(3)
C(5H)-O(1H)-C(2H)	104.7(3)	C(17)-C(18)-C(13)	120.5(3)
C(5H)-O(1H)-K(1)	121.2(2)	O(1C)-C(18C)-C(17C)	108.7(3)
C(2H)-O(1H)-K(1)	104.6(2)	C(20)-B(19)-C(24)	116.8(3)
C(5T)-O(1T)-C(2T)	105.1(3)	C(20)-B(19)-P(2)	120.9(3)
C(5T)-O(1T)-K(1)	104.9(2)	C(24)-B(19)-P(2)	122.3(3)
C(2T)-O(1T)-K(1)	118.0(2)	C(21)-C(20)-B(19)	119.4(3)
C(31)-P(2)-C(25)	100.38(16)	C(22)-C(21)-C(20)	121.9(3)
C(31)-P(2)-B(19)	106.84(15)	C(21)-C(22)-C(23)	120.6(3)
C(25)-P(2)-B(19)	104.27(16)	C(24)-C(23)-C(22)	121.8(3)
C(31)-P(2)-Ir(1)	109.65(11)	C(23)-C(24)-B(19)	119.5(3)
C(25)-P(2)-Ir(1)	115.62(11)	C(30)-C(25)-C(26)	117.2(3)
B(19)-P(2)-Ir(1)	118.31(13)	C(30)-C(25)-P(2)	122.4(3)
O(1C)-C(2C)-C(3C)	109.2(3)	C(26)-C(25)-P(2)	120.5(3)
C(1)-C(2)-C(3)	120.2(3)	C(27)-C(26)-C(25)	121.4(3)
O(1H)-C(2H)-C(3H)	104.2(3)	C(26)-C(27)-C(28)	120.6(3)
O(1H)-C(2H)-K(1)	51.24(17)	C(27)-C(28)-C(29)	119.2(3)
C(3H)-C(2H)-K(1)	96.0(2)	C(30)-C(29)-C(28)	119.9(4)
O(1T)-C(2T)-C(3T)	106.3(3)	C(29)-C(30)-C(25)	121.7(3)
C(4)-C(3)-C(2)	120.0(4)	C(36)-C(31)-C(32)	118.5(3)
O(4C)-C(3C)-C(2C)	107.1(3)	C(36)-C(31)-P(2)	119.5(3)
C(4H)-C(3H)-C(2H)	104.3(3)	C(32)-C(31)-P(2)	121.9(2)
C(2T)-C(3T)-C(4T)	103.8(3)	C(33)-C(32)-C(31)	120.2(3)
C(3C)-O(4C)-C(5C)	112.2(3)	C(34)-C(33)-C(32)	120.8(3)
C(3C)-O(4C)-K(1)	120.05(19)	C(35)-C(34)-C(33)	119.9(3)
C(5C)-O(4C)-K(1)	117.03(19)	C(34)-C(35)-C(36)	119.7(3)
C(5)-C(4)-C(3)	120.2(3)	C(31)-C(36)-C(35)	120.9(3)
C(5T)-C(4T)-C(3T)	103.4(3)		
C(3H)-C(4H)-C(5H)	104.8(3)		
C(4)-C(5)-C(6)	120.5(3)		
O(4C)-C(5C)-C(6C)	107.8(3)		
O(1T)-C(5T)-C(4T)	106.5(3)		
O(1T)-C(5T)-K(1)	51.56(18)		
C(4T)-C(5T)-K(1)	97.2(2)		
O(1H)-C(5H)-C(4H)	105.1(3)		
O(7C)-C(6C)-C(5C)	109.9(3)		
C(5)-C(6)-C(1)	120.2(3)		
C(8C)-O(7C)-C(6C)	111.2(3)		
C(8C)-O(7C)-K(1)	108.48(19)		
C(6C)-O(7C)-K(1)	110.83(18)		
C(8)-C(7)-C(12)	117.8(3)		
C(8)-C(7)-P(1)	119.9(2)		
C(12)-C(7)-P(1)	122.3(2)		
C(9)-C(8)-C(7)	120.8(3)		